2000

Dynamic wavelength routing in multifiber WDM networks

Ling Li
Iowa State University

INFORMATION TO USERS

This manuscript has been reproduced from the microfilm master. UMI films the text directly from the original or copy submitted. Thus, some thesis and dissertation copies are in typewriter face, while others may be from any type of computer printer.

The quality of this reproduction is dependent upon the quality of the copy submitted. Broken or indistinct print, colored or poor quality illustrations and photographs, print bleedthrough, substandard margins, and improper alignment can adversely affect reproduction.

In the unlikely event that the author did not send UMI a complete manuscript and there are missing pages, these will be noted. Also, if unauthorized copyright material had to be removed, a note will indicate the deletion.

Oversize materials (e.g., maps, drawings, charts) are reproduced by sectioning the original, beginning at the upper left-hand corner and continuing from left to right in equal sections with small overlaps.

Photographs included in the original manuscript have been reproduced xerographically in this copy. Higher quality 6" x 9" black and white photographic prints are available for any photographs or illustrations appearing in this copy for an additional charge. Contact UMI directly to order.

Bell & Howell Information and Learning
300 North Zeeb Road, Ann Arbor, MI 48106-1346 USA

UMI®
800-521-0600

Dynamic wavelength routing in multifiber WDM networks

by

Ling Li

A dissertation submitted to the graduate faculty

in partial fulfillment of the requirements for the degree of

DOCTOR OF PHILOSOPHY

Major: Computer Engineering

Major Professor: Arun K. Somani

Iowa State University

Ames, Iowa

2000

UMI Number: 9962830

UMI Microform 9962830

Bell & Howell Information and Learning Company
300 North Zeeb Road
P.O. Box 1346
Ann Arbor, MI 48106-1346

Graduate College
Iowa State University

This is to certify that the Doctoral dissertation of

Ling Li

has met the dissertation requirements of Iowa State University

Signature was redacted for privacy.

Major Professor

Signature was redacted for privacy.

For the Major Program

Signature was redacted for privacy.

For the Graduate College

TABLE OF CONTENTS

LIST OF TABLES

LIST OF FIGURES

ACKNOWLEDGEMENTS

First and foremost, this dissertation, simply put, would not have been possible without the continuous support of my advisor Professor Arun K. Somani. He showed me different ways to approach a research problem and the need to be persistent to accomplish any goal. His advise to me as a friend as well as an advisor cannot be measured. I thank him from the bottom of my heart.

Next, I wish to thank Professor Suresh Subramaniam, whose suggestions are something I can always trust and count on. I am also thankful to Professor Manimaran Govindarasu, Professor Satish S. Udpa, Professor Degang Chen, Professor Murti Salapaka and Professor Ahmed Kamal with whom my discussions have been quite enjoyable. Also thanks to the folks at the Dependable Computing and Networking Laboratory, Seongwoo Kim, Hue-Sung Kim, Srini Ramasubramanian, Murari Sridharan, Sashisekaran Thiagarajan, Ra'ed Al-Omari, Jim-Eng Ng, Liang Zhao, Tao Wu, and former members Govind Krishnamurthi and Mohan Gurusamy, for interesting discussions and having fun together.

I would also like to thank Ms. Barbara Berry, my host family in Seattle, who taught me how to love and enjoy life. I enjoyed the weekends and holidays we spent and many places we visited together like a family. A special thank you is due to my friends, Mr. Jack Ovens in Ames, who has been meeting me every week for three years. We talked a lot of things together and enjoyed the dark coffee in Memory Union. He also helped me proofread my first journal paper.

I want to thank my parents, Sitong Li and Qingzhi Shi, not only for having me in

the first place, but unconditional support and encouragement to pursue my interests. I love them from the bottom of my heart. Their blessings have been a source of strength to me. I dedicate this work to them.

Last, but far from least, I want to express my deep appreciation and love for my wife and best friend, Wei Zhao, who has turned a blind eye to the dereliction of duty that occurred in our family over the past few years. I cannot imagine that I could have completed this work without her support.

ABSTRACT

Routing and wavelength assignment algorithms play a key role in improving the performance of wavelength-routed, wavelength-division-multiplexed (WDM) all-optical networks. We study networks with dynamic wavelength routing and develop accurate analytical models for evaluating the blocking performance under dynamic input traffic in different topologies. We also develop algorithms with linear complexity to optimally place a given number of wavelength converters on a path of a network. Finally we consider the effect of multiple fibers on WDM networks without wavelength conversion. We develop analytical models for evaluating the blocking performance of multifiber networks. The number of fibers required to provide high performance in multifiber networks with different routing algorithms is also studied.

1 INTRODUCTION

Computer and communication networks have changed the world dramatically in the 20th century, and will continue to do so in the future. Two major networks of networks, the public switched telephone network (PSTN) and the Internet, exist today. The PSTN is based on circuit switches that provide a very high quality of service for large-scale, advanced voice services. The PSTN is a low-delay, fixed-bandwidth network of networks. The Internet is based mainly on packet switches that provide very flexible data services, for example, e-mail and access to the World Wide Web. At the same time, however, it is a variable-delay, variable-bandwidth network that provides no guarantee on the quality of service (QoS). Internet traffic volumes continue to grow exponentially. A conservative estimate of Internet traffic growth is that it is doubling every 6 months. Current predictions indicate that data traffic principally made up of the Internet will exceed voice traffic in North America in the year 2001 [1]. As data traffic surpasses voice traffic, and as it becomes possible to provide high levels of QoS on packet networks - particularly for voice and other real-time services - it will be desirable to converge the multiple networks around a single packet-based core network [2]. The electronic-switched, connection-oriented network of the past 125 years will be replaced by a packet-switched IP network [3].

1.1 Next-Generation Network Architecture

Different networks, e.g., PSTN, IP, ATM, and Sonet/SDH, exist today. However, it is likely that the existing networks will converge to share a common high-level architecture in the next-generation networks, as shown in Figure 1.1.

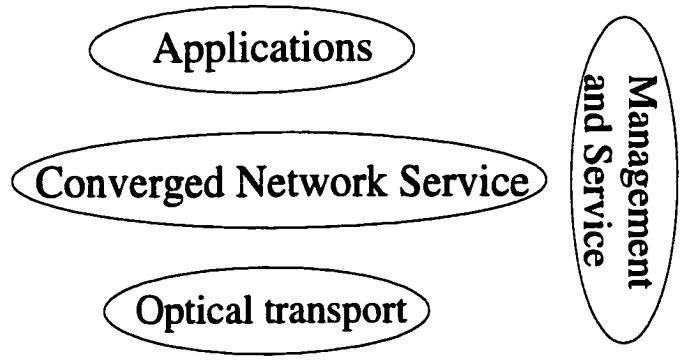

Figure 1.1 A next-generation network architecture.

The application signals have widely varied characteristics, e.g., signal format and transmission speed. To transport the varied application signals on the optical transport network, a network service layer is needed to map the signals to optical channel signals along with associated "overhead" to assure proper networking functions. This layer will capture today's IP and ATM capabilities with statistical multiplexing and QoS guarantee. New protocols such as multiprotocol label switching (MPLS), resource reservation protocol (RSVP), and differentiated services (DiffServ) will likely play a major role to support the required QoS across a wide set of applications. The network service layer relies entirely on the transport layer for the delivery of multi-gigabit bandwidth where and when it is needed to connect to their peers.

The optical transport layer delivers managed multi-gigabit bandwidth and provides highly reliable, wavelength-level network interfaces to the service platforms. It has advanced features such as optical channel routing and switching and supports flexible, scalable, and reliable transport of a wide variety of client signals at ultra-high speed. This next-generation network will dramatically increase, and maximally share, backbone network infrastructure capacity and provide sophisticated service differentiation for emerging data applications. Transport networking enables the service layer to operate more effectively, freeing them from constraints of physical topology to focus on the sufficiently large challenge of meeting service requirements [4]. The design and operation

of optical transport networks are the focuses of this dissertation.

1.2 Research Issues in Optical Transport Networks

Over the past two decades, optical fibers have revolutionized the communications industry. Researchers have been driven by a vision of accessing a larger fraction of the approximately 50-THz theoretical information bandwidth of a single-mode fiber. A natural approach to utilize the fiber bandwidth efficiently is to partition the usable bandwidth into non-overlapping wavelength band. Each wavelength, operating at several gigabits per second, is used at the electronic speed of the end-users. This mechanism is called wavelength division multiplexing (WDM) [5], and is the most promising candidate for improving fiber bandwidth utilization in future optical networks. The research, development, and deployment of WDM technology are now evolving at a rapid pace to fulfill the increasing bandwidth requirement and deploy new network services.

1.2.1 Wavelength-Routed WDM Networks

With the advancement of optical technologies, a wide variety of optical components of building WDM networks have been developed, such as wide-band optical amplifiers (OAs), optical add/drop multiplexers (OADMs) and optical cross-connects (OXCs). It becomes possible to route data to their respective destinations based on their wavelengths. The use of wavelength to route data is referred to as wavelength routing, and a network which employs this technique is known as a *wavelength-routed* network [6]. In such networks, each connection between a pair of nodes is assigned a path through the network and a wavelength on that path such that connections whose paths share a common link in the network are assigned different wavelengths. The optical communication path between two nodes is called a *lightpath*. All-optical networks employing wavelength-division multiplexing and wavelength routing are a viable solution for future wide-area networks (WANs) and metropolitan-area networks (MANs). These wavelength-routed WDM networks offer the advantages of protocol transparency and simplified manage-

ment and processing compared to routing in telecommunications systems using digital cross-connects [7].

The research issues in WDM networks can be broadly classified into two categories: network design and network operation. The network design problem is generally an optimization problem [8, 9]. The inputs to the problem are a static traffic demand, a general network topology, and some specific requirements, e.g., network reliability and/or restoration time. The objective of the optimization problem could be minimizing the resources, including the number of wavelengths, the number of fibers, or the number of cross-connect ports, to meet the requirements. The outputs may include the network configuration, and the route and wavelength for each source-destination pair. The network design problem can be formulated as an integer liner programming (ILP) or mixed integer liner programming (MILP) problem. Since the number of variables and constraints can be very large in WDM networks, heuristics are usually used to find fast solutions.

After a network is built, one critical problem is how to operate the network such that the network performance is optimized under dynamic traffic. The traffic intensity of the dynamic traffic is usually known while the individual demands arrive and depart randomly. Since network resources are typically not sufficient enough to guarantee that every dynamic demand can be accommodated in the network, the average blocking probability for a given utilization is one of the metrics to measure the network performance. Some other metrics include control overhead and algorithm complexity.

In a wavelength-routed WDM network, the path of a signal is determined by the location of the signal transmitter, the wavelength on which it is transmitted, and the state of the network devices. An example of such a network with 2 wavelengths on each link is shown in Figure 1.2. There are two sessions that are in progress, one from node 1 to node 2 using wavelength λ_1, another from node 2 to node 3 using wavelength λ_2. A connection request from node 1 to node 3 has to be blocked, although free wavelengths are available on both link 1 and link 2. This is because of the wavelength continuity constraint, that is, the same wavelength must be assigned to a connection on

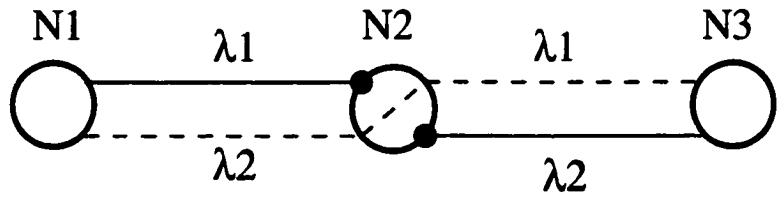

Figure 1.2 A demonstration for the wavelength continuity constraint on a two-hop path

every link on a path if wavelength converters are not available at the switching nodes. Connection requests encounters higher blocking probability than it does in electronic-switched networks because of the wavelength continuity constraint.

1.2.2 Routing and Wavelength Assignment (RWA) Algorithms

Routing and wavelength assignment algorithms are responsible for selecting a suitable route and a wavelength among the many possible choices for establishing a connection. Good routing and wavelength assignment algorithms are critically important to improving the performance of WDM networks.

Routing algorithms have been extensively studied in telecommunications (circuit-switched) networks [10] and computer (packet-switched) networks [11]. The routing algorithms can be broadly classified into two, namely, *static routing* and *dynamic routing.* In the static routing, the routes for node-pairs are fixed, i.e., the routes do not change with the network status. The static routing typically includes *fixed-path routing (FPR)* and *alternate path routing (APR).* In the dynamic routing, the routes for node-pairs are dynamically selected according to the current network status. A typical example of the dynamic routing is least-congestion routing (LCR). All of these routing algorithms were first proposed in circuit-switched networks and have been applied to optical WDM networks.

The fixed-path routing is the simplest among the three algorithms. Many research papers on wavelength assignment algorithms and analytical models assume fixed-path

routing because of its simplicity. However, its simplicity also results in performance degradation because only one path is provided for each node-pair. A connection request is blocked if no wavelength is available on the path. Alternate path routing, in which more than one candidate paths are provided for a connection request, improves the network performance significantly [12, 13, 14] compared to the fixed-path routing. However, the candidate paths and their orders are predetermined without considering the current network status. The performance cannot be further improved with these static routing algorithms. The least-congestion routing, which take the current network status into account, select the least congested path to establish a connection. The results in [15] show that the blocking probability of using least-congestion routing is one to two order of magnitude lower than alternate path routing in mesh-torus networks.

Wavelength assignment problem is a unique problem in WDM networks. Unlike in circuit-switched networks, the same wavelength has to be free on all of the links of a path for establishing a connection in all-optical WDM networks without wavelength conversion. If full-range wavelength converter is available at every node, wavelength assignment is a trivial problem. However, the technology of all-optical wavelength conversion is not mature yet. Wavelength converters are likely to be costly devices in the near future. Therefore, good wavelength assignment algorithms along with routing algorithms are critically important to improving the network performance and reducing the network cost.

The wavelength assignment algorithms in the literature can be broadly classified into two categories: the algorithms proposed for single-fiber networks and that for multifiber networks. The following algorithms are first proposed for single-fiber networks:

1. *Random (R)*: The random wavelength assignment algorithm choose one of the available wavelengths randomly with a uniform distribution to establish a connection.

2. *First-Fit (FF)*: Assume that the wavelengths are arbitrarily ordered, e.g., $\lambda_1, \lambda_2, \ldots, \lambda_W$, where W is the maximum number of wavelengths per fiber. The first-fit algorithm

checks the status of the wavelengths sequentially and chooses the first available wavelength to establish a connection.

3. *Most-Used (MU)*: The free wavelength that is used on the most number of links in the network is chosen to establish a connection.

4. *Least-Used (LU)*: The free wavelength that is used on the least number of links in the network is chosen to establish a connection.

The random wavelength assignment algorithm is usually assumed by analytical models because of its simplicity. However, the used wavelengths are randomly distributed and mixed up with free wavelengths in the network. It is hard for a connection request to find a wavelength free on consecutive links from a source to a destination node. The least-used algorithm attempts to route a connection on the least utilized wavelength in order to achieve a near-uniform distribution of the load over the wavelength set. The results in [16] show that both of the random and the least-used algorithms distribute the load evenly over the wavelengths. The first-fit and the most-used method attempt to pack the connections together to use fewer wavelengths, and leave more wavelengths consecutively free. The simulation results in [17, 18, 16] show that the blocking probability of the random and least-used wavelength assignment algorithms are higher than that of the first-fit and most-used algorithms. The random assignment algorithm has a performance close but better than the least-used algorithm. The first-fit algorithm with fixed-path routing is considerably lower than the blocking probability with the random wavelength assignment algorithm. However the most-used algorithm performs slightly better than the first-fit algorithm [19].

With the development of networks and optical technology, more and more researchers have realized that a single-fiber network may not have enough capacity to support the dramatically increasing bandwidth requirement. In fact, most of the optical networks, if not all, consist of multiple fibers on each link. The wavelength continuity constraint is relaxed in multifiber networks because a wavelength that cannot continue on one fiber can be switched to anther fiber using optical cross-connect as long as the same

wavelength is available on the other fibers on the out-going link. The effects of multiple fibers on the network performance will be further discussed in the following sections. We focus on the wavelength assignment algorithms in multifiber networks here. Several wavelength assignment algorithms have been proposed for multifiber WDM networks in the literature:

1. *Least-loaded (LL)*: the LL algorithm proposed in [18] selects the wavelength that has the largest residual capacity on the most loaded link along a path;

2. *Minimum sum (MS)*: the MS algorithm proposed in [18] chooses the wavelength that has the minimum average utilization.

   Both MS and LL algorithms select the most used wavelength when multiple wavelengths are tied, hence they reduce to the most-used rule in the single-fiber case.

3. $M\sum$: the $M\sum$ algorithm in [19] chooses the wavelength that leaves the network in a "good" state for future calls. The goodness of a state is measured by a new concept called the *value* of the network. The value function $V(\alpha)$ of the resulting state α after a call is established is restricted to be functions of path capacities, i.e., $V(\alpha) = g([C(\alpha, p) : p : P])$ where P is the set of all possible paths, and $C(\alpha, p)$ is the path capacity of p in an arbitrary state ϕ.

4. *Relative Capacity Loss (RCL)*: the relative capacity loss algorithm in [20] chooses the wavelength that minimize the relative capacity loss. The relative capacity loss of path p on wavelength λ^*, denoted by $R_c(p, \lambda^*)$, is defined as

$$R_c(p, \lambda^*) = \frac{P_c(p, \lambda^*) - P_c'(p, \lambda^*)}{\sum_\lambda P_c(p, \lambda)} . \tag{1.1}$$

   where $P_c(p, \lambda)$ is the wavelength path capacity of path p on wavelength λ [20].

Note here that the random, first-fit, most-used, and least-used algorithms are first proposed for single fiber network, but they can also be used in multifiber networks with or without modifications. The results in [18] show that the LL and MS algorithms performs better than the Random, first-fit, and most-used algorithms in multifiber networks.

The $M\sum$ algorithm in [19] performs considerably better than other algorithms except the RCL algorithm at the cost of increased computational complexity. The blocking probability of using the RCL algorithm is $5\% - 30\%$ better than the $M\sum$ depending on the traffic demands and network topology, but has the same worst cast time complexity of $M\sum$ (at least asymptotically) [20].

In the above discussions we separate a connection establish procedure into two steps: select a route first (if not fixed-path routing), and then select a wavelength from the available free wavelengths. The routing and wavelength assignment algorithm can also be solved jointly as proposed in [16] and [18]. The route-wavelength pair that meets the specified criteria, i.e., maximizes the residual capacity, over all wavelengths and considered paths is selected jointly. These joint routing and wavelength assignment algorithms outperform the disjoint approaches.

1.2.3 Wavelength Conversion in WDM Networks

A WDM network without wavelength conversion is referred as *wavelength selective (WS)* network. The network performance can be improved by using wavelength converters at the switching nodes, which can convert data on one wavelength along a link into another wavelengths at an intermediate node and forward it along the next link. The networks with wavelength conversion is called *wavelength interchanging (WI)* networks [21]. The first solution for wavelength conversion is opto-electronic wavelength conversion, in which the optical signal is converted into the electronic domain first. The electronic signal is then used to drive the input of a tunable laser tuned to the desired wavelength of the output. Since this technique is not transparent to data bit rate and data format, which is one of the mayor advantages of using optical networking, the opto-electronic wavelength conversion is not preferred to using in the future networks. All-optical wavelength conversion, in which no opto-electronic conversion is involved, can be divided into the following categories [22]:

- Wavelength conversion using wave-mixing, including *four-wave mixing* [23, 24] and *difference frequency generation (DFG)* [25].

- Wavelength-conversion using cross modulation, including *Semiconductor Optical Amplifiers (SOAs) in XGM and XPM mode* [26, 27], and semiconductor lasers [28].

All-optical wavelength converters are being prototyped in research laboratories [29]. However, the techniques have not mature yet so far. Wavelength converters are likely to remain costly devices in the near future. Many papers have been published on evaluating the benefits of wavelength converters using analytical models and simulation. These benefits depend on the topology of the network, the traffic demand, the number of available wavelengths, and the routing and wavelength assignment algorithms, among other factors. As the network becomes denser, one would expect the usefulness of converters to decrease, since the paths get shorter. In the limiting case with a link between every node pair, wavelength converters have no effect on the blocking performance, since all connections are one-hop connections[1]. On the other hand, a sparsely connected network tends not to mix calls well and thus causes a load correlation in successive links. This reduces the usefulness of wavelength converters [30].

1.3 Contributions and Outline of the Dissertation

The rest of the dissertation is organized as follows. Good routing and wavelength assignment algorithms are critically important to increasing the efficiency of WDM networks. We present two new routing algorithms, fixed-path least-congestion (FPLC) routing and neighborhood-information-based routing, in Chapter 2 to improve the network performance. The FPLC routing algorithm routes a connection request on the least-congested path out of a set of predetermined paths. A set of routes [2] connecting the source-destination pair is searched in parallel and the route with the maximum number of idle wavelengths is selected to set up the connection. If a request cannot be accommodated by any of the routes, it is blocked.

[1]This assumes that the direct link is always used in this case. If alternate path routing is allowed, wavelength converters may still be of some benefit.

[2]The words "path" and "route" are used interchangeably throughout this dissertation

The FPLC still has higher setup delay and higher control overhead. To overcome these shortcomings, a new routing method using neighborhood information is also investigated in Chapter 2. In this method, for each source-destination pair, a set of preferred paths are pre-computed. Instead of searching all the nodes on the preferred routes, only the first k links on each path are searched. A route is selected based on availability of free wavelengths on the first k links on the preferred paths. An essential observation here is that the parameter k depends on the size and structure of the network and the network performance requirement.

We develop new analytical models to compute the blocking performance of the FPLC routing and the neighborhood-information-based routing with the consideration of link-load correlation. The analytical models are validated and verified by comparing the analytical results with the simulation results. It is shown that the FPLC routing performs one to two orders of magnitude better than the alternate-path routing and the fixed-path routing in a 4×4 mesh-torus network and in the NSFNET T1 backbone network. A value of $k = 2$ is generally enough to ensure good network performance these networks.

Since the cost of an all-optical wavelength converter is likely to remain high, sparse wavelength conversion and limited wavelength conversion are studied in [31, 32]. A network with only a few nodes having full conversion capability is called a network with sparse wavelength conversion. The results in [31] show placing converters on a fraction of nodes of a network is sufficient to ensure high network performance.

An interesting problem in sparse wavelength conversion networks is how to place a small number of converters so that the network performance is optimized. This problem has been studied in [33, 34, 36]. The complexity of the optimal converter placement algorithm is $O(N^2K)$ when the blocking probability of end to end calls is optimized on a path. Here N is the number of nodes on the path, and K is the number of converters being placed.

We present a new linear complexity algorithm to place converters on a path to minimize the blocking probability in Chapter 3. Given the number of nodes, N, and the

number of converters, K, the basic idea of our algorithm is that we divide the path into K+1 segments such that the blocking probability on each segment is equal. It is shown that the blocking probability is minimized if each segment has the same blocking probability. However, it is not always possible to divide a path into segments with equal blocking probabilities, due to the arbitrary values of the loads on each link. Three algorithms are proposed in the chapter to divide a path into segments such that each segment has approximately equal blocking probabilities. The results of using these algorithms are compared with the optimal solutions obtained by using dynamic programming method of [33].

An alternative solution to conquer the wavelength continuity constraint is to use multifiber WDM networks. In multifiber networks, each link consists of multiple fibers, and each fiber carries information on multiple wavelengths. A wavelength that cannot continue on the next hop can be switched to another fiber using an optical cross-connect (OXC) if the same wavelength is free on one of the other fibers. We study the performance of multifiber WDM networks with different routing and wavelength assignment algorithms in Chapter 4, 5, and 6. We present a new analytical model, multifiber link-load correlation (MLLC) model, in 4 to compute the blocking performance of multifiber networks with fixed-path routing. Comparing to the link independence model in [19], the MLLC model is an more accurate and general model that is applicable to not only regular networks but also irregular networks.

The effects of multiple fibers in WDM networks with the alternate-path routing (APR) is studied in Chapter 5. The question we attempt to answer is how many fibers per link are required to guarantee high performance in a WDM network with the APR. We use and extend the MLLC model in Chapter 4 to analyze the performance of WDM networks with the APR. We observe that the number of fibers required to guarantee high performance is slightly higher in the APR than the FPR. However, a limited number of fibers are still sufficient to guarantee that the blocking performance of a multifiber WDM network is similar to the blocking performance of a full-wavelength-convertible network.

As we show in Chapter 2 that dynamic routing algorithms can significantly improve the network performance compared to the fixed-path routing and alternate-path routing. However, most of the current research on dynamic routing has focused on single-fiber WDM networks. We study the blocking performance of multifiber WDM networks with the fixed-paths least-congestion (M-FPLC) routing in Chapter 6. Two routing algorithms are studied in the chapter: wavelength-trunk (WT)-based FPLC and light-path (LP)-based FPLC. We use and extend the multifiber link-load correlation model developed in 4 to analyze the performance of multifiber WDM networks with the WT-based FPLC routing. We observe that the number of fibers required to provide high performance in a multifiber network with dynamic routing is higher than those multifiber networks with fixed-path routing and alternate-path routing. However, multifiber networks with dynamic routing can still achieve similar blocking performance to full-wavelength-convertible networks with limited number of fibers.

A parametric system cost model for both multifiber networks and single-fiber wavelength-convertible WDM networks is developed in Chapter 7. By comparing the cost of different network configurations, we show that a multifiber network is a cost-effective solution under current technology. Conclusions and directions for future research are presented in Chapter 8.

2 FIXED-PATHS LEAST-CONGESTION ROUTING AND ROUTING USING NEIGHBORHOOD INFORMATION

2.1 Introduction

One of the main requirements in all-optical WDM networks is that the same wavelength must be assigned to a connection on every link on a path if wavelength converters are not available at the switching nodes. A connection request encounters higher blocking probability than it does in circuit-switched networks because of the wavelength continuity constraint. Therefore, routing and wavelength assignment algorithms play a key role in improving the performance of WDM networks [6, 7]. Many researchers have proposed the use of the shortest path routing and alternate shortest path routing. In [12, 13, 17, 18, 37, 38, 39, 40] the performance of the shortest path (SP) routing and the alternate shortest paths (ASP) routing methods are investigated through approximate analysis and simulation. A new alternate routing method, alternate routing with limited trunk reservation, is introduced in [12] to improve the blocking probability and fairness among connection requests. Since the shortest paths are statically computed and an attempt is made to set up a connection request on fixed paths without acquiring the information of current network status, it is not possible to further improve the network performance in terms of blocking probability by using these routing approaches.

Dynamic routing approaches are more efficient than static routing methods [12, 13, 15, 18, 37, 41, 42, 43, 44]. In [12], simulation results show that the dynamic routing method can significantly improve the network performance compared to the SP and the ASP. Routing and wavelength assignments are considered jointly and adaptively

in [16]. All feasible paths between a source-destination pair are computed and one of them is selected according to a specific criterion to set up a request. Least loaded routing (LLR) algorithms are introduced as dynamic routing methods in [39, 41, 42]. However, only fully connected networks are investigated and no performance comparison is provided between LLR and static routing algorithms in these papers. Dynamic routing methods are also discussed in [18, 43]. The main problems with these dynamic routing methods are longer setup delays and higher control overheads including, in some cases, the introduction of a central control node that keeps track of the network's global state.

In this chapter, we consider alternate dynamic routing algorithms in all-optical networks. We first introduce a dynamic routing algorithm, called fixed-paths least-congestion routing (FPLC), and compare its performance to that of the SP and the ASP. This algorithm routes a connection request on the least-congested path out of a set of predetermined paths. A set of routes [1] connecting the source-destination pair are searched in parallel and the route with the maximum number of idle wavelengths is selected to set up the connection. If a request cannot be accommodated by any of the routes, it is blocked.

The FPLC still has higher setup delay and higher control overhead. To overcome these shortcomings, a new routing method using neighborhood information is also investigated in this chapter. In this method, for each source-destination pair, a set of preferred paths are pre-computed. Instead of searching all the nodes on the preferred routes, only the first k links on each path are searched. A route is selected based on availability of free wavelengths on the first k links on the preferred paths. If several free wavelengths are available on the selected route, a wavelength is selected according to a pre-specified wavelength assignment algorithm. If no free wavelengths are available on all the preferred routes, the request is blocked. An essential observation here is that the parameter k depends on the size and structure of the network and the network performance requirement. It is shown that a value of $k = 2$ is generally enough to ensure good network performance in a 4×4 mesh-torus network and in the NSFNET T1 backbone

[1] The words "path" and "route" are used interchangeably throughout this dissertation

network depicted in Figure 2.2 and Figure 2.11, respectively.

Wavelength assignment is another unique problem of optical networks. Algorithms for improving network performance using different information are proposed in [18, 19, 45, 46]. In [19], a dynamic wavelength assignment algorithm, the Max_Sum ($M\Sigma$), is proposed and compared to other algorithms, i.e., the First-Fit (FF), the Most-Used (MU), the Min-Product (MP), the Least Loaded (LL) and the Random (R). However, global information is required in most of these algorithms. Since distributed algorithms are considered in this chapter, two general wavelength assignment methods are examined:

1. Random Assignment: The assigned wavelength is selected randomly from the available wavelengths. The approximate analysis and the corresponding simulations in this chapter are based on this method.

2. First-fit Assignment: The wavelength is assigned according to a predefined order [17]. We assume that the wavelengths are indexed and the free wavelength with the smallest index is selected.

Several approximate analytical methods on the blocking probabilities of networks are proposed in the literature. In [47], a model to compute the approximate blocking probability with Poisson traffic input is presented. However, the model is inappropriate for networks with sparse topologies because it does not consider the correlation among the use of wavelengths between successive links of a path. This model is improved in [48] with the consideration of this dependence. A Markov chain based reduced load model with state-dependent arrival rate is presented in [17, 39]. A more accurate model in [31] accounts for link load correlation. We compute approximate blocking probabilities for our algorithms using both of the analytical methods, i.e., the link load correlation model [31] and the approximate reduced load model [17, 39], and compare the results. We show that the model considering link load correlation is simpler and more accurate than the reduced load model.

This chapter is organized as follows. In Section 2, we discuss the performance of the FPLC, and compare it to the SP and the ASP with different wavelength assignment

methods. Routing using neighborhood information is introduced and analyzed in Section 3. Section 4 presents results for applications of our routing methods to an irregular network, the NSFNET T1 backbone network, and a large-scale regular network, a 7×7 mesh-torus network. In Section 5, we present our conclusions and future work that we are undertaking.

2.2 Fixed-Paths Least-Congestion Routing

Distributed network control for WDM networks is discussed in [49, 50]. Two reservation protocols, source initiated reservation (SIR) and destination initiated reservation (DIR) are introduced and compared in [50]. The results show that DIR performs better than SIR when the propagation delay is small. However, the DIR cannot improve throughput when the propagation delay is large and no wavelength converter is available at the network. The control protocol for our FPLC routing algorithm is similar to DIR. However, to help the destination to make a correct decision in the absence of wavelength converters, we also include information in the request message going towards the destination regarding how many different requests may be competing for a wavelength on the same link. For this purpose, we assume that each node keeps a counter for each wavelength on the links connected to this node. When a wavelength is requested by a wavelength-searching message from a source node, the corresponding counter is increased by one before the request is forwarded. This counter information is added to the searching message as a hint to indicate the probability of other paths using this wavelength. This hint can be used by the wavelength assignment algorithm to avoid a possible duplicate use of a wavelength. The details of the FPLC algorithm is described as follows:

2.2.1 The Routing Rules

For a given topology, we first statically compute a set of routes to be used for each source-destination pair and store the routes information at each source node. In this

chapter, we only use two edge-disjoint shortest paths for analysis and simulation. We refer to these routes as the first and second route. We restrict the number of preferred routes to two because network resources cannot be used efficiently if many longer routes are allowed in the network. One reason that the two routes are required to be edge-disjoint is that we try to search two paths in parallel. Another consideration is fault tolerance. If one path fails, the connection can be rerouted to another path[51, 52, 53, 54]. We also noticed that using more than two paths does not significantly improve performance [21].

The routing algorithm consists of two steps:

- Step 1. Upon arrival of a connection setup request destined to node d, node i performs the following steps:

    1. If i is the source node, search the available number of wavelengths on two routes in parallel by sending *needle packets* [2] requesting a path setup towards the next nodes on the two routes. The counters of the available wavelengths on the outgoing link, S_λ, are increased by one, and the path information are also included in the *needle packet.*

    2. If i is an intermediate node, compute $S_\lambda = S_\lambda \cap S_{available}$. If $S_\lambda \neq \phi$, increase the counters for these wavelengths, add the counter information to the packet, and forward it to the next node. If $S_\lambda = \phi$, node i responds to the source node with a nack-packet, but also continues sending a nack-packet indicating no free wavelength available on the route to the destination node for a resolution.

    3. If $i = d$, this request has found the route to the destination. Wait for the second request to arrive. Select the route that has the maximum number of free wavelengths available and one wavelength from the available wavelengths on the route according to the wavelength assignment method to set up the request. If two routes have the same number of idle wavelengths, the first

[2]The *needle packets* can be sent out through a control network, either out-of-band or inband, as proposed in [49]

route is selected. Reserve the selected wavelength for the request, then send an ack-packet to the source node on the selected route and a nack-packet to the source node on other routes (it is not necessary to send back any packet on the route on which a nack-packet is received, as a nack-packet has already been sent back by an intermediate node).

- Step 2. Upon arrival of a responding packet on the return path, node i performs the following steps:

  1. If i is an intermediate node, reserve the selected wavelength for the request, decrease the wavelengths counters related to the request, and forward the packet towards the source node. If the selected wavelength has been reserved by another request, send a nack-packet to the source node. The reserved wavelength on previous links from the destination node is released after a short period of time if no request is set up on it.
  2. If $i = s$, the source node is reached. The connection is set up on the selected route using the selected wavelength. If no wavelength is available on any of the two routes, the connection request is blocked

2.2.2 Analysis of the FPLC Routing

To analyze the FPLC routing algorithm, we first use and extend the analysis of a link load correlation model in [31]. This model has been used on regular network topologies using the fixed path routing. Results show that this correlation model is more accurate than the models presented in [17, 39, 47]. The notations used here are similar to that in [31] and described below.

We assume that call requests arrive at each source-destination pair according to a Poisson process with rate λ. The destination of a call is uniformly distributed to other nodes. Call holding time is exponentially distributed with mean $(1/\mu)$. The number of wavelengths, F, is same on all links. Wavelengths are randomly assigned to a session

from the set of free wavelengths on the associated path. To make the analysis tractable, we also assume that the wavelength searching and reservation time is negligibly small.

2.2.2.1 Link Load Correlation Model

The basic idea of the link load correlation model is that the blocking probability on a two-hop path can be computed with the consideration of link load correlation. Then the blocking probability on a l-hop path can be computed recursively by viewing the first $l-1$ hops as the first hop and the lth hop as the second hop of a two-hop path. The following steady-state probabilities are defined to obtain the blocking probabilities.

- $Q(w_f) = \Pr\{w_f$ wavelengths are free on a link$\}$.
- $S(y_f|x_{pf}) = \Pr\{y_f$ wavelengths are free on a link of a path $|$ x_{pf} wavelengths are free on the previous link of the path$\}$.
- $U(z_c|y_f, x_{pf}) = \Pr\{z_c$ calls (wavelengths) continue to the current link from the previous link of a path $|$ x_{pf} wavelengths are free on the previous link, and y_f wavelengths are free on the current link$\}$.
- $R(n_f|x_{ff}, y_f, z_c) = \Pr\{n_f$ wavelengths are free on a two-hop path $|$ x_{ff} wavelengths are free on the first hop of the path, y_f wavelengths are free on the second hop, and z_c calls continue from the first to the second hop$\}$.
- $T^{(l)}(n_f, y_f) = \Pr\{n_f$ wavelengths are free on an l-hop path and y_f wavelengths are free on hop $l\}$.

For a two-hop path as shown in Figure 2.1, let C_l be the number of calls that enter the path at node 0 and leave at node 1, let C_c be the number of calls that enter the path at node 0 and continue on to the second link, and let C_n be the number of calls that enter the path at node 1. We also denote λ_l the arrival rate of calls that enter at node 0 and leave at node 1, λ_c the arrival rate of calls that enter at node 0 and continue on to node 2, and λ_e the arrival rate of calls that enter at node 1. The corresponding Erlang

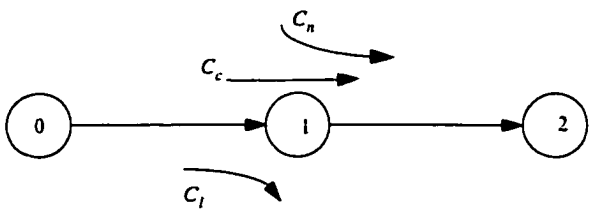

Figure 2.1 Calls arriving and leaving on a two-hop path.

load is denoted by $\rho_e = \lambda_e/\mu$, $\rho_c = \lambda_c/\mu$, and $\rho_l = \lambda_l/\mu$. The steady-state probability of state (c_l, c_c, c_n) as [11] is given by

$$\pi(c_l, c_c, c_n) = \frac{\frac{\rho_l^{c_l}}{c_l!}\frac{\rho_c^{c_c}}{c_c!}\frac{\rho_e^{c_n}}{c_n!}}{\sum_{j=0}^{F}\sum_{i=0}^{F-j}\sum_{k=0}^{F-j}\frac{\rho_l^i}{i!}\frac{\rho_c^j}{j!}\frac{\rho_e^k}{k!}}, \quad 0 \le c_l + c_c \le F, \quad 0 \le c_c + c_n \le F \ .$$

The probabilities $R(n_f|x_{ff}, y_f, z_c)$ $U(z_c|y_f, x_{pf})$, $S(y_f|x_{pf})$, and $Q(w_f)$ are similar as in [31] and are reproduced here for completeness.

$$R(n_f|x_{ff}, y_f, z_c) = \begin{cases} \frac{\binom{x_{ff}}{n_f}\binom{F-x_{ff}-z_c}{y_f-n_f}}{\binom{F-z_c}{y_f}} & \text{for } \min(x_{ff}, y_f) \ge n_f \ge \max(0, x_{ff} + y_f + z_c - F), \\ 0, & \text{otherwise.} \end{cases}$$

$$\begin{aligned} U(z_c|y_f, x_{pf}) &= P(C_c = z_c \mid C_n + C_c = F - y_f, C_l + C_c = F - x_{pf}) \\ &= \frac{\pi(F - x_{pf} - z_c, z_c, F - y_f - z_c)}{\sum_{x_c=0}^{\min(F-x_{pf}, F-y_f)} \pi(F - x_{pf} - x_c, x_c, F - y_f - x_c)}, \end{aligned} \tag{2.1}$$

$$\begin{aligned} S(y_f|x_{pf}) &= P(C_n + C_c = F - y_f \mid C_l + C_c = F - x_{pf}) \\ &= \frac{\sum_{x_c=0}^{\min(F-x_{pf}, F-y_f)} \pi(F - x_{pf} - x_c, x_c, F - y_f - x_c)}{\sum_{x_c=0}^{F-x_{pf}} \sum_{x_n=0}^{F-x_c} \pi(F - x_{pf} - x_c, x_c, x_n)}, \end{aligned} \tag{2.2}$$

and

$$Q(w_f) = P(C_l + C_c = F - w_f)$$

$$= \sum_{x_c=0}^{F-w_f} \sum_{x_n=0}^{F-x_c} \pi(F - w_f - x_c, x_c, x_n) \ .$$

The steady-state probability of a l-hop path P can be recursively computed as

$$T_P^{(l)}(n_f, y_f) = \sum_{x_{pf}=0}^{F} \sum_{z_c=0}^{\min(F-x_{pf}, F-y_f)} \sum_{x_{ff}=0}^{x_{pf}}$$
$$R(n_f|x_{ff}, z_c, y_f) U(z_c|y_f, x_{pf}) S(y_f|x_{pf}) T_P^{(l-1)}(x_{ff}, x_{pf}). \tag{2.3}$$

Let $Q_P(w)$ be the free wavelength distribution of this path. $Q_P(w)$ becomes

$$Q_P(w) = \sum_{y_f=0}^{F} T_P^{(l)}(w, y_f). \tag{2.4}$$

A fundamental assumption made in the correlation model is that the path used by a call does not depend on the state of the links on the path. For a fixed shortest path routing on regular networks, it is possible to assume that the effect of blocking probability on the carried load can be neglected, and the arrival rate on each link is the same for keeping the analysis simple. However, these assumptions become invalid when the FPLC is used. In this case, a path for a request is selected using the current network status. Thus the arrival rate on each link is continuously changing. No steady-state is reached in the strict sense when the FPLC is used. We propose to use a technique based on the Erlang Fixed-Point method for Alternate routing [55] to solve this problem. The details of this method are described as follows:

The reduced load approximation model in [12, 17, 39] significantly increased the complexity by computing the arrival rate on each link for different link status. We show that more accurate results can be obtained without considering the different arrival rate for different link status when the link load correlation model is used. We need the following further notations:

1. Let $R_j^{(1)}$ be the set of first shortest routes that employ link j, and $R_j^{(2)}$ be the set of second shortest routes that employ link j. More formally,

   $R_j^{(1)} = \{P_j | P_j$ is the first shortest route for a source-destination pair that employ link j $\}$, and

$R_j^{(2)} = \{P_j | P_j$ is the second shortest route for a source-destination pair that employ link j $\}$.

2. Let $R_{i,j}^{(1)}$ be the set of first shortest routes that have a subset of route from link i to j. Let $R_{i,j}^{(2)}$ be the set of second shortest routes that have a subset of route from link i to j.

3. Let $Pr(P_\alpha^1)$ and $Pr(P_\alpha^2)$ be the probability that a call for a source-destination pair α is set up on the first shortest path and the second shortest path, P_α^1, P_α^2, respectively.

In the FPLC, a call request is set up on the first shortest path if the number of free wavelengths on the second shortest path is less than the number of free wavelengths on the first shortest path. Otherwise, it is set up on the second shortest path assuming that the path has at least one free wavelengths. Therefore,

$$Pr(P_\alpha^1) = \sum_{i=1}^{F} Q_{P_\alpha^1}(i)(\sum_{n=0}^{i} Q_{P_\alpha^2}(n)), \tag{2.5}$$

$$Pr(P_\alpha^2) = \sum_{i=1}^{F} Q_{P_\alpha^2}(i)(\sum_{n=0}^{i-1} Q_{P_\alpha^1}(n)). \tag{2.6}$$

Recall that λ is the call arrival rate at each node. The arrival rate of calls that enter at link i and continue to link j, $\rho_c(i,j)$, becomes

$$\rho_c(i,j) = \sum_{P_j \in R_{i,j}^1} \lambda Pr(P_j) + \sum_{P_j \in R_{i,j}^2} \lambda Pr(P_j).) \tag{2.7}$$

The arrival rate of calls that leave from link i, $\rho_l(I)$, includes calls that use link I as the first or second route, but do not continue to link j. $\rho_l(i)$ is given by

$$\rho_l(i) = \sum_{P_i \in R_i^1} \lambda Pr(P_i) + \sum_{P_i \in R_i^2} \lambda Pr(P_i) - \rho_c(i,j). \tag{2.8}$$

The arrival rate of calls that enter at link j $\rho_e(j)$, includes calls that use link j as the first or the second route, but do not include calls that continue from link i to link j,

$$\rho_e(j) = \sum_{P_j \in R_j^1} \lambda Pr(P_j) + \sum_{P_j \in R_j^2} \lambda Pr(P_j) - \rho_c(i,j). \tag{2.9}$$

Given the arrival rate to each link, the blocking probability can be computed using Eqs. (2.3) and (2.4). Let L_a be the blocking probability for source-destination pair a,

$$L_a = Q_{P_a^1}(0) \times Q_{P_a^2}(0). \tag{2.10}$$

Let J be the number of links on a network. Let ϵ be a small positive number that is used as convergence criterion. The algorithm given below iteratively computes the approximate blocking probabilities for the traffic on all the routes.

1. Initialization. For each source-destination pair a let $\bar{L}_a = 0$. Choose $\rho_e(i)$, $\rho_c(i,j)$, and $\rho_l(i), i,j = 1,\ldots,J$ arbitrarily for all links.

2. Calculate $Q_P(w)$ for each source-destination pair using Eqs. (2.3) and (2.4);

3. Calculate the blocking probability $\bar{L}_a$ for all source-destination pair a using Eq. (2.10). If $\max_a |L_a - \bar{L}_a| < \epsilon$ then terminate. Otherwise let $\bar{L}_a = L_a$, go to next step .

4. Calculate ρ_e, ρ_l, and ρ_c for each link using Eqs. (2.7, 2.8, 2.9), then go back to step 2.

Since the arrival rate for each link can be computed individually, this method is suitable for analysis of irregular networks. With the assumption that the arrival rate is not dependent on the link status, the complexity of our method is significantly reduced. The method can also be extended to alternate routing approaches with small modifications of Eqs. 2.5 and 2.6.

2.2.2.2 Time Complexity of the Correlation Model

The computational time complexity of the analytical model can be analyzed as follows. Given call arrival rates, $\rho_l(i)$, $\rho_c(i,j)$, and $\rho_e(j)$, the conditional probability matrices, R, U, and S in Eq. (2.3) can be computed in $O(F^3)$ time units. Let H be the maximal number of links along a path over all possible paths, i.e., H is the diameter of the network. We know from Eqs. (2.3) and (2.4) that the time needed to compute

$Q_P(w_f)$ is $O(HF^4)$. Let N be the number of node in a network. The total source-destination pairs in such a network is $N*(N-1)$. Hence, step 2 in the algorithm can be finished in $O(N^2HF^5)$ time units. Given every element of Q obtained in step 2, the arrival rates of each link can be computed in $O(F^3)$ units. Therefore, the time complexity of the algorithm is dominated by the computation of the free wavelength distribution matrix, Q, which takes $O(N^2HF^5)$ time units in the worst case. In the implementation, multiple iterations are required to solve the Erlang fixed-point equation. We observed that most of the results shown in the next section are obtained in less than 10 iterations.

Note that the computational complexity mainly results from the link-load correlation model, which is the best model available so far in the literature in terms of accuracy while maintaining reasonable complexity. The reduced load model in [39] has also been extended to analyze the performance of the FPLC in the next subsection. The results show that the reduced load model is more complex and less accurate than the correlation model. We must also point out that the complexity of the analytical model does not affect the efficiency of the routing algorithms.

2.2.2.3 Reduced Load Model

The reduced load model proposed in [17, 39] is also extended to the FPLC in this section. We present the model here for comparison with the link load correlation model. The results are compared and discussed in the next section.

The arrival rate on each link for different link status is considered in the reduced load model. We assume that the inter-arrival time on link j be exponentially distributed with parameter $\alpha_j(m_j)$ when link j has m_j free wavelengths.

Let X_j be a random variable representing the number of wavelengths available on link j in a steady state. The idle capacity distribution on link j is denoted by

$$q_j(m_j) = Pr[X_j = m_j], m_j = 0, \ldots, F \ .$$

Following [39, 17, 12, 41], we also assume that X_j's are independent. Thus X_j can be viewed as a birth-and-death process. Using the result of [39], the idle capacity

distribution of X_j is given by

$$q_j(m_j) = \frac{F(F-1)\dots(F-m_j+1)}{\alpha_j(1)\alpha_j(2)\dots\alpha_j(m_j)} \tag{2.11}$$

where

$$q_j(0) = \left[1 + \sum_{m_j=1}^{F} \frac{F(F-1)\dots(F-m_j+1)}{\alpha_j(1)\alpha_j(2)\dots\alpha_j(m_j)}\right]^{-1}. \tag{2.12}$$

Let the link set of P_j be $\{j, j_1, j_2, \dots, j_{h(P_j)-1}\}$. Link numbers in the set are not in order. Let $p_i(.)$ be the probability that i wavelengths are available on route P_j given that each link has $m_j, m_{j_1}, \dots, m_{j_{h(P_j)-1}}$ free wavelengths, respectively. Then,

$$p_i(m_{j_1}, \dots, m_{j_n}) = \sum_{k=0}^{F} p_i(k, m_{j_n}) p_k(m_{j_1}, \dots, m_{j_{n-1}}) \tag{2.13}$$

where $p_i(x, y)$ is the probability that there are i free wavelengths on two-hop path on which each link has x and y wavelengths available, respectively. From [17], this conditional probability is

$$p_i(x,y) = \frac{\binom{x}{i}\binom{F-x}{y-i}}{\binom{F}{y}}.$$

Let $u_i(m_j; P_j)$ be the probability that there are i free wavelengths available on route P_j given that m_j wavelengths are idle on link j. $u_i(m_j; P_j)$ is given by

$$\begin{aligned} u_i(m_j; P_j) \;=\; & \sum_{m_{j_1}=i}^{F} \sum_{m_{j_2}=i}^{F} \dots \sum_{m_{j_{h(P_j)-1}}=i}^{F} q_{j_1}(m_{j_1}) q_{j_2}(m_{j_2}), \dots, q_{j_{h(P_j)-1}}(m_{j_{h(P_j)-1}}) \\ & \times p_i(m_j, m_{j_1}, m_{j_2}, \dots, m_{j_{h(P_j)-1}}). \end{aligned}$$

The probability that there are i wavelengths available on route P_j is given by

$$v_i(P_j) = \sum_{m_j=i}^{F} q_j(m_j) u_i(m_j; P_j).$$

Let $X_{P_j^1}$ be a random variable representing the number of idle wavelengths on route P_j^1. Let $X_{P_j^2}$ be a random variable representing the number of idle wavelengths on route

P_j^2. The inter-arrival time distribution parameter on link j, $\alpha_j(m_j)$, is given by

$$\begin{aligned}\alpha_j(m_j) &= \sum_{P_j^1 \in R_j^1} \lambda(\sum_{i=1}^{m_j} u_i(m_j; P_j^1) Pr[X_{P_j^2} \leq i]) \\ &+ \sum_{P_j^2 \in R_j^2} \lambda(\sum_{i=1}^{m_j} u_i(m_j; P_j^2) Pr[X_{P_j^1} < i]) \end{aligned} \tag{2.14}$$

where $Pr[X_{P_j^1} \leq i])$ denotes the probability that the number of idle wavelengths on route P_j^1 is less than or equal to i and it is given by

$$Pr[X_{P_j^1} \leq i] = 1 - \sum_{k=i+1}^{F} v_i(P_j^1).$$

The same relation gives

$$Pr[X_{P_j^2} < i] = 1 - \sum_{k=i}^{F} v_i(P_j^2).$$

In the formulation of Eq. (2.14), the first term is for selecting the first route from set R_j^1 that has i idle wavelengths and P_j^2 (the corresponding alternate path) has less than or equal to i free wavelengths; second term is for selecting the route from set R_j^2 where the corresponding alternate path has less than i free wavelengths.

The blocking probability L_a becomes

$$L_a = Pr[X_{P_a^1} = 0] Pr[X_{P_a^2} = 0] \tag{2.15}$$

where P_a^1 and P_a^2 denote the first and second shortest routes connecting the source-destination pair a.

Due to a circular relationship between $q_j(m_j)$ and $\alpha_j(m_j)$, it is not easy to compute L_a. Therefore we again fall back on an iterative algorithm to compute the approximate blocking probabilities.

1. Initialization. For all source-destination pair a let $\bar{L}_a = 0$. Choose $\alpha_j(.), j = 1, \ldots, J$ arbitrarily for all links.

2. Determine $q_j(.)$, $j = 1, \ldots, J$, using Eqs.(2.11) and (2.12).

3. Calculate $\alpha_j(.)$, $j = 1, \ldots, J$, using Eq. (2.14).

4. Calculate the blocking probability L_a for all source-destination pair a using Eq. (2.15). If $\max_a |L_a - \bar{L}_a| < \epsilon$ then terminate. Otherwise let $\bar{L}_a = L_a$, go to step 2.

2.2.3 Numerical Results and Discussion

The analytical methods of the previous sections are used here to calculate blocking probabilities. The physical network that is studied, a mesh-torus network with 16 nodes, is depicted in Figure 2.2 in which all adjacent nodes are connected by bi-directional links. The analytical results are then compared to blocking probabilities obtained by simulation.

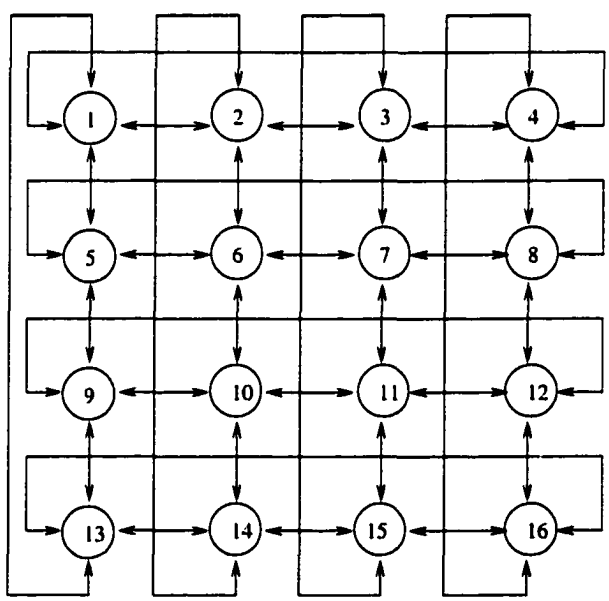

Figure 2.2 A mesh-torus network with 16 nodes

Two edge-disjoint shortest paths are required for each source-destination pair in the network. Different route selection methods will yield different network performance because some links maybe over-used and others maybe under-used if route selection is not symmetric. Since uniform traffic is employed and the arrival rate to all source-destination pairs is assumed to be identical, we try to distribute traffic evenly on each link by using x-y and y-x routing. In x-y and y-x routing, each node is denoted by

an integer pair (x, y). The rules to determine the first path and the second path for a connection setup request from (x_1, y_1) to (x_2, y_2) is as follows:

1. The first path first uses x-links connecting (x_1, y_1) to (x_2, y_1) and then uses y-links connecting (x_2, y_1) to (x_2, y_2).

2. The second path first uses y-links connecting (x_1, y_1) to (x_1, y_2) and then uses x-links connecting (x_1, y_2) to (x_2, y_2).

3. If two nodes are on the same row (or column), the shortest path on the row (or column) is selected as the first path. The second path is the shortest of the following two possible paths. If two possible paths have the same length, one of them is randomly selected as the second path.

   (a) The path in reverse direction of the first path, i.e., $(x_1, y_1) \rightarrow ((x_1 - 1) \bmod N, y_1) \rightarrow \ldots (x_2, y_2)$.

   (b) Go to the next column (or row) first, then go to the destination using shortest path, i.e., $(x_1, y_1) \rightarrow (x_1, (y_1 + 1) \bmod N) \rightarrow \ldots (x_2, y_2)$.

Figure 2.3 shows the network blocking probability versus the traffic load per source-destination pair for a given number of wavelengths on each link, $F = 4$ and $F = 8$. In this figure, curves are for analytical results and points are for simulation results. In the approximate analysis, iteration is required and the convergence criteria is set to be 10^{-6} for the blocking probabilities. Each data point in the simulations was obtained using 10^7 call arrivals. The same criterion is set for all the analysis and simulation results in this chapter. Note that for the same source-destination pair traffic load, if F is small then the traffic load per wavelength is heavy and vice-versa. From the figure, we observe that analytical results are in good agreement with simulation results for heavy to moderate traffic ($F = 4$) for both of the models. However, the blocking probabilities are slightly overestimated for light traffic ($F = 8$). The analytical results are not very accurate when traffic load is extremely light ($F = 8$ and source-destination pair traffic load ≤ 0.30). In any case, the link load correlation model always gives more accurate

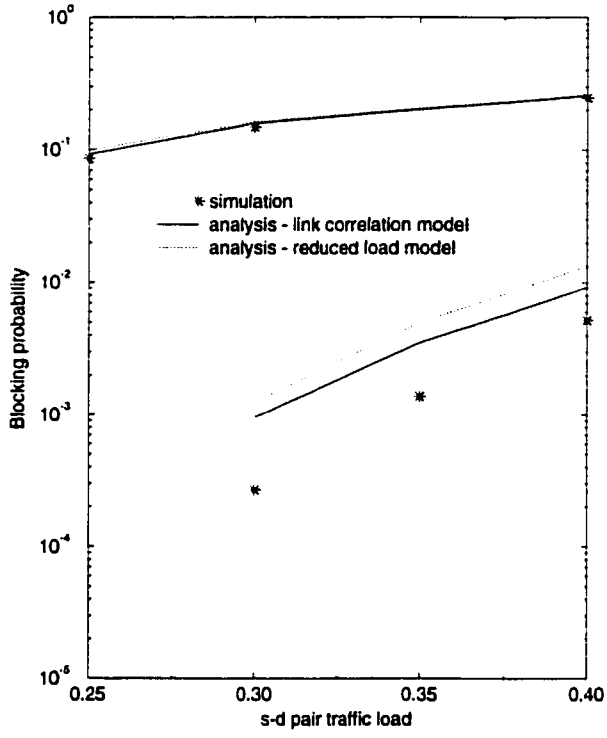

Figure 2.3 Blocking probability versus traffic load in a 4 × 4 mesh-torus network

results compared to the reduced load model. It is also faster to compute as the results can be obtained in a few minutes, while the reduced load model took several hours to analyze a 4 × 4 mesh-torus network on a sun Ultra-1 workstation. Therefore we use only the link correlation model in the following sections.

2.2.4 Performance Comparison

In this section, we compare three different routing methods based on our analytical models and simulation results. The 4 × 4 mesh-torus network topology depicted in Figure 2.2 is used. The following routing methods are employed for comparison purposes.

1. Shortest Path routing (SP): This method searches all the links on the shortest path. If there are any free wavelengths available on the path, one wavelength is

selected according to the specified wavelength assignment algorithm. A connection request is blocked if there is no idle wavelength available on the path.

2. Alternate Shortest Path routing (ASP): This method first tries to set up a connection request on the first shortest path. If there is no wavelength available on the the first shortest path, the request is overflowed to the second path. The request is blocked if it cannot be set up on either of the two paths.

3. Fixed-Paths Least-Congestion routing (FPLC): Two preselected shortest paths are searched in parallel and the path with the maximum number of free wavelengths is employed to set up the connection. If no wavelength is idle on the two paths, the request is blocked.

Figure 2.4, 2.5 and 2.6 show the performance results for the three different routing methods. We plot average link utilization, average wavelength utilization, and average blocking probability in these figures, respectively. The average link utilization shown in Figure 2.4 is computed using the following equation,

$$\overline{L_u}(j) = \sum_{w=0}^{F} (F - w) Q_j(w).$$

The average wavelength utilization illustrated in Figure 2.5 is defined as the ratio of the number of links that have w idle wavelengths to the total number of links in the network,

$$\overline{W_u}(w) = \frac{\sum_{j=1}^{J} Q_{P_j}(w)}{J}.$$

For Figure 2.4 and Figure 2.5, the corresponding traffic load for each source-destination pair is 0.3 and the number of wavelengths is $F = 8$. We observe from Figure 2.4 that the FPLC approach slightly increases the average link utilization compared to the ASP and the SP. The reason for this increase is that this algorithm does not use the shortest paths all the time. In the FPLC, longer paths are allowed to be used even when there are idle wavelengths on the shortest path. Another, and more important, reason is that more connection requests are accommodated by using the FPLC than the ASP and the

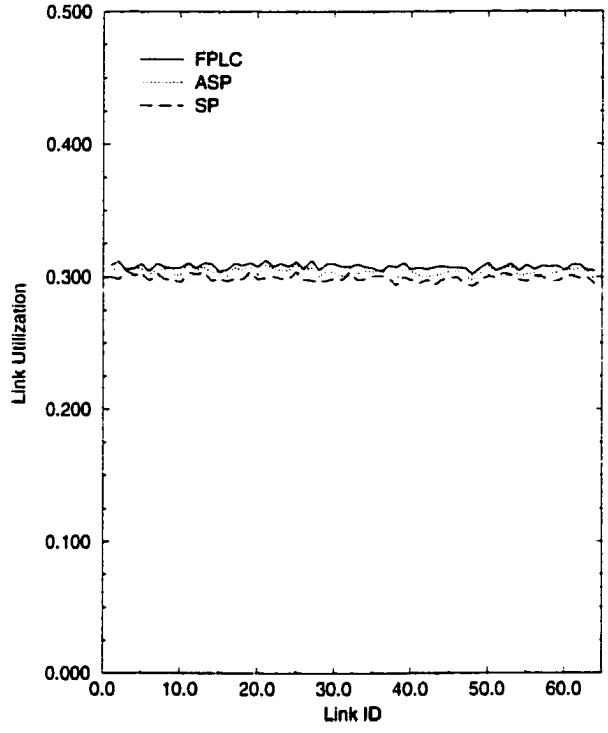

Figure 2.4 Average link utilization for different routing methods

SP as the blocking probability is small. This can be observed from Figure 2.6 (F=8) where the FPLC improves the blocking probability when the traffic load is low. As the traffic load increases, the performance of the FPLC gets closer to the ASP.

One of the reasons that the FPLC performs better than the ASP and the SP can be seen from Figure 2.5. The horizontal axis in the figure shows the number of busy wavelengths on a link. The vertical axis shows the probability that these many wavelengths on an average are busy. An ideal routing method should produce a curve with a sharp peak depicting better distribution of traffic load. Figure 2.5 shows that the FPLC tends to get a sharper peak compared to the ASP and the SP.

We also notice that in the FPLC, the network performance can be significantly improved by using the first-fit wavelengths assignment compared to the random wavelength assignment. Figure 2.7 shows the difference of the ASP and the FPLC using different

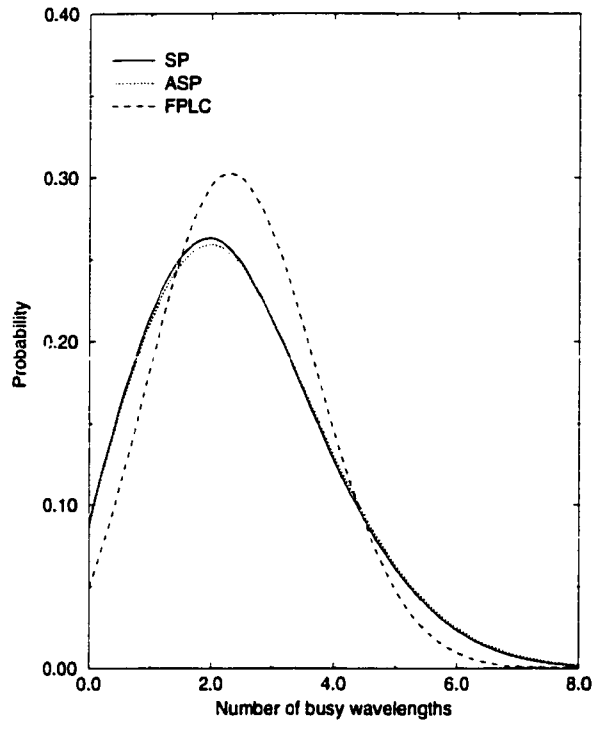

Figure 2.5 Average wavelength utilization for different routing methods

wavelength assignment methods through simulation. As reported in [12], the first-fit wavelength assignment strategy can slightly improve the blocking probability in the ASP. While using the FPLC, the first-fit wavelength assignment performs much better than the random strategy under light load condition. The reason can be explained intuitively as follows:

Compact wavelength assignment methods (i.e. most-used) perform better than spread wavelength assignments (i.e. least-used) as suggested in [18, 56]. In the FPLC, a request is set up on the least congested route. The wavelengths with lower index have more chances to be employed when compared to the ASP. Using the first-fit wavelength assignment, this compact wavelength assignment effect is enhanced. For example, two wavelengths (λ_1, and λ_2) are used on the first shortest path, λ_3 may be used to set up a request on the first shortest path for ASP. However, in the FPLC using first-fit wavelength assignment, λ_1 and λ_2 still have higher chance to be used to set up a request

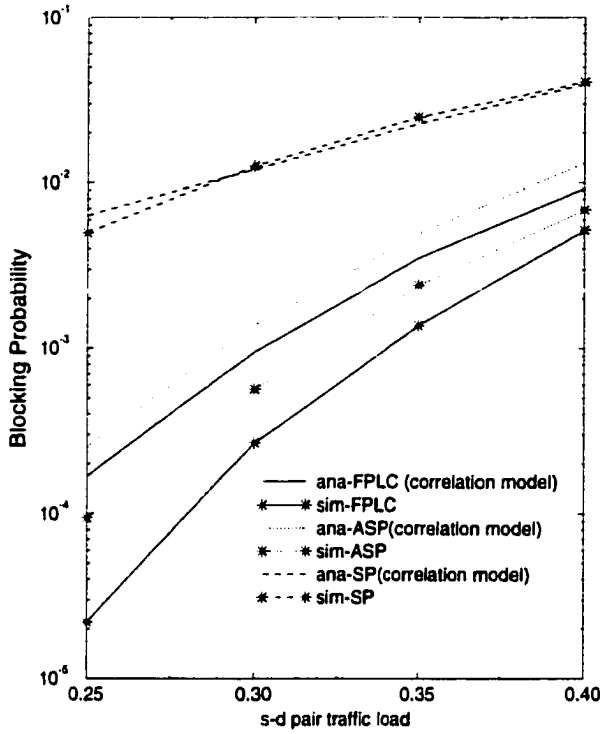

Figure 2.6 Performance comparison for three routing methods

on the second shortest path. This compact wavelength assignment effect leaves more free wavelengths in the network. Thus the performance is improved. In mesh-torus networks, it seems that the second shortest path for a source-destination pair may not be longer than the first shortest path. However, among the 240 first shortest paths in a 4×4 mesh-torus network, 64 of them are 1-hop long. The corresponding second shortest paths are 3-hop long. We also show in Section 2.4.1 that the FPLC achieves better performance than the SP and the ASP in the NFSNET T1 backbone in which the second shortest path could be 4-hop longer than the first shortest paths.

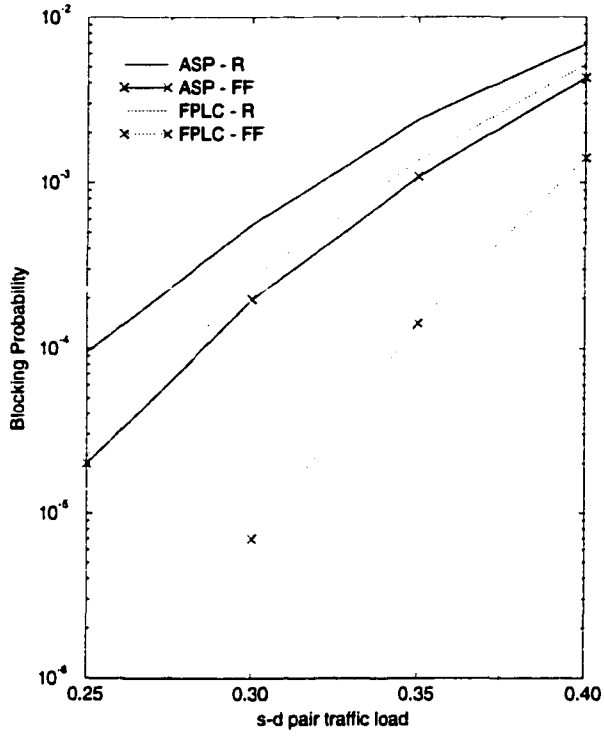

Figure 2.7 Performance comparison for the ASP and the FPLC using different wavelength assignment methods

2.3 Routing Using Neighborhood Information

We have seen in the previous section that the fixed-paths least-congestion routing method improves network performance compared to static routing approaches. However, problems still exist when using this dynamic routing method in a large network. Although we use a distributed parallel algorithm to overcome some of the problems, the main difficulties remaining are the control overhead, setup delay, and possible conflicts in wavelength usage when multiple paths are being set up simultaneously on one link. In this section, we propose a new routing algorithm using neighborhood information in which the setup efficiency and lower control overhead of static routing versus the low blocking probability trade-off is introduced. Using analytical and simulation methods,

it is shown that routing using neighborhood information can achieve good performance compared to static routing approaches which overcomes some of the difficulties. The possible conflicts in wavelength usage is also reduced by using this approach.

In the neighborhood-information-based routing, similar to the FPLC, a set of edge-disjoint shortest paths are statically computed and stored at each node. Upon the arrival of a connection request, the source node first decides on which route to set up the request. This route selection process is similar to that in the FPLC. However, instead of searching all the links on the preferred paths, only the neighborhood including the nodes up to distance k are searched and the results are compared to decide which route to select. There are two possibilities for collecting the neighborhood information: it can be either collected when needed or exchanged periodically. After a route is selected, the source node initiates a wavelength assignment process by sending a *needle packet* to the destination on the selected route. The intermediate nodes on the route first compute S_λ using the same equation as in the FPLC, increase the counters for the requested wavelengths, then forward the packet to the next node. One wavelength is selected at the destination node to set up the request using an appropriate wavelength assignment algorithm. A responding packet is sent back by the destination node to the source node. If no wavelength is available on the selected route, the connection request is blocked. The counters related with the request are decreased by one when a response packet is received by an intermediate node. This routing algorithm is called $FPLC - N(k)$.

2.3.1 The Routing Rules

To set up a connection request destined to node d, the source node s first collects and analyzes the neighborhood information on two edge-disjoint routes for the first k links only. This information is gathered by exchanging neighborhood information (periodically or on demand) with nodes up to distance k. The number of free wavelengths on the two paths up to distance k are compared and a path that has the maximum number of idle wavelengths is selected. The source node s then initiates a wavelength assignment process by sending a *needle packet* to the next node on the selected path. A set of

wavelengths, S_λ, which are available on the outgoing link, and the path information are included in the *needle packet.* If no common wavelength is free on any of the two routes up to distance k, the request is blocked.

Each intermediate node i computes $S_\lambda = S_\lambda \cap S_{available}$. If $S_\lambda \neq \phi$, it increases the requested wavelength counter and forwards the packet to the next node on the route. The counters are decreased when a response packet on the path is returned. If $S_\lambda = \phi$, the intermediate node responds to the source node with a nack-packet.

The destination node selects a wavelength from the set of available wavelengths according to the pre-specified wavelength assignment methods and assigns it to the request. It responds to the source node with an ack-packet and the selected wavelength.

2.3.2 Analysis of the FPLC-N(k)

We extend the approximate analytical models discussed in the previous section to the FPLC-N(k). We use the same terminologies as before.

Let $\hat{Q}^k_{P_j}(w)$ present the probability that there are w free wavelengths available on route P_j up to neighborhood distance k. $\hat{Q}^k_{P_j}(w)$ is given by

$$\hat{Q}^k_{P_j}(w) = \sum_{y_f=0}^{F} T^{(k)}_{P_j}(w, y_f).$$

Let $V^l_P(n_f, x_{pf})$ be the probability that n_f wavelengths are free on an l-hop path P, and x_{pf} wavelengths are free on the first link. Then,

$$V^l_P(n_f, x_{pf}) = \sum_{y_f=0}^{F} \sum_{z_c=0}^{\min(F-x_{pf}, F-y_f)} \sum_{x_{ff}=0}^{y_f} R(n_f | x_{pf}, z_c, x_{ff}) \\ U(z_c | y_f, x_{pf}) S(y_f | x_{pf}) V^{(l-1)}_P(x_{ff}, y_f) \ . \tag{2.16}$$

Considering the first k hops as the first hop, as we do in the previous section, $V^{(l-k)}(0, x_{pf})$ is the probability that x_{pf} wavelengths are available on the first k hops of an l-hop path, but none of the x_{pf} wavelengths is available on the following $l-k$ hops.

Let $\widehat{Pr}(P^1_\alpha)$ be the probability that a call for a source-destination pair α is set up on the first shortest path P^1_α, and $\widehat{Pr}(P^2_\alpha)$ be the probability that a request is set up on

the second shortest path P_α^2 using neighborhood information. In the FPLC-N(k), a call request is attempted to be set up on the path that has more free wavelengths on the first k links. The request is successfully set up if at least one wavelength is free on the first k links, and at least one of the free wavelengths can continue on the following links of the path. Therefore,

$$\widehat{Pr}(P_\alpha^1) = \sum_{i=1}^{F} \hat{Q}_{P_\alpha^1}^k(i)(\sum_{n=0}^{i} \hat{Q}_{P_\alpha^2}^k(n))(1 - V_{P_\alpha^1}^{(l-k)}(0,i)), \tag{2.17}$$

$$\widehat{Pr}(P_\alpha^2) = \sum_{i=1}^{F} \hat{Q}_{P_\alpha^2}^k(i)(\sum_{n=0}^{i-1} \hat{Q}_{P_\alpha^1}^k(n))(1 - V_{P_\alpha^2}^{(l-k)}(0,i)). \tag{2.18}$$

The arrival rate of calls that enter at link i and continue to link j becomes

$$\rho_c(i,j) = \sum_{P_j \in R_{i,j}^1} \lambda\widehat{Pr}(P_j) + \sum_{P_j \in R_{i,j}^2} \lambda\widehat{Pr}(P_j). \tag{2.19}$$

The arrival rate of calls that leave from link i becomes

$$\rho_l(i) = \sum_{P_i \in R_i^1} \lambda\widehat{Pr}(P_i) + \sum_{P_i \in R_i^2} \lambda\widehat{Pr}(P_i) - \rho_c(i,j). \tag{2.20}$$

The arrival rate of calls that enter at link j becomes

$$\rho_e(j) = \sum_{P_j \in R_j^1} \lambda\widehat{Pr}(P_j) + \sum_{P_j \in R_j^2} \lambda\widehat{Pr}(P_j) - \rho_c(i,j). \tag{2.21}$$

Blocking probability L_α for the FPLC-N(k) consists of three terms: (1) the probability that the first route is selected using neighborhood information (there are i free wavelengths on the first route up to neighborhood distance k and the corresponding alternate route has less than or equal to i idle wavelengths up to neighborhood distance k), but blocked at other links on the first route after distance k; (2) the probability that the second route is selected using neighborhood information (there are i free wavelengths on the second route up to neighborhood distance k and the corresponding alternate route has less than i idle wavelengths up to neighborhood distance k), but blocked at other links on the second route after distance k; and (3) the probability that no wavelength is available on any of the two routes up to distance k. Thus,

$$L_\alpha = \sum_{i=1}^{F} \hat{Q}_{P_\alpha^1}^k(i)(\sum_{n=0}^{i} \hat{Q}_{P_\alpha^2}^k(n)) V_{P_\alpha^1}^{(l-k)}(0,i)$$

$$+ \sum_{i=1}^{F} \widehat{Q}^{k}_{P^2_a}(i)(\sum_{n=0}^{i-1} \widehat{Q}^{k}_{P^1_a}(n))V^{(l-k)}_{P^2_a}(0,i)$$
$$+ \widehat{Q}^{k}_{P^1_a}(0)\widehat{Q}^{k}_{P^2_a}(0) \qquad (2.22)$$

Using the same algorithm given in Section 2.2.2, we can compute the blocking probabilities for the traffic on all the routes.

2.3.3 Numerical Results and Discussion

We assess the accuracy of our approximation in this section. The physical network, a 4×4 mesh-torus network depicted in Figure 2.2, is employed. The routes used for each source-destination pair are similar to those used in the FPLC as described in Section 2.2.

Figure 2.8 shows the blocking probability versus the traffic load for a given number of wavelengths on each link ($F = 8$) using the FPLC-N(1). The route to set up a connection request is determined by 1-neighborhood information. Similar to the original observation for the FPLC, we again notice that the analytical and the simulation results match when the traffic load is heavy to moderate, but analytical results are less accurate for light traffic.

The performance of the FPLC-N(k) with different values of k is compared using analytical results shown in Figure 2.9 (F=8). The diameter of our network topology is 4, so the FPLC-N(3) is the same routing method as the FPLC. Thus, the FPLC is the lower bound on the FPLC-N(k). It is observed from the figure that the blocking probability is not linearly decreasing with the increase of neighborhood distance. The difference of the blocking probabilities between $k = 0$ and $k = 1$ is much higher than the difference between $k = 1$ and $k = 2$ and the difference between $k = 2$ and $k = 3$ under light traffic conditions.

From Figure 2.7 we know that for the FPLC, the first-fit wavelength assignment method performs much better than random strategy under light traffic. The same is true for the FPLC-N(k) as shown by our simulation results depicted in Figure 2.10 (F=8).

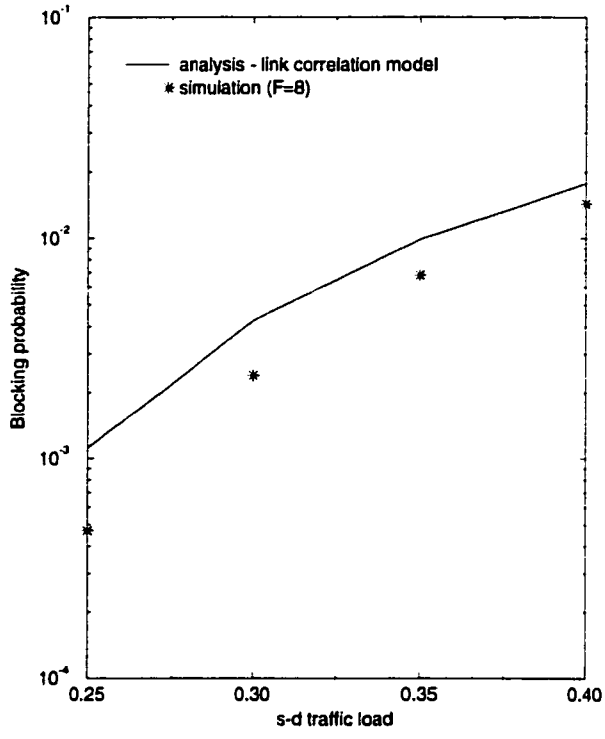

Figure 2.8 Blocking probability versus traffic load using the FPLC-N(1)

In comparison to the results of Figure 2.8, we note from Figure 2.10 that the blocking probability is significantly improved when the first-fit wavelength assignment is used. The FPLC-N(1) can achieve the performance similar to the ASP. Thus, we conclude that 1-neighborhood information is sufficient to ensure good network performance in terms of blocking probability in a 4×4 mesh-torus network.

2.4 Irregular and Large Scale Regular Networks

In this section, we investigate two other networks: the NSFNET T1 backbone network (irregular topology) depicted in Figure 2.11 and a 7×7 mesh-torus network (regular topology). We have shown in the previous section that the first-fit wavelength assignment method can achieve a better network performance than the random assignment strategy

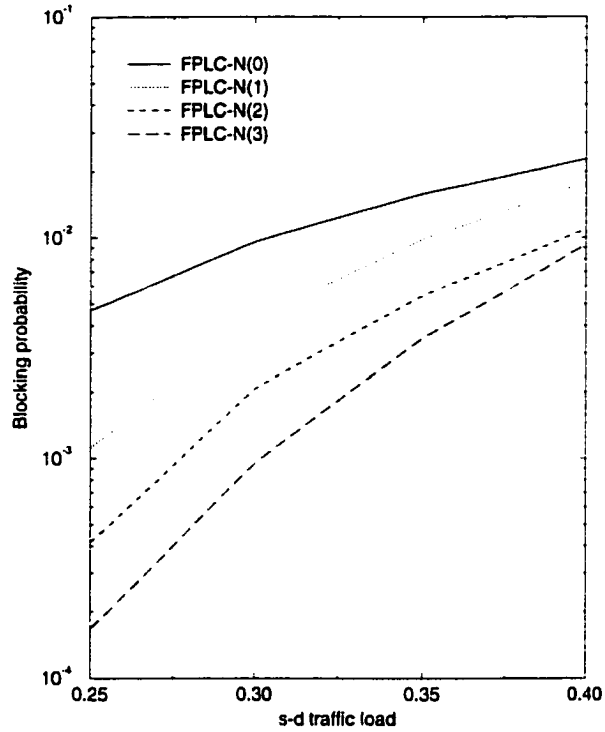

Figure 2.9 Performance comparison using different neighborhood information

in the FPLC and the FPLC-N(k), but the first-fit wavelength assignment method is more difficult to analyze. Therefore, we provide simulation results to support our conclusion that neighborhood-information-based routing is also efficient in these two networks.

2.4.1 The NSFNET

The analytical results using the link correlation model compared to simulation results are shown in Figure 2.12. We see from the figure that the link correlation model performs well on the NSFNET. The analytical results are accurate under heavy and moderate traffic load. It is not very accurate under light traffic. No analytical results using the reduced load model is shown because the reduced load model becomes too complex in terms of computing time for the NSFNET to get any meaningful results in a reasonable

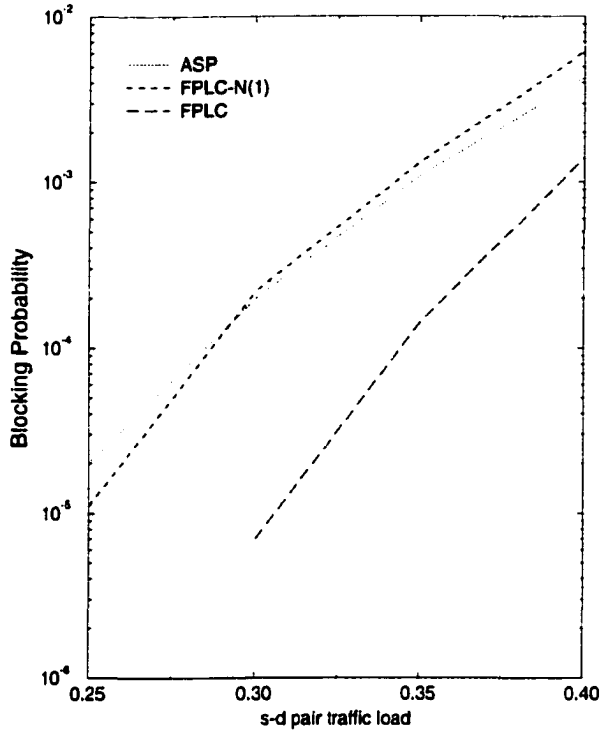

Figure 2.10 Performance comparison of the ASP, the FPLC-N(1) and the FPLC

time. Some routes in the NSF network are 5-hop long. The number of states dramatically increases with the number of hops on a route when the reduced load model is used. Therefore, the reduced load model becomes impractical for the NSFNET. However, the complexity required for each data point using the link correlation model is acceptable (within a few minutes), since no arrival rate for different link state is considered.

The simulation results for the NSFNET using the first-fit wavelength assignment are shown in Figures 2.13, 2.14, and 2.15. The corresponding source-destination pair traffic load is 0.2 for Figures 2.13 and 2.14. The number of wavelengths on each link, F, is 8. Figure 2.13 shows the average link utilization distribution. The horizontal axis in the figure shows link ID while the vertical axis shows the average link utilization. The difference of overall average network link utilization between the SP and the ASP is

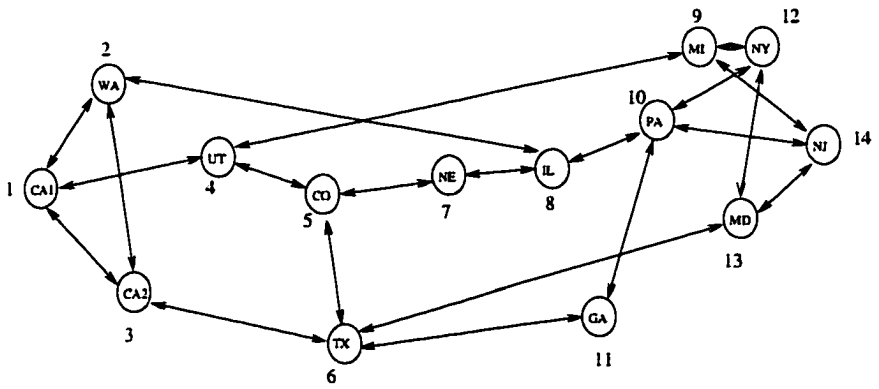

Figure 2.11 The NSFNET T1 backbone network

small. The reason is that under the light load condition, few of the connection requests are overflowed to the second shortest path. However, for the FPLC, the link utilization is much higher than that in the SP and the ASP. Also notice that the link utilization is not evenly distributed among all links. The minimum link utilization for the FPLC is 0.14 and the maximum is 0.37. These can be explained as follows:

In mesh-torus networks, the first shortest path and the second shortest path have the same length except when the two nodes are on the same row (or column). Therefore, employing the second shortest path does not increase the use of resources much. This is confirmed in Figure 2.4, which illustrates that average link utilization is only slightly increased by using the FPLC. However, in an irregular network, the second shortest path between a source-destination pair could be much longer than the first shortest path. For example, in Figure 2.11 there is a 1-hop path between node WA and IL, but the second shortest path is 5-hop long: $WA \rightarrow CA1 \rightarrow UT \rightarrow CO \rightarrow NE \rightarrow IL$, $WA \rightarrow CA2 \rightarrow TX \rightarrow CO \rightarrow NE \rightarrow IL$, or $WA \rightarrow CA2 \rightarrow TX \rightarrow GA \rightarrow PA \rightarrow IL$. Therefore, the FPLC is likely to use more network resources than the SP and the ASP. Another difficulty of using the FPLC routing algorithm in the NSFNET is that it is impossible to distribute traffic evenly among links as in a regular mesh-torus network by using x-y and y-x routing methods. Since uniform traffic is employed in our analytical and simulation model, each node generates connection requests to any other nodes with

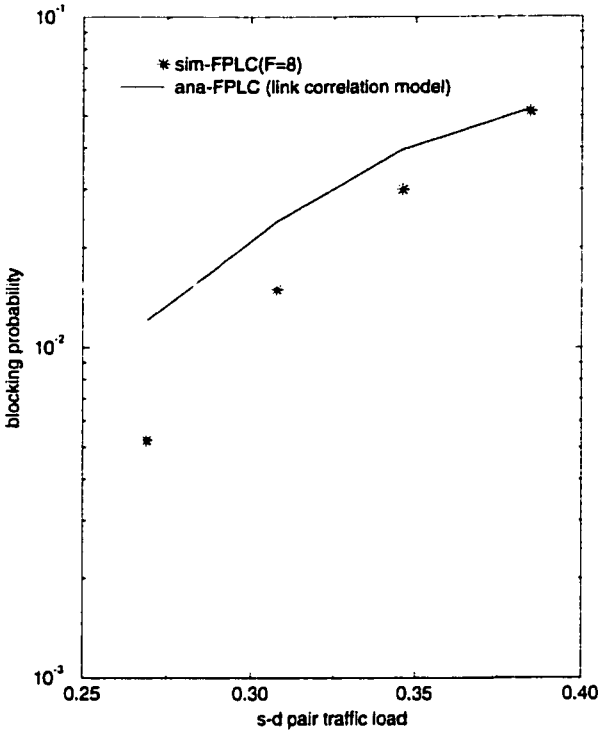

Figure 2.12 Blocking probability versus traffic load in the NSFNET

the same probability. Thus inevitably some links are over-used and the others are under-used. These can be observed from the results of Figure 2.13. The unbalanced traffic distribution also leads to higher blocking probability. However, the advantage of using the FPLC could be observed from Figure 2.14 which shows that the load distribution is better than that in the ASP and the SP.

The performance comparison in terms of average blocking probability versus traffic load for the ASP, the FPLC, the FPLC-N(1) and the FPLC-N(2) is shown in Figure 2.15. The performance of the FPLC is better than the ASP in the NSFNET when the traffic load is light and it gets closer to the ASP as the traffic load increases. Routing using neighborhood information does not perform as well in the NSFNET as it does in mesh-torus network. However, the performance of the FPLC-N(1), which employs 1-neighborhood information, is close to the ASP. By using 2-neighborhood information,

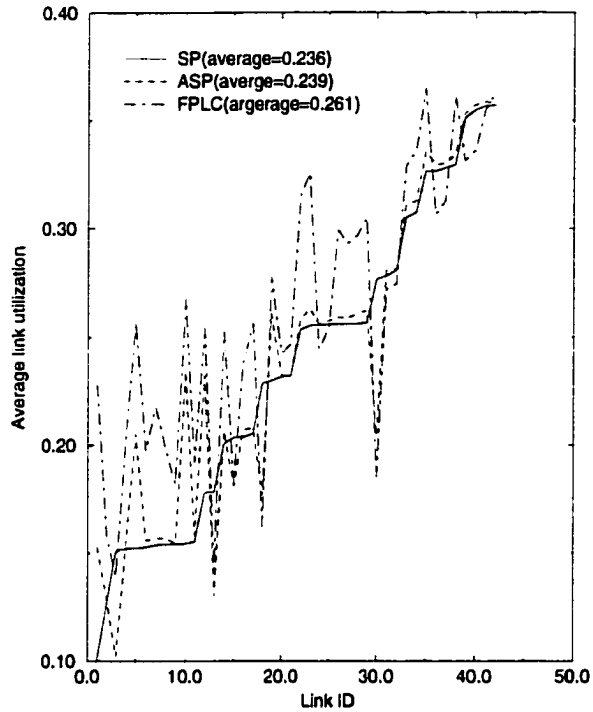

Figure 2.13 Average link utilization for different routing algorithms

the FPLC-N(2) can achieve similar performance to the ASP. Thus one can use the FPLC-N(1) or the FPLC-N(2) to achieve the similar performance as the ASP and keep the setup time and control overhead low.

The network performance could be further improved by using wavelength reservation, protection threshold, or limited trunk reservation methods proposed in [39, 12]. We, however, do not pursue them here.

2.4.2 A 7×7 Mesh-Torus Network

In this section, we present results for a 7×7 mesh-torus network using the first-fit wavelength assignment. The FPLC-N(k) is investigated and compared to the ASP and the FPLC using a simulation method. The results are shown in Figure 2.16.

We observe that the FPLC performs much better than the ASP when the traffic load is light. It soon converges to the ASP with the increasing load. Using 1-neighborhood

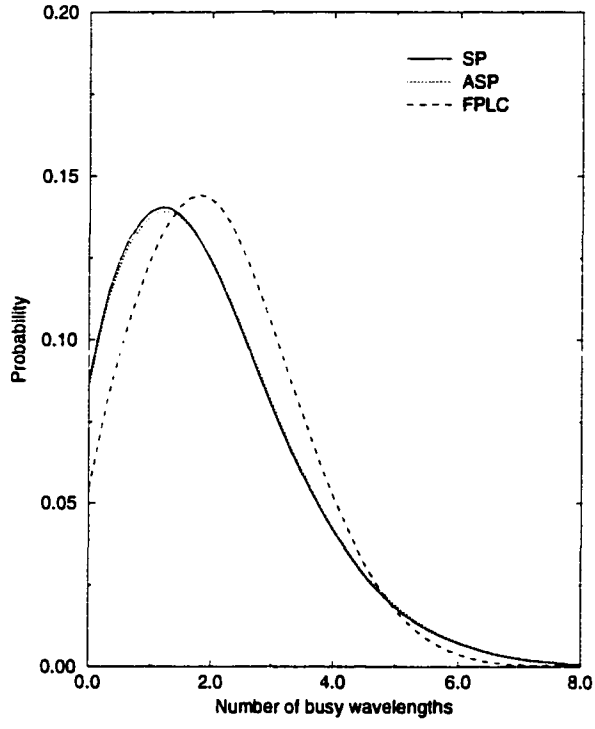

Figure 2.14 Average wavelength utilization for different routing algorithms

information gives a reasonable performance in a 7×7 mesh-torus network, but using 2-neighborhood information achieves performance similar to ASP.

2.5 Conclusions

In this chapter, we have proposed two new dynamic routing methods in all-optical wavelength-routed networks. Approximate analytical approaches are developed for the fixed-paths least-congestion routing and the routing using neighborhood information algorithms. Numerical results show that the fixed-paths least-congestion routing with the first-fit wavelength assignment method significantly improves network performance compared to the alternate paths routing algorithms. The reason is that more wavelengths are left free on a network when the FPLC with the first-fit wavelength assignment method is used.

The routing using neighborhood information algorithm is employed as a trade-off

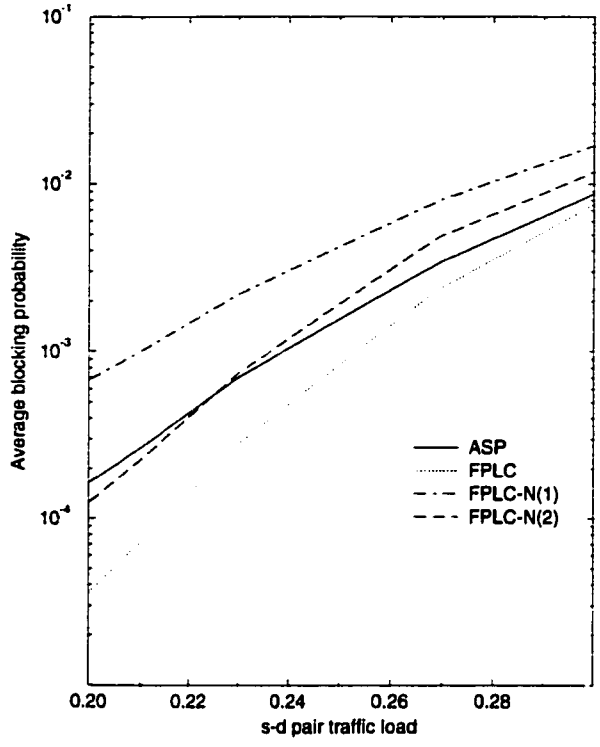

Figure 2.15 Blocking probability in the NSFNET

between network performance in terms of blocking probability versus setup delay and control overhead when using dynamic routing algorithms. It is shown that the routing using neighborhood information method achieves good performance when compared to static routing approaches. 1-neighborhood information is sufficient to ensure network performance in a 4×4 mesh-torus network and in the NSF T1 backbone network. 2-neighborhood information can achieve similar performance to that achievable with the alternate routing method in a 7×7 mesh-torus network.

We have shown results using the first-fit wavelength assignment and under uniform traffic only for different network topologies. The network performance using the FPLC and the neighborhood-information-based routing using other wavelength assignments under non-Poisson traffic [57] is an open problem for further research. The impacts of non-uniform traffic in irregular networks are also under investigation.

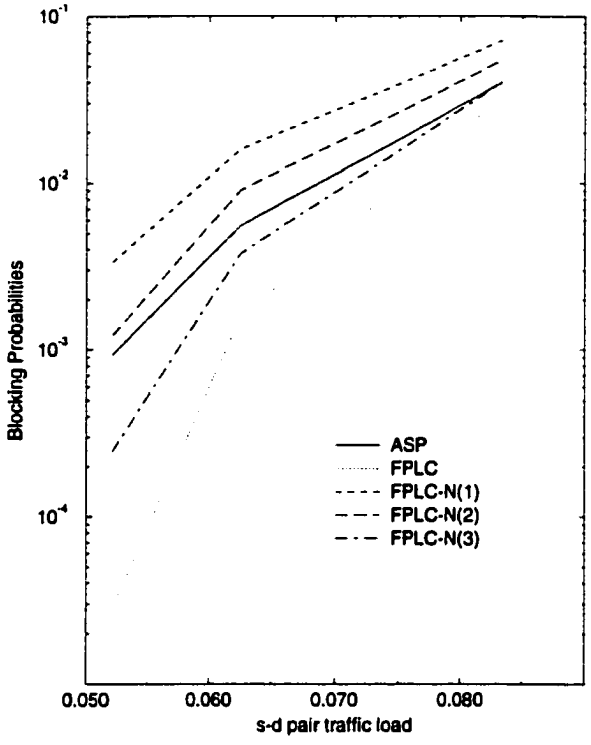

Figure 2.16 Blocking probability for various algorithms in a 7×7 mesh-torus network

3 EFFICIENT ALGORITHMS FOR WAVELENGTH CONVERTER PLACEMENT

3.1 Introduction

We presented two dynamic routing algorithms in the previous chapter to improve the network performance. The routing algorithms can be used in networks with or without wavelength conversion. In wavelength-routed all-optical networks, the wavelength continuity constraint, assigning the same wavelength to route a connection on every link on a path, is a well-known problem. To reduce the blocking probability, wavelength converters, which can change an incoming wavelength to another, are proposed to use [58]. The benefits of employing wavelength converters are discussed in [17, 47]. Since the cost of an all-optical wavelength converter is likely to remain high, sparse wavelength conversion and limited wavelength conversion are studied in [31, 32]. A network with only a few nodes having full conversion capability is called a network with sparse wavelength conversion. The results in [31] show placing converters on a fraction of nodes of a network is sufficient to ensure high network performance.

An interesting problem in sparse wavelength conversion networks is how to place a small number of converters so that the network performance is optimized. This problem has been studied in [33, 34, 35, 36]. A solution using dynamic programming was proposed to optimize the performance on a path, a bus network, and a ring network. However, the complexity of this solution is $O(N^2K)$ when the blocking probability of end to end calls is optimized on a path. Here N is the number of nodes on the path, and K is the number of converters being placed.

We present a new linear complexity algorithm to place converters on a path to minimize the blocking probability (maximize the success probability) in this chapter. Given the number of nodes, N, and the number of converters, K, the basic idea of our algorithm is that we divide the path into K+1 segments such that the blocking probability on each segment is equal. It is shown that the blocking probability is minimized if each segment has the same blocking probability. However, it is not always possible to divide a path into segments with equal blocking probabilities, due to the arbitrary values of the loads on each link. Three algorithms are proposed in this chapter to divide a path into segments such that each segment has approximately equal blocking probabilities. The results of using these algorithms are compared with the optimal solutions obtained by using dynamic programming method of [33].

This chapter is organized as follows. The end-to-end optimal converter placement is studied using a link-load independence model in Section 3.2. We first prove that the optimal placement is obtained if the blocking probability on each segment is equal. Three algorithms with linear complexities are proposed to obtain the segments with approximately equal blocking probabilities. An optimal converter placement algorithm is developed in Section 3.3 with the consideration of link-load correlation. An analytical approximation is proposed and shown that the segmentation algorithms are also applicable when the link-load correlation model is used. We make some concluding remarks in Section 3.4.

3.2 Converter Placement with End-to-End Performance Optimization

We consider a path of length N, as shown in Figure 3.1. Let the number of converters to be placed be K. Let the nodes along the path be numbered $0, 1, \ldots, N$, and let the link loads per wavelength on link i be $\rho_i, i = 0, \ldots, N-1$. We employ a binomial model [47] to compute the performance; that is, we assume that a wavelength on link i is occupied with probability ρ_i, and the occupancy is statistically independent of other

wavelengths on the same link and on other links. The converter placement for minimizing the blocking probability for end-to-end calls (from node 0 to node N) is considered in this section. A segmentation idea is introduced and proved that optimal placement can be obtained by dividing a path into K+1 segments such that each segment has equal blocking probability. Three implementation algorithms of this idea are also proposed in this section.

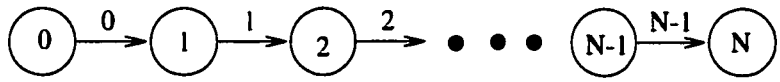

Figure 3.1 A path with N links

3.2.1 A Segmentation Method for Converter Placement on A Path

We define a *segment* to be the set of links between two consecutive converters. Thus K converters divide the N link path into $K+1$ segments. Let $V = (0, v_1, \ldots, v_K, N)$ be the converter placement vector denoting the first node, the converter locations, and the last node of the path. v_i is the node with the ith converter. The ith segment is from node v_{i-1} to node v_i (the first segment is from node 0 to node v_1, and the $K+1$ segment is from node v_K to node N). Without any loss of generality, we count converter locations from the left to the right. Let $L(v_{i-1}, v_i)$ be a set of links on segment i from node v_{i-1} to node v_i.

When the wavelength utilization on each link is assumed equal and the link-load correlation is neglected, intuition suggests that the optimal solution is to place converters uniformly (each segment has the equal length) on the path. This placement has been proved optimal in [33]. We consider a more general scenario in which link loads may non-uniformly distributed. We assume in this section that link loads are independent. The effect of link-load correlation is studied in the next section. Let F be the number of wavelengths on each link. Let $S(V)$ be the success probability of an end-to-end call

given the placement vector is V,

$$S(V) = \prod_{i=1}^{K+1} f_i \tag{3.1}$$

where f_i is the success probability on segment i and is given by

$$f_i = [1 - (1 - \prod_{j \in L(v_{i-1}, v_i)} \bar{\rho}_j)^F] \tag{3.2}$$

and $\bar{\rho}_j = 1 - \rho_j$, is the success probability on link j.

Since we assume that wavelength utilization may or may not uniformly distributed over links, p_i may or may not equal to p_j if $i \neq j$. Our goal is to select a placement vector V such that $S(V)$ is maximized. Instead of dividing the path into equal length segments as in [33], we divide the path such that the success probability on each segment is the same. We show that the placement obtained using this idea is optimal by proving the following results:

Lemma 1 *Let $Z = (z_1, z_2, \ldots, z_{K+1})$ be a vector of $K+1$ real numbers z_i, $-\infty \leq z_i \leq 0$, $i = 1, 2, \ldots, K+1$, the function*

$$G(Z) = \prod_{i=1}^{K+1} (1 - (1 - e^{z_i})^F) \quad \textit{given} \quad \sum_{i=1}^{K+1} z_i = \textit{constant}$$

is maximized if

$$z_1 = z_2 = \ldots = z_{K+1}.$$

The proof of this lemma is shown in the appendix.

Theorem 1 *An optimal placement for end-to-end performance is achieved if the success probability on each segment is equal on the path.*

Proof: Let Y_i be the success probability on one wavelength on segment i. Then,

$$Y_i = \prod_{j \in L(v_{i-1}, v_i)} \bar{\rho}_j. \tag{3.3}$$

It is ready to see that $0 \leq Y_i \leq 1$. Since $\bar{\rho}_j = 1 - \rho_j$ is known on every link, $\prod_{i=1}^{K+1} Y_i = \prod_{j=0}^{N-1} (\bar{\rho}_j)$ is a constant. $S(V)$ from Eqs. 3.1, 3.2 and 3.3 becomes

$$S(V) = \prod_{i=1}^{K+1} (1 - (1 - Y_i)^F). \tag{3.4}$$

The goal is to prove that $S(V)$ is maximized when $Y_1 = Y_2 = \ldots = Y_{K+1}$ given $\prod_{i=1}^{K+1} Y_i$ =constant. However, the global maximum value is hard to prove because the constraint of Y_i is not a convex set. We use the following substitution to convert the constraint to a convex set.

Let $Y_i = e^{z_i}, -\infty \leq z_i \leq 0$. Then $S(V)$ becomes

$$S(V) = \prod_{i=1}^{K+1} (1 - (1 - e^{z_i})^F) \tag{3.5}$$

From lemma 1 we know that the maximum value of $S(V)$ is obtained when $z_1 = z_2 = \ldots = z_{K+1}$, that is, $Y_1 = Y_2 = \ldots = Y_{K+1}$. ■

Theorem 1 provides insight into the converter placement problem and helps us solve the problem without computing the blocking probability for every s-d pair. Let the wavelength utilization on all the links (a set of positive real numbers between 0 and 1) be represented by an indexed set. The optimal solution is obtained by dividing the set into K+1 subsets such that each subset consists of consecutive elements in the set and the product of elements in each subset are all equal.

3.2.2 Implementation of the Segmentation Method

To divide an N link path into $K+1$ segments such that each segment has the equal success probability ($f_1 = f_2 = \ldots = f_{K+1}$) is not trivial. One of the difficulties is that the success probabilities on links, $\bar{\rho}, 0 \leq j \leq N-1$, may vary significantly. From Eq. 3.2, we know that

$$f_i = f_j \text{ if and only if } Y_i = Y_j \ .$$

A key observation here is that the geometric mean of the success probability on one wavelength on each segment can be easily obtained. To identify a segment, we compute the success probability on one wavelength of successive links and compare it with the geometric mean of the success probability. The success probabilities on all the segmentations are approximately equal if all of them are approximately equal to the geometric mean of the success probability.

Let M be the geometric mean of the success probability on each segment for one wavelength. Then,

$$M = \sqrt[K+1]{\prod_{i=1}^{K+1} Y_i} = \sqrt[K+1]{\prod_{j=0}^{N-1} \bar{\rho}_j} \ . \tag{3.6}$$

Recall that v_{i-1} is the placement of the $(i-1)$th converter. The next converter placement, v_i, is obtained by selecting consecutive links after node v_{i-1} on the path such that the product, $f_i' = \prod_{j \in L(v_{i-1}, v_i)} \bar{\rho}_j \simeq M$. It is possible that two consecutive nodes j and $j+1$ on the path satisfy the approximation requirement. Then v_i is to be chosen out of the two nodes. In the following we present three algorithms to make such a selection.

Algorithm LtoR: The first algorithm, called LtoR, computes the success probability of each segment from link 0 to link N-1 (left to right). If the success probability of a segment from link i to link j ($j > i$) is closer to M than that of the segment from link i to link $j+1$, a converter is placed at node j. Otherwise, a converter is placed at node $j+1$.

The following function, Get_next_placement() as shown in Table 3.1, computes the location for the next converter and the success probability for the current segment, Y', given that the last converter location *last* and the geometric mean M. We use the same function for all the three algorithms. The value of Y' may or may not be used by some of the algorithms.

The placement procedure continues until the last converter is placed or the end of the path is reached. A detailed description of this algorithm, LtoR, is given in Table 3.2.

Algorithm $LM_{recomputed}$: The problem of using the algorithm, LtoR, is that all the approximation errors in Y_i for different segmentation may accumulate. Thus the last segment may have a large variation from the desired value of M. To reduce the effect of the approximation errors, the second algorithm, called $LM_{recomputed}$, is introduced. In this algorithm, instead of using the same value of M computed at the beginning of the

Table 3.1 Function: Get_next_placement()

```
int Get_next_placement(int last, float M, float *Y')
var float Y''; int i;
begin
   *Y' = ρ̄_last;
   for( i = last+1; i < N; i++) begin
     Y'' = *Y' ρ̄_i;
     if(fabs(*Y' − M) < fabs(Y'' − M) )
       return i;
     else
       *Y' = Y''
   end;
end.
```

algorithm, we recompute M every time a converter is placed. The success probability in a segment is compared with the new M. This algorithm is described in Table 3.3.

Algorithm LorR: Both of the above algorithms compute the success probability Y_i and compare it with M from the left nodes to the right nodes on a path. The same method can also be applied by computing Y_i and comparing it with M from the right nodes to left nodes on the path. To reduce the approximation errors and make the best selection so that each segment has the success probability as close as possible, we combine the above ideas together into algorithm three, LorR. In this algorithm, we compute the success probabilities of segments from both side of a path. A segment, which has success probability closer to M is selected regardless of being on the left or on the right, and a converter is placed at the node of that location. By viewing the unselected links as a new path, M is recomputed. This algorithm is shown in Table 3.4.

Note that the actual locations of converters may vary but the overall blocking probability may still be the same if each segment has equal success probability on a path. To see this, consider a path with four nodes, n_0, n_1, n_2, n_3, and three links, l_0, l_1, l_2, with link loads $\rho_0 = \rho_1 = \rho_2$. A single converter can be placed at the node n_1 or n_2 to obtain the same blocking probability.

Table 3.2 From Left to Right

LtoR($\bar{\rho_i}, N, K$)
var int np = i = 0; float $M = \sqrt[K+1]{\prod_{j=0}^{N-1} \bar{\rho_j}}$, $Y' = 0$;
begin
  while((i < K+1) & (np < N)) *begin*
    /*Compute the next converter placement
    given the last placement is at node np. */
    np ← Get_next_placement(np, M, &Y');
    Place a converter at np;
    i++;
  end;
end.

In the next section we show the results of using the above three algorithms, and compare them with the optimal solutions under different wavelength utilization on each link. Note that the first algorithm is the simplest and the third is the most complex among the three algorithms. Each of these three algorithms has linear complexity.

3.2.3 Numerical Results and Discussions

The three algorithms discussed above are evaluated in this section to find the optimal placement on a 10-hop path (N=10) as shown in Figure 3.1. The number of wavelength (F) on each link is also assumed to be 10. Five different wavelength utilization patterns are used as shown in Table 3.5. Linear (**l**) utilization in the table represents the wavelength utilization increasing linearly from 0.05 on link 0 to 0.1 on link N-1. The utilization of m-linear (**ml**) increases from link 0 to the middle of the path and then decreases to link N-1 with different rate. The utilization pattern **e** represents that the wavelength utilization are exponentially distributed on each link with mean 0.1 and variance 0.1. The wavelength utilization of m_exponential (**me**) increase with rate of 2 from link 0 to the middle of the path and then decreases with rate of $\frac{1}{2}$ to link N-1, and **u** represents the random utilization uniformly distributed between 0.2 and 0.3 on each link.

Table 3.3 From Left to Right: recompute M

```
LM_recomputed(float ρ_i, int N, int K)
var int np = i = 0; float M = ^{K+1}√(∏_{j=0}^{N-1} ρ̄_j), Y' = 0;
begin
   while((i < K+1) & (np < N)) begin
      /*Compute the next converter placement
      given the last placement is at node np. */
      np ← Get_next_placement(np, M, &Y');
      Place a converter at np;
      /*recompute M*/
      M = ^{K-i}√(M^{K+1-i} / Y');
      i++;
   end;
end.
```

The results of using the three algorithms are shown in Table 3.6 with different utilization patterns. The dynamic programming method guarantees to yield the optimal results that are shown in the table for comparision. It is noticed that all the algorithms yield optimal solutions for $K = 1, 2, 3$ on the 10-hop path. The results of placing $K = 4$ converters are shown in the table. Since we consider sparse wavelength converter networks, $K > 4$ is not of interest. We see from the table that optimal solutions are obtained under most of the utilization patterns. Some of the placements of using the segmentation algorithms are different from the dynamic programming results (i.e., algorithm 2, algorithm 3 and the optimal algorithm give three different solutions under the m_exponential utilization). However, all of them are optimal since the blocking probabilities are equal. Recall that the optimal result may not be unique. Among the three segmentation algorithms, the third algorithm is the most accurate. As mentioned earlier, although this algorithm is a little more complex than the others, it still has linear complexity. Many other utilization patterns are also tested and they support our observations. The results are not shown here because of the space limitation.

We noticed that an optimal result might not be obtained using the segmentation algorithm when the link loads are dramatically different; that is, some link loads are

Table 3.4 From Left or Right: recompute M

1. Compute M of the path as $M = \sqrt[K+1]{\prod_{j=0}^{N-1} \bar{\rho}_j}$;
2. Compute f'_L and f'_R from left to right and from right to left, respectively, using the function Get_next_placement().
3. Set $Y' = \min($ fabs(f'_L -M), fabs(f'_R -M)), and place a converter on the corresponding node;
5. If there are links not being considered, the links are viewed as a new path; recompute M as $M = \sqrt[k']{\frac{M^{k'+1}}{Y'}}$, where k' is the number of converters have not been placed; goto step 2;
   Else, stop.

extremely high and other loads are extremely low. Under such utilization patterns, some links which have extremely light utilization, have little weight to the success probability ($\bar{\rho}_i > 0.9$) of a segment. Then the segmentation algorithms may incorrectly put such links in a segment. However, the blocking probability is affected very little by the lightly loaded links.

3.3 Converter Placement on A Path Considering Link-Load Correlation

In the previous section we considered the optimal converter placements to optimize the performance of the end-to-end calls. Two basic assumptions are made in order to deploy the binomial model: the call requests arrive at different wavelengths are statistically independent, and the link loads on a path are independent of each other. The wavelength independence is assumed to make the analysis simple. However, the second assumption may not be appropriate if the interfering traffic [47] arrives at each node, as is the case in a bus, a ring, or a path in an arbitrary topology network. A performance model considering link-load correlation was proposed in [47, 48]. In this section, we show that our segmentation algorithm is also applicable when the link-load correlation is considered, i.e., we assume that link loads are dependent.

Table 3.5 Wavelength utilization on a 10-hop path

links	l_1	l_2	l_3	l_4	l_5
linear(**l**)	0.050	0.056	0.061	0.067	0.072
m-linear(**ml**)	0.100	0.125	0.150	0.175	0.200
exponential(**e**)	0.086	0.150	0.024	0.083	0.037
m-exponential(**me**)	0.006	0.012	0.024	0.048	0.096
uniform(**u**)	0.221	0.211	0.239	0.221	0.234
links	l_6	l_7	l_8	l_9	l_10
linear(**l**)	0.078	0.083	0.089	0.094	0.100
m-linear(**ml**)	0.200	0.175	0.150	0.125	0.100
exponential(**e**)	0.261	0.257	0.044	0.178	0.101
m-exponential(**me**)	0.096	0.048	0.024	0.012	0.006
uniform(**u**)	0.203	0.204	0.232	0.208	0.218

Table 3.6 Converter placements and blocking probabilities for different algorithms compared to optimal solution

	l	*ml*	*e*	*me*	*u*
Alg. 1	3 5 7 9	3 5 7 9	3 6 7 9	4 5 6 8	2 4 6 8
	4.61e-08	5.81e-05	2.80e-5	2.44e-10	4.26e-04
Alg. 2	3 5 7 9	3 5 6 8	3 6 7 9	4 5 6 7	2 4 6 8
	4.61e-08	4.22e-05	2.80e-5	2.39e-10	4.26e-04
Alg. 3	3 5 7 9	3 5 6 8	2 5 6 8	3 4 5 6	2 4 6 8
	4.61e-08	4.22e-05	7.49e-6	2.39e-10	4.26e-04
Opt.	3 5 7 9	3 5 6 8	2 5 6 7	2 5 6 7	2 4 6 8
	4.61e-08	4.22e-05	7.49e-6	2.39e-10	4.26e-04

3.3.1 Segmentation Method Using the Link-Load Correlation Model

The assumption of the previous section, i.e., the success probabilities in disjoint segments are statistically independent, is still needed when link-load correlation is considered. With this assumption, the success probability of an end-to-end call, $S(V)$, can still be computed as

$$S(V) = \prod_{i=1}^{K+1} f_i \tag{3.7}$$

where f_i is the success probability on segment i.

For lack of space, we omit explaining of the details of the link-load correlation model

and ask the reader to refer to [47, 48] when necessary. Referring to Figure 3.1, we denote $P_n(i)$ be the probability that a new call enters the network at node i and uses link i on wavelength λ_1 given that λ_1 is not used by another call on link i. Let F be the number of wavelengths per fiber. Then the success probability on segment i, $f_i, (i \leq K+1)$, is given by

$$f_i = 1 - [1 - \bar{\rho}(v_{i-1}) \prod_{j \in L(v_{i-1}+1, v_i)} \bar{P}_n(k)]^F , \tag{3.8}$$

where $\bar{\rho}(i) = 1 - \rho(i)$ and $\bar{P}_n(i) = 1 - P_n(i)$.

Let Y_i be the success probability on one wavelength on segment i. Thus,

$$Y_i = \bar{\rho}(v_{i-1}) \prod_{j \in L(v_{i-1}+1, v_i)} \overline{P}_n(j) . \tag{3.9}$$

Our goal is to select a placement vector V to maximize $S(V)$ with

$$f_i = 1 - (1 - Y_i)^F . \tag{3.10}$$

We cannot apply Theorem 1 directly here because the product of Y_i is not a constant any more. Instead of having a set of positive numbers as in the link-load independence model, we have two sets of positive numbers, $\bar{\rho}(i)$ and $\bar{P}_n(i)$. For each segment, we need to select $\bar{\rho}(i)$ for the first link and $\bar{P}_n(i)$ for other links in each segment so that the product in each segment is approximately equal.

Note again that we are considering a sparse wavelength conversion network. The nodes, which have converters, are a small fraction of all nodes in the network. The success probability on segment i, Y_i defined in Eq. 3.9, usually include one $\bar{\rho}(i)$ and several $\bar{P}_n(i)$s. For a reasonable blocking probability of end-to-end calls, $\bar{\rho}(i)$, is not small. Therefore Y_i would be dominated by the product of $\bar{P}_n(i)$. Knowing these facts, we propose to use the following approximation:

Let X be the geometric mean of the ratios of $\bar{\rho}(i)$ to $\bar{P}_n(i)$; that is,

$$X = \sqrt[N]{\prod_{i=0}^{i=N-1} \frac{\bar{\rho}_i}{\bar{P}_n(i)}} .$$

X is a constant since both $\bar{\rho}_i$ and $\bar{P}_n(i)$ are known. Then $\bar{\rho}(i)$ can be approximately computed as

$$\bar{\rho}(i) \simeq \bar{P}_n(i) X$$

The product of $Y_i = \bar{\rho}(v_{i-1}) \prod_{j \in L(v_{i-1}+1, v_i)} \bar{P}_n(j)$ for all the segments is given as

$$\begin{aligned} \prod_{i=1}^{K+1} Y_i &= \prod_{i=1}^{K+1} (\bar{\rho}(v_{i-1}) \prod_{j \in L(v_{i-1}+1, v_i)} \bar{P}_n(j)) \\ &\simeq \prod_{i=1}^{K+1} (X \bar{P}_n(v_{i-1}) \prod_{j \in L(v_{i-1}+1, v_i)} \bar{P}_n(j)) \\ &= X^{K+1} \prod_{i=0}^{N-1} \bar{P}_n(i) \, . \end{aligned} \tag{3.11}$$

Since X is a constant and the product of $\bar{P}_n(i)$ is also a constant on a path, the product of Y_i becomes a constant too, and $0 < Y_i < 1$. This approximation is shown to be valid when we compare the results obtained using this approximation with the optimal results in the next section. Note from Eqs 3.7, 3.10 and 3.11 that Theorem 1 is applicable to this problem because $\prod_{i=1}^{i=K+1} Y_i$ in Eq. 3.11 is a constant. Thus an optimal placement with the consideration of link-load correlation can be achieved if the success probability of each segment is equal on the path.

Following the previous section, to identify a segment, we can compute the success probability on one wavelength of successive links and compare it with the geometric mean of the success probability of each segment. The geometric mean of Y_i, M, can be derived as

$$M = X \sqrt[K+1]{\prod_{i=0}^{i=N-1} \bar{P}_n(i)} \, . \tag{3.12}$$

By computing Y_i for each segment and comparing it with the target constant M, a path can be easily divided into $K+1$ segment. The first and second algorithms described in the previous section can also be applied here after a little modification: Eq. (3.12) is used instead of Eq. (3.6) to compute the geometric mean of the success probability on a segment. The function Get_next_placement(), used to compute the next converter location given the last converter is placed at node *last*, is replaced by a new function, Get_next_LtoR() shown in Table 3.7. In the new function, we compute the success probability using both ρ_i and $\bar{P}_n(i)$.

The third algorithm, selecting a segment from both left side and right side, cannot be applied directly because the first element of a segment success probability Y_i is $\bar{\rho}(i)$. It is

Table 3.7 Get next converter location from left to right considering link-load correlation

```
int Get_next_LtoR(int last, float M, float& Y')
var float Y''; int i;
begin
   Y' = ρ̄_last;
   for( i = last+1; i < N; i++) begin
    Y'' = Y' P̄_n(i);
    if(fabs(Y' − M) < fabs(Y'' − M) )
      return i;
    else
      Y' = Y''
    end;
end.
```

difficult to predict where the first element is if we compute Y_i from right to left. However, this problem can be solved by considering the product of $\bar{\rho}_{i-1}$ and $\bar{P}_n(i)$ together instead of $\bar{\rho}_i$ or $\bar{P}_n(i)$ individually, when we compute a converter location from right to left. If the temporary success probability Y' is not close to M, the segment is expanded to the next link, and Y' is computed as $Y' = \frac{Y'}{\bar{\rho}_i}\,\bar{\rho}_{i-1}\bar{P}_n(i)$. A new version of the function Get_next_placement is given in Table 3.8.

Table 3.8 Get next converter location from right to left considering link-load correlation

```
int Get_next_RtoL(int last, floatM, float& Y')
var float Y''; int i;
begin
   Y' = ρ̄_last;
   for( i = last; i > 0; i−−) begin
    Y'' = (Y'/ρ̄_i) ρ̄_{i−1} P̄_n(i) ;
    if(fabs(Y' − M) < fabs(Y'' − M) )
      return i;
    else
      Y' = Y''
    end;
end.
```

Table 3.9 From left or right considering link-load correlation

```
LorR_LLC(ρ̄, P̄_n, N, K)
var float f'_L=f'_R=0, Y' = 1, M = (K+1)√(X^K ∏_{i=0}^{i=N-1} P_n(i));
var int Lp=Rp = 0, path_begin = 0, path_end = N-1, i = 0;
begin    while( (i < K + 1) & (Lp < Rp)) begin
      M = √(M^{k'+1} / Y')
      Lp = Get_next_LtoR(path_begin, M, f'_L);
      Rp = Get_next_RtoL(path_end, M, f'_R);
      If ( fabs(f'_L - M) < f'_R - M)) begin
         /*f'_L is closer to M*/
         Place a converter at Lp;
         Y' = f'_L;
         path_begin = Lp;
         end;
      Else begin /*f'_R is closer to M*/
         Place a converter at Rp;
         Y' = f'_R;
         path_end = Rp;
         end;
      i++;
   end;
end.
```

The idea of selecting converter location from both sides can be used when link-load correlation is considered. A detailed description of the algorithm is shown in Table 3.9.

3.3.2 Numerical Results and Discussions

The converter placement for different traffic matrices considering link-load correlation is compared with optimal results using dynamic programming in this section. Similar to the previous section, we set N = 10, and F=10. The link loads as shown in Table 3.10 are computed from the traffic matrix $[\lambda_{sd}]$. The constant link load is achieved by setting $\rho_n(0) = \rho$, and $\rho_n(i) = \rho - \sum_{j=0}^{i-1} \frac{H-i}{H-j}\rho_n(i-1), i = 1, 2, \ldots, N-1$, and $\lambda_{ij} = \frac{\rho_n(i)}{H-i}$ for $j > i$ [33]. The second utilization pattern, m-linear, is obtained by setting $\lambda_{ij} = 0.01, i, j = 0, 1, \ldots, N$. The traffic matrix of the third utilization pattern is set to

Table 3.10 Wavelength utilizations computed from the traffic matrices

links	l_1	l_2	l_3	l_4	l_5
constant(**c**)	0.30	0.30	0.30	0.30	0.30
m-linear(**ml**)	0.10	0.12	0.24	0.28	0.30
nonuniform(**nu**)	0.12	0.19	0.24	0.27	0.28
uniform(**u**)	0.07	0.14	0.18	0.21	0.23
links	l_6	l_7	l_8	l_9	l_10
constant(**c**)	0.30	0.30	0.30	0.30	0.30
m-linear(**ml**)	0.30	0.28	0.24	0.12	0.10
nonuniform(**nu**)	0.28	0.27	0.24	0.19	0.12
uniform(**u**)	0.23	0.22	0.18	0.14	0.07

Table 3.11 Converter placements and blocking probabilities with the consideration of the link-load correlation

	nu_2	u_2	c_4	ml_4
Alg. 1	4 6	4 6	3 5 7 9	3 4 5 6
	2.88e-04	3.83e-06	1.71e-04	3.24e-05
Alg. 2	4 7	4 5	3 6 8 9	3 4 5 6
	3.52e-04	5.80e-06	1.63e-04	3.24e-05
Alg. 3	4 6	4 6	3 6 8 9	3 4 5 7
	2.88e-04	3.83e-06	1.63e-04	3.13e-05
Opt.	4 6	4 6	3 6 8 9	3 4 5 7
	2.88e-04	3.83e-06	1.63e-04	3.13e-05

$\lambda_{sd} = 0.04/|i-j|, i, j = 0, 1, \ldots, N$, which may be more practical in a path network. The last traffic matrix is randomly generated with uniform distribution U(0.005, 0.01).

The link loads are shown in Table 3.10. The corresponding converter locations and the blocking probabilities using the three algorithms are shown in Table 3.11. We observed from Table 3.11 that when the number of nodes with wavelength converters are small in a network and the link loads are not high for the reasonable blocking probability, the results obtained are same as that of using the dynamic programming method, which has the complexity of $O(N^2K)$.

A ring is a popular topology in optical networks. After placing a converter at a node

in a ring network, the ring can be divided into a path as in [33]. Our results show that the algorithms are also applicable to ring networks. The results are omitted for lack of space.

3.4 Conclusions

In this chapter, we considered the optimal converter placement problem for a given number of converters on a path topology. We first proposed and proved that optimal placement considering end-to-end calls are obtained when the segments on a path have equal success probability. The result in [33] showing that uniform placement of converters is optimal for the end-to-end performance when the link loads are uniform is a natural corollary included in this result. Then the theory was used to achieve optimal converter placement using both the link-load independence model and the link-load correlation model. Three implementation algorithms with linear complexity were introduced.

The results indicate that the optimal placement considering end-to-end calls can be obtained with linear complexity using the segmentation algorithm under different traffic patterns. Since a ring topology can be easily divided into a path [33], the algorithms can also be applied to ring networks.

4 MUTIFIBER WDM NETWORKS

4.1 Introduction

In the previous chapter, we introduced efficient algorithms to place wavelength converters in sparse wavelength conversion networks. However, as we mentioned in Chapter 1, the technologies of wavelength conversion have not been mature yet. The cost of an all-optical wavelength converter is likely to remain high in the near future. Multifiber WDM network is an alternative solution to conquer the wavelength continuity constraint [20, 59, 60]. In multifiber WDM networks, each link consists of multiple fibers, and each fiber carries information on multiple wavelengths. A wavelength that cannot continue on the next hop can be switched to another fiber using an optical cross-connect (OXC) if the same wavelength is free on one of the other fibers. Thus, multiple fibers in WDM networks have similar effect as the limited wavelength conversion.

There have been considerable interests to analyze the blocking performance of multifiber WDM networks. The independent wavelength load model in [47] is extended to multifiber networks in [21]. The results of this model are not numerically accurate for Poisson traffic because of the assumption that the load on one wavelength is independent of those on the other wavelengths on a link. The link load independence model proposed in [17] is extended to multifiber networks in [19]. However, this independent model is not accurate [19]. It overestimates the blocking performance for $F = 1$ and underestimates for $F > 1$ in a mesh-torus network. The blocking performance models for first-fit wavelength assignment in [16, 18] are also proposed to be applicable in multifiber networks. However, both of these models require intensive computation due to their iterative procedure to solve the Erlang fixed-point equation. Multifiber WDM net-

works have also been studied in [20, 59]. Much research has been done in the literature on WDM networks with limited wavelength conversion [61, 62, 63, 64]. Several analytical models have been proposed to analyze the blocking performance of such networks. A simple analytical model is developed in [32] for two-hop and multi-hop paths. An model to compute blocking probabilities for mesh-torus networks is presented in [63]. A more general model that can be used in any topology is proposed in [64]. However, this model can only be used in networks with small values of conversion degree, because of the approximation made in the model. Since link-load correlation is not considered, the analysis may not be accurate for sparse network topologies.

We study the effect of multiple fibers in circuit-switched all-optical WDM networks in this chapter. A new analytical model, a multifiber link-load correlation (MLLC) model, is proposed in Section 4.2 to compute the blocking performance in multifiber networks. To our knowledge, this is the first analytical model taking into account the link-load correlation in multifiber WDM networks. Comparing to the link independence model in [19], the MLLC model is an accurate and general model that is applicable to not only regular networks but also irregular networks. In Section 4.3 we show that our correlation model is accurate for a variety of network topologies by comparing the analytical results with the simulation results. We show, by using analytical and simulation models, that a limited number of fibers is sufficient to provide similar performance as that in full-wavelength-convertible networks. Our conclusions are presented in Section 4.4.

4.2 A Multifiber Link-Load Correlation Model

We propose a new analytical model to compute the blocking performance of multifiber WDM networks in this section. Our model is based on the Markov-chain (MC) model in [31], which is accurate and has modest computing complexity in single-fiber WDM networks. The MC model has been introduced in Chapter 2. Similar to the assumptions in the MC model, we assume Poisson input traffic with arrival rate λ at each node and exponentially distributed call holding time with mean $1/\mu$. A single path

is preselected for each source-destination (s-d) pair, and a wavelength assigned to a connection is randomly selected with uniform distribution from the set of free wavelengths on that path. We assume that F, the number of fibers/link, and W, the number of wavelengths/fiber, are the same on all links and fibers, respectively. We also assume that an incoming request on one channel can be switched to any output port using OXC as long as the output port has the same wavelength free regardless of which fiber it is on. If the wavelength is not free on all of the F fibers, the request is blocked on this wavelength. No wavelength converter is available at any node.

We define a Light Channel (LC) as a wavelength on a fiber on a link. A lightpath (LP) is a connection between a s-d pair using the same wavelength on all the links of a path. Note that a lightpath consists of several LCs on successive links. However, the LCs on a path may or may not be on the same fiber. Let a wavelength trunk (WT) λ_i be a collection of the LCs/LPs using λ_i on all the fibers. We define a WT "free" on a link if the wavelength is free on at least one of the fibers on the link. A WT is "busy" on the link otherwise. A WT is "free" on a path if that WT is free on all of the links constituting the path. A WT is "busy" on the path otherwise.

The blocking probability on a l-hop path can be computed recursively by viewing the first $l-1$ hops as the first hop and the lth hop as the second hop of a two-hop path [31, 17]. Thus we study a two-hop path first with F fibers on each hop and W wavelengths on each fiber as shown in Figure 4.1. Let $R_{WTLC}(\widehat{N}_{f_2}|\widehat{X}_{f_1}, z_{c_2}, y_{f_2})$ be the probability that $\widehat{N}_{f_2}$ WTs are free on a two-hop path given that $\widehat{X}_{f_1}$ WTs are free on the first hop of the path, y_{f_2} LCs are free on the second hop, and z_{c_2} LCs are busy on both of the link occupied by continuing calss from the first to the second hop[1]. Note that the recursive condition to compute the blocking performance of a multihop path is satisfied if we can find a closed-form expression of $R_{WTLC}(\widehat{N}_{f_2}|\widehat{X}_{f_1}, z_{c_2}, y_{f_2})$ [31]. The following notations are needed to obtain the blocking probabilities:

- Let w be the number of considered WTs on a link, $w \leq W$. w is used as a

[1]We put a hat on the variables for the number of WTs, to differentiate them from the variables for the number of LCs on a link, throughout this chapter.

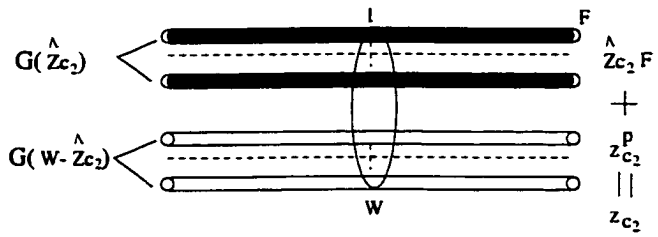

Figure 4.1 The W WTs are divided into two groups

subscript in the expressions of this chapter to indicate that the computation of the expressions is on w WTs.

- Let $z_{c_2}^p$ be the number of continuing calls on a two-hop path which occupy only part of a WT, i.e., do not use all the F LCs on any WT. In other words, no busy WT is occupied completely by $z_{c_2}^p$ calls.

- Let y_{b_2} be the number of busy LCs occupied by entering calls on the second link of the two-hop path. We know that $y_{b_2} = WF - y_{f_2} - z_{c_2}$.

4.2.1 Computation of $R_{WTLC}(\widehat{N}_{f_2}|\widehat{X}_{f_1}, z_{c_2}, y_{f_2})$

The difficulty in computing $R_{WTLC}(\widehat{N}_{f_2}|\widehat{X}_{f_1}, z_{c_2}, y_{f_2})$ results from the continuing calls from the first hop to the second hop. To simplify the computation, we divide the W WTs on the two-hop path into different groups. The conditional distribution of continuing calls is computed in each group. We first divide the W WTs on the two-hop path into two groups as shown in Figure 4.1. The first group, $G(\hat{Z}_{c_2})$, consists of $\hat{Z}_{c_2}$ busy WTs that are occupied completely by continuing calls on both of the links. The other $(W - \hat{Z}_{c_2})$ WTs belongs to the second group, $G(W - \hat{Z}_{c_2})$, which has $(z_{c_2} - \hat{Z}_{c_2}F)$ continuing calls but no busy WT is occupied completely by the continuing calls. $R_{WTLC}(\widehat{N}_{f_2}|\widehat{X}_{f_1}, z_{c_2}, y_{f_2})$ is given by

$$R_{WTLC}(\widehat{N}_{f_2}|\widehat{X}_{f_1}, z_{c_2}, y_{f_2}) = \sum_{\hat{Z}_{c_2}=0}^{\lfloor \frac{z_{c_2}}{F} \rfloor}$$

$$P_1(\hat{Z}_{c_2}|\widehat{X}_{f_1}, z_{c_2}, y_{f_2})_W P_2(\widehat{N}_{f_2}|\widehat{X}_{f_1}, z^p_{c_2}, y_{f_2})_{W-\hat{Z}_{c_2}}\ , \tag{4.1}$$

where $z^p_{c_2} = z_{c_2} - \hat{Z}_{c_2}F$. Here $P_1(\hat{Z}_{c_2}|\widehat{X}_{f_1}, z_{c_2}, y_{f_2})_{w=W}$ is the probability that $\hat{Z}_{c_2}$ busy WTs are occupied completely by continuing calls given that $\widehat{X}_{f_1}$ WTs are free on the first hop of the path, y_{f_2} LCs are free on the second hop, and z_{c_2} busy LCs continue from the first to the second hop. We assume here that the calls are arranged on the two links such that all possible LC configurations to reach the state $(\widehat{X}_{f_1}, z_{c_2}, y_{f_2})$ are equiprobable[2]. Thus we can distribute the z_{c_2} continuing calls to the two links first, then distribute the leaving and entering calls on the first and second link to reach the state $(\widehat{X}_{f_1}, z_{c_2}, y_{f_2})$. $P_1(\hat{Z}_{c_2}|\widehat{X}_{f_1}, z_{c_2}, y_{f_2})_{w=W}$ can be computed as

$$P_1(\hat{Z}_{c_2}|\widehat{X}_{f_1}, z_{c_2}, y_{f_2})_w = \begin{cases} 0 & \hat{Z}_{c_2} + \widehat{X}_{f_1} > W\ , \\ 0 & y_{f_2} + z_{c_2} > WF\ , \\ \dfrac{\binom{W}{\hat{Z}_{c_2}} f(z^p_{c_2}, w, F)}{\binom{wF}{z_{c_2}}} & otherwise\ , \end{cases} \tag{4.2}$$

where $z^p_{c_2} = z_{c_2} - \hat{Z}_{c_2}F$, and $f(z, w, F)$ is the number of ways of distributing z LCs to w WTs such that every WT is free. Note that each WT consists of F fibers. Suppose $j = \lfloor \frac{z}{F} \rfloor$. $f(z, w, F)$ is given by [19]

$$f(z, w, F) = \begin{cases} 0 & z > (F-1)w \\ \binom{wF}{z} & j = 0 \\ \binom{wF}{z} - \sum_{i=1}^{j} \binom{w}{i} f(z - iF, w - i, F) & otherwise. \end{cases} \tag{4.3}$$

[2]The arrival rates actually change with the state of the Markov chain because of blocking on other links of the network. However, modeling it in multifiber case would considerably complicate the model. We show later that the loss in accuracy due to our assumption is not significant.

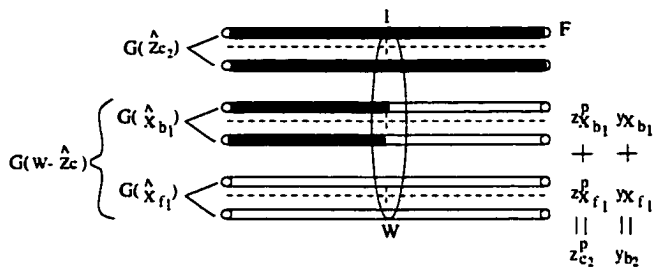

Figure 4.2 The WTs in the $G(W-\hat{Z}_{c_2})$ group are divided further into two groups

In Eq. (4.1), $P_2(\widehat{N}_{f_2}|\widehat{X}_{f_1}, z^p_{c_2}, y_{f_2})_{W-\hat{Z}_{c_2}}$ is the probability that $\widehat{N}_{f_2}$ WTs are free on a two-hop path with $w = W-\hat{Z}_{c_2}$ WTs, given that $\widehat{X}_{f_1}$ WTs are free on the first hop of the path, y_{f_2} LCs are free on the second hop, $z^p_{c_2}$ calls continue from the first to the second hop but no busy WT is occupied completely by these continuing calls. To compute $P_2(\widehat{N}_{f_2}|\widehat{X}_{f_1}, z^p_{c_2}, y_{f_2})_{W-\hat{Z}_{c_2}}$, we divide the second WT group further into $G(\widehat{X}_{b_1})$ group and $G(\widehat{X}_{f_1})$ group as shown in Figure 4.2. $G(\widehat{X}_{b_1})$ group consists of $\widehat{X}_{b_1} = W-\widehat{X}_{f_1}-\hat{Z}_{c_2}$ busy WTs on the first hop, occupied by continuing calls, or leaving calls, but no busy WT is occupied completely by continuing calls. The WTs in the $G(\widehat{X}_{f_1})$ group are free WTs on the first hop. The WTs in these two groups may or may not busy on the second hop. Recalling our definition of a "free" WT, some LCs may be set up on the WTs in $G(\widehat{X}_{f_1})$, but the number of busy LCs on a WT is less than F. Let $z^p_{X_{b_1}}$ be the number of continuing calls distributed in the $G(\widehat{X}_{b_1})$ group. Then the number of continuing calls distributed on the $G(\widehat{X}_{f_1})$ group is $z^p_{X_{f_1}} = z^p_{c_2} - z^p_{X_{b_1}}$. Recall that y_{b_2} is the busy LCs occupied by entering calls on the second link of the two-hop path. Let $y_{X_{b_1}}$ be the number of entering calls at the second link in the $G(\widehat{X}_{b_1})$ group, then the number of entering calls in the $G(\widehat{X}_{f_1})$ group is $y_{X_{f_1}} = y_{b_2} - y_{X_{b_1}}$. The probability $P_2(\widehat{N}_{f_2}|\widehat{X}_{f_1}, z^p_{c_2}, y_{f_2})_{w=W-\hat{Z}_{c_2}}$ in Eq. (4.1) is given by

$$P_2(\widehat{N}_{f_2}|\widehat{X}_{f_1}, z^p_{c_2}, y_{f_2})_{w=W-\hat{Z}_{c_2}} =$$

$$\sum_{z^p_{X_{b_1}}=0}^{z^p_{c_2}} \sum_{y_{X_{b_1}}=0}^{wF-z_{c_2}-y_{f_2}} P_4(y_{X_{b_1}}|z^p_{X_{b_1}}, z^p_{X_{f_1}}, y_{b_2}, \widehat{X}_{b_1}, \widehat{X}_{f_1})_w$$

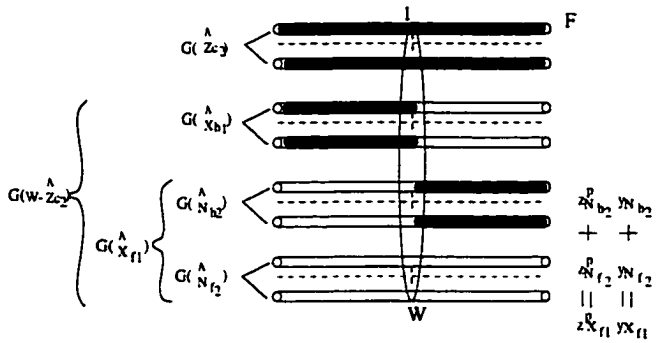

Figure 4.3 The WTs in the $G(\widehat{X}_{f_1})$ group are divided again into two groups

$$P_3(z^p_{X_{b_1}}|z^p_{c_2}, \widehat{X}_{b_1}, \widehat{X}_{f_1})_w P_5(\widehat{N}_{f_2}|\widehat{X}_{f_1}, z^p_{X_{f_1}}, y_{X_{f_1}})_{\widehat{X}_{f_1}}\ , \tag{4.4}$$

where $\widehat{X}_{b_1} = W - \widehat{X}_{f_1} - \hat{Z}_{c_2}$, $z^p_{X_{f_1}} = z^p_{c_2} - z^p_{X_{b_1}}$ and $y_{X_{f_1}} = y_{b_2} - y_{X_{b_1}}$. Here $P_3(z^p_{X_{b_1}}|z^p_{c_2}, \widehat{X}_{b_1}, \widehat{X}_{f_1})_w$ is the probability that $z^p_{X_{b_1}}$ continuing calls are in the subgroup $G(\widehat{X}_{b_1})$ given that $z^p_{c_2}$ calls are randomly distributed in the group $G(W - \hat{Z}_{c_2})$ and no busy WT is occupied completely by $z^p_{c_2}$ calls. $P_3(z^p_{X_{b_1}}|z^p_{c_2}, \widehat{X}_{b_1}, \widehat{X}_{f_1})_w$ is given by

$$P_3(z^p_{X_{b_1}}|z^p_{c_2}, \widehat{X}_{b_1}, \widehat{X}_{f_1})_w =$$

$$\frac{f(z^p_{X_{b_1}}, \widehat{X}_{b_1}, F) f(z^p_{X_{f_1}}, z^p_{c_2} - \widehat{X}_{b_1}, F)}{f(z^p_{c_2}, w, F)}\ . \tag{4.5}$$

$P_4(y_{X_{b_1}}|z^p_{X_{b_1}}, z^p_{X_{f_1}}, y_{b_2}, \widehat{X}_{b_1}, \widehat{X}_{f_1})_w$ in Eq. (4.4) is the probability that $y_{X_{b_1}}$ LCs are distributed in the subgroup $G(\widehat{X}_{b_1})$, given $z^p_{X_{b_1}}$, $z^p_{X_{f_1}}$, and y_{b_2} calls are distributed in group $G(\widehat{X}_{b_1})$, $G(\widehat{X}_{f_1})$, and $G(W - \hat{Z}_{c_2})$, respectively. Thus,

$$P_4(y_{X_{b_1}}|z^p_{X_{b_1}}, z^p_{X_{f_1}}, y_{b_2}, \widehat{X}_{b_1}, \widehat{X}_{f_1})_w =$$

$$\frac{\binom{\widehat{X}_{b_1} F - z^p_{X_{b_1}}}{y_{X_{b_1}}} \binom{\widehat{X}_{f_1} F - z^p_{X_{f_1}}}{y_{b_2} - y_{X_{b_1}}}}{\binom{wF - z^p_{X_{b_1}} - z^p_{X_{f_1}}}{y_{b_2}}}\ . \tag{4.6}$$

$P_5(\widehat{N}_{f_2}|\widehat{X}_{f_1}, z^p_{X_{f_1}}, y_{X_{f_1}})_{w=\widehat{X}_{f_1}}$ in Eq. (4.4) is the probability that $\widehat{N}_{f_2}$ WTs are free on the two-hop path with w WTs, given that all of the WTs are free on the first hop, $y_{X_{f_1}}$

LCs are free on the second hop, and $z^p_{X_{f_1}}$ calls continue from the first hop to the second hop. To compute $P_5(\widehat{N}_{f_2}|\widehat{X}_{f_1}, z^p_{X_{f_1}}, y_{X_{f_1}})_{w=\widehat{X}_{f_1}}$, we divide the $G(\widehat{X}_{f_1})$ group again into two groups. The group $G(\widehat{N}_{f_2})$ consists of $\widehat{N}_{f_2}$ WTs that are free on both of the first hop and the second hop. The other group, $G(\widehat{N}_{b_2})$, consists of $\widehat{N}_{b_2} = \widehat{X}_{f_1} - \widehat{N}_{f_2}$ WTs, which are free on the first hop but busy on the second hop as shown in Figure 4.3. Let $z^p_{N_{b_2}}$ be the number of continuing calls distributed in the group $G(\widehat{N}_{b_2})$. Then the number of continuing calls distributed in the group $G(\widehat{N}_{f_2})$ is $z^p_{N_{f_2}} = z^p_{X_{f_1}} - z^p_{N_{b_2}}$. Let $y_{N_{b_2}}$ be the number of entering calls distributed on the $\widehat{N}_{b_2}$ WTs. The number of entering calls distributed on the $\widehat{N}_{f_2}$ WTs is $y_{N_{f_2}} = y_{X_{f_1}} - y_{N_{b_2}}$. $P_5(\widehat{N}_{f_2}|\widehat{X}_{f_1}, z^p_{X_{f_1}}, y_{X_{f_1}})_w$ is derived as

$$P_5(\widehat{N}_{f_2}|\widehat{X}_{f_1}, z^p_{X_{f_1}}, y_{X_{f_1}})_w = \sum_{z^p_{N_{b_2}}=0}^{z^p_{X_{f_1}}}$$

$$\frac{\binom{\widehat{X}_{f_1}}{\widehat{N}_{f_2}} f(z^p_{N_{b_2}}, \widehat{N}_{b_2}, F) g(\widehat{N}_{f_2}, z^p_{X_{f_1}} - z^p_{N_{b_2}}, y_{X_{f_1}} - y_{N_{b_2}})}{f(z^p_{X_{f_1}}, \widehat{X}_{f_1}, F) \binom{\widehat{X}_{f_1} F - z^p_{X_{f_1}}}{y_{X_{f_1}}}}.$$

where $g(\widehat{N}_{f_2}, z^p_{N_{f_2}}, y_{N_{f_2}})$ is the number of ways to distribute $z^p_{N_{f_2}}$ continuing calls and $y_{N_{f_2}}$ entering calls to $\widehat{N}_{f_2}$ WTs such that every WT is free. $g(\widehat{N}_{f_2}, z^p_{N_{f_2}}, y_{N_{f_2}})$ is given by

$$g(\widehat{N}, z, y) = \binom{\widehat{N}F}{z} \binom{\widehat{N}F - z}{y} - \sum_{i=1}^{\lfloor \frac{z+y}{F} \rfloor} \sum_{j=0}^{min(iF, z)}$$

$$\times \binom{\widehat{N}}{i} \binom{iF}{j} g(\widehat{N} - i, z - j, y - (iF - j)).$$

A closed-form expression of $R_{WTLC}(\widehat{N}_{f_2}|\widehat{X}_{f_1}, y_{f_2}, z_{c_2})$ is obtained as

$$R_{WTLC}(\widehat{N}_{f_2}|\widehat{X}_{f_1}, y_{f_2}, z_{c_2}) =$$

$$\sum_{\widehat{Z}_{c_2}=0}^{\lfloor \frac{z_{c_2}}{F} \rfloor} \sum_{z^p_{X_{b_1}}=0}^{z_{c_2} - \widehat{Z}_{c_2} F} \sum_{y_{X_{b_1}}=0}^{(W - \widehat{Z}_{c_2})F - z_{c_2} - y_{f_2}}$$

$$P_1(\widehat{Z}_{c_2}|\widehat{X}_{f_1}, z_{c_2}, y_{f_2}) P_3(z^p_{X_{b_1}}|z^p_{c_2}, \widehat{X}_{b_1}, \widehat{X}_{f_1})$$

$$P_4(y_{X_{b_1}}|z^p_{X_{b_1}}, z^p_{X_{f_1}}, y_{b_2}, \widehat{X}_{b_1}, \widehat{X}_{f_1})$$

$$P_5(\widehat{N}_{f_2}|\widehat{X}_{f_1}, z^p_{X_{f_1}}, y_{X_{f_1}}) \tag{4.7}$$

4.2.2 Computation of Average Blocking Probability

Let $P_6^{(l)}(\widehat{N}_{f_l}, y_{f_l})$ be the probability that $\widehat{N}_{f_l}$ wavelengths are free on an l-hop path and y_{f_l} LCs are free on hop l. We continue to assume that the load on the lth hop is dependant only on the load on the $(l-1)$-hop. By viewing the first $l-1$ hops as the first hop and the lth hop as the second hop of a two-hop path, we can compute the blocking probability on the l-hop path using the results for a two-hop path in Eq. (4.7).

$$\begin{aligned} P_6^{(l)}(\widehat{N}_{f_l}, y_{f_l}) = \sum_{x_{f_{l-1}}=0}^{FW} \sum_{z_{c_l}=0}^{\min(FW-x_{f_{l-1}}, FW-y_{f_l})} \sum_{\widehat{N}_{f_{l-1}}=0}^{\lfloor \frac{x_{f_{l-1}}}{F} \rfloor} \\ R_{WTLC}(\widehat{N}_{f_l}|\widehat{N}_{f_{l-1}}, z_{c_l}, y_{f_l}) U(z_{c_l}|y_{f_l}, x_{f_{l-1}}) \\ S(y_{f_l}|x_{f_{l-1}}) P_6^{(l-1)}(\widehat{N}_{f_{l-1}}, x_{f_{l-1}}) \quad l > 1 \,. \end{aligned} \tag{4.8}$$

where $U(z_{c_2}|x_{f_1}, y_{f_2})$ is the probability that z_{c_2} LCs are occupied by continuing calls from the first link to the second link given that x_{f_1} LCs are free on the first link, and y_{f_2} LCs are free on the second link; and $S(y_{f_2}|x_{f_1})$ is the probability that y_{f_2} LCs are free on the second link of a path given that x_{f_1} LCs are free on the first link of the path. The conditional probabilities, $U(z_{c_2}|x_{f_1}, y_{f_2})$ and $S(y_{f_2}|x_{f_1})$, can be obtained using Eqs. 2.1 and 2.2, respectively. The probability that $\widehat{N}_{f_2}$ wavelengths and y_{f_1} LCs are free on the first link of a path is $P_6^{(1)}(\widehat{N}_{f_1}, y_{f_1}) = P_1(\widehat{N}_{f_1}|0, 0, FW - y_{f_1})_W$.

4.2.3 Computation of the Parameters

Let P_j^α be a route between a s-d pair α using link j, $P_{i,j}^\alpha$ as a route continuing from link i to link j. Let R_i be a set of fixed routes for calls that use link i, and $R_{i,j}^c$ be the set of fixed routes for calls that continue from link i to link j. Let λ_i^e, λ_j^l, and $\lambda_{i,j}^c$ be the arrival rates of calls entering at link i, leaving link j, and continuing from link i to link j, respectively. λ_i^e, λ_j^l, and λ_{ij}^c are given by

$$\lambda_{i,j}^c = \sum_{P_{i,j}^\alpha \in R_{i,j}^c} \lambda_\alpha \,, \tag{4.9}$$

$$\lambda_i^l = \sum_{P_i^\alpha \in R_i} \lambda_\alpha - \lambda_{i,j}^c \,, \tag{4.10}$$

$$\lambda_j^c = \sum_{P_j^\alpha \in R_j} \lambda_\alpha - \lambda_{i,j}^c \,, \tag{4.11}$$

These arrival rates are used to compute the steady-state probability $U(z_{c_2}|x_{f_1}, y_{f_2})$ and $S(y_{f_2}|x_{f_1})$ defined in Eqs. 2.1 and 2.2 in Chapter 2, respectively. Let $l(\alpha)$ be the length of a path between a s-d pair α. Let R be the number of s-d pairs in the network, and P_B be the network-wide average blocking probability. P_B is given by

$$P_B = \sum_{\alpha} \sum_{y_f=0}^{FW} P_6^{l(\alpha)}(0, y_f)/R. \tag{4.12}$$

4.2.4 Implementation and Complexity Analysis

The above equations shows an approach on how to compute the steady-state probability of a path that has i free wavelength trunks. The performance analyses of different routing algorithms in the next section are based on these equations. Comparing to the link-load correlation model for single fiber networks [31], the MLLC model has the same computational complexity except for the computation of the free WT distribution on a two-hop path, $R_{WTLC}(\widehat{N}_{f_2}|\widehat{X}_{f_1}, y_{f_2}, z_{c_2})$. However, $R_{WTLC}(\widehat{N}_{f_2}|\widehat{X}_{f_1}, y_{f_2}, z_{c_2})$ does not depend on any network topology and traffic arrival rate. The only parameters needed to compute $R_{WTLC}(\widehat{N}_{f_2}|\widehat{X}_{f_1}, y_{f_2}, z_{c_2})$ is the number of fibers per link, F, and the number of wavelengths per fiber, W. Thus $R_{WTLC}(\widehat{N}_{f_2}|\widehat{X}_{f_1}, y_{f_2}, z_{c_2})$ can be computed offline. The results can be used repeatedly in different topologies and traffic patterns, as long as they have the same number of fibers per link and wavelengths per fiber.

We present a new analytical model that can be used for both regular and irregular multifiber WDM networks in this section. In the next section, we evaluate the call blocking performance for three different topologies.

4.3 Numerical Results and Analysis

In this section, we assess the accuracy of the MLLC model by comparing it with the simulation results. We also compare the MLLC model with the multifiber independence

model presented in [19] and show that the MLLC model yields closer solutions to the simulation results than the independence model. The MLLC model is applied to two regular topologies, the ring and the mesh-torus networks, and an irregular NSF T1 backbone network (NSFnet) [15]. We are interested in finding the effect of multifibers on these networks. The question we attempted to answer is how many fibers are required to provide similar performance as that in a full-wavelength-convertible network.

In the networks we studied, the link capacity is fixed at 24 light channels, i.e., $FW = 24$ on each link. We vary the number of fibers on each link, F, from $1, 2, 3, 4, 6, 8, 12$ to 24, and the number of wavelengths on each fiber is varied by $W = 24/F$ accordingly. We assume Poisson traffic arrives at each node, and the destination for an arrival request is uniformly distributed among other nodes[3]. We adjust the traffic load such that the blocking probabilities are around 10^{-3}. Each data point in the simulations was obtained using 10^6 call arrivals.

We first study a 10-node unidirectional ring network in which the gain of using wavelength converters is limited. The call blocking probability against the number of fibers per link is plotted in Figure 4.4. The traffic load is 2 Erlangs per node. Wavelength converters are useful to reduce the blocking probability in the mesh-torus networks. A 5×5 mesh-torus network with node traffic of 17 Erlangs is studied. The results are shown in Figure 4.5. Analytical and simulation results are plotted for different fiber-wavelength pair configurations. The close match between the analytical and simulation results and the fact that the analytical results follow the trend of the simulation results indicate that the model is adequate in analytically predicting the performance in ring and mesh-torus topologies. For comparison, we also plot the analytical results obtained from the independence model in [19]. It is seen that the independence model severely overestimated the blocking probability when the number of fibers per link, F, is small, and underestimated the blocking when F is larger. We observed that 6 fibers per link in the ring and 4 fibers per link in the mesh-torus, are sufficient to provide similar per-

[3]The MLLC model could also be used for non-uniformly distributed traffic using Eqs. (4.9), 4.10) and (4.11). The uniform distribution assumption is made only for simplicity. Note that link loads in NSFnet are non-uniformly distributed.

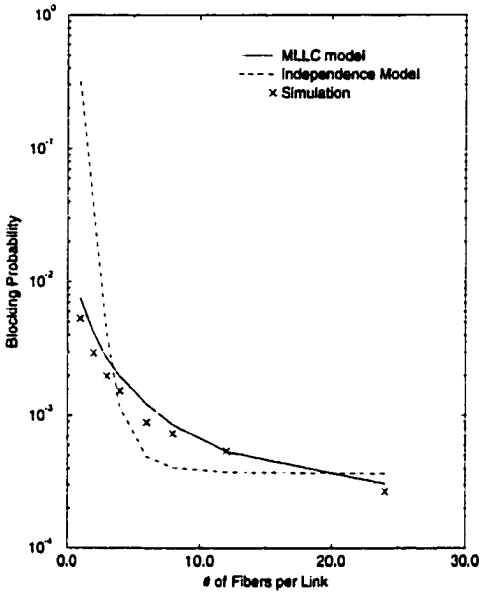

Figure 4.4 Blocking probability versus the number of fibers in a 10-node unidirectional ring network. The number of LCs per link are fixed at 24

formance as that in full-wavelength-convertible networks (F=24, W=1). Recalling that multiple fibers has similar effect as limited wavelength conversion in WDM networks, our observation is coincident with the results in [32], which showed that with a conversion bandwidth that covers only 25% of the whole transmission bandwidth, the blocking probability is almost identical to the one with full-range conversion.

The above two regular topologies have been intensively studied in the literature [32, 21]. However, few analytical models are applicable in irregular multifiber networks. We apply the MLLC model to the NSFnet and show the results in Figure 4.6. The traffic load per node is 12 Erlangs. It is seen that the analytical results follow the trend of the simulation results. No result of the independence model is shown in the figure because the independence model is not applicable in irregular networks. We observe that the full wavelength conversion (F=24, W=1) in the NSFnet does not improve much the performance compared to no wavelength conversion (F=1, W=24). It is also interesting to note that only 4 fibers per link is sufficient to provide similar performance as that of

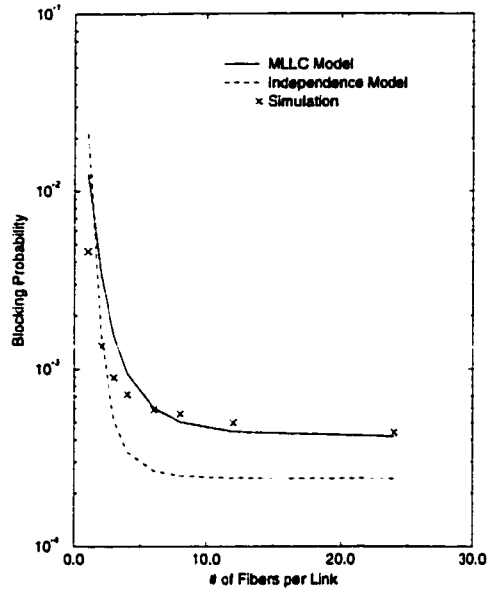

Figure 4.5 Blocking probability versus the number of fibers in a 5×5 mesh-torus network. The number of LCs per link are fixed at 24

using full wavelength converters in the NSFnet.

From the above simulation and analytical results, we know that the MLLC model is applicable for both regular and irregular networks. The analytical results are close to the simulation results in all of the three examined topologies. We also observe that good performance is guaranteed in multifiber networks with a limited number, i.e., $2-4$, of fibers.

4.4 Conclusions

We have studied the effect of multiple fibers in circuit-switched all-optical WDM networks. To evaluate the blocking performance of such networks, we have developed an analytical model taking the link-load correlation into account. We have shown that the model is accurate for a variety of network topologies by comparing the analytical results with the simulation results. Comparing to the independence model of [19], the MLLC model is more accurate both in regular networks (the ring, the mesh-torus) and

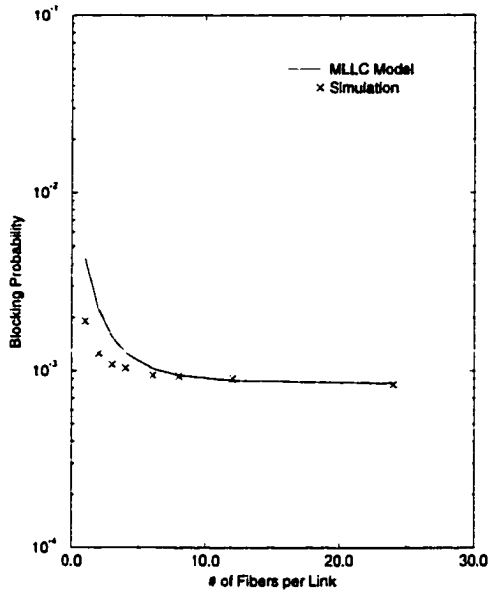

Figure 4.6 Blocking probability versus the number of fibers in the NSFnet. The number of LCs per link are fixed at 24

irregular networks (the NSFnet).

An important conclusion of our study is that a multifiber network has similar blocking performance as that in a full-wavelength-convertible network, if we select the wavelength-fiber-pairs adequately. A limited number of fibers is sufficient to guarantee high network performance. Most of the current optical networks are built on multiple fibers. Multifiber WDM networks without wavelength conversion is not only a feasible, but also a desirable choice under current technologies.

5 FIBER REQUIREMENT IN MULTIFIBER WDM NETWORKS WITH ALTERNATE-PATH ROUTING

5.1 Introduction

We presented an analytical model to compute the blocking performance of multifiber WDM networks with fixed-path routing in Chapter 4. Since the cost of a multifiber network is likely to be higher than a single-fiber network (more amplifiers and multiplexer/demultiplexer), the design goal of a multifiber network is to achieve high network performance with the minimum number of fibers per link. Thus an important problem in multifiber networks is to determine how many fibers are required on each link to guarantee high network performance that is similar to a network with full-range wavelength converters at every node. This fiber requirement may depend on many factors, e.g., the network topology, traffic patterns, the number of wavelengths per fiber, and the routing algorithm employed in the network. A similar problem has been studied in [54, 60] under static traffic. We study the fiber requirement under dynamic traffic in different topologies with alternate-path routing in this chapter.

The wavelength assignment problem in multifiber WDM networks has been studied in [19, 20]. Different wavelength assignment algorithms in multifiber networks are compared in [19]. A sophisticated wavelength assignment algorithm, $M\sum$, is developed. The results show that the $M\sum$ algorithm performs much better than other algorithms in multifiber networks. A relative capacity loss (RCL)wavelength assignment algorithm is presented in [20]. The blocking probability of the RCL algorithm is $5\% - 30\%$ better than the $M\sum$ depending on the traffic demands and network topology, but has the

same worst cast time complexity of $M \sum$ (at least asymptotically) [20]. There have been considerable interests to analyze the blocking performance of multifiber WDM networks [19, 21]. A review of the literature is shown in Chapter 4. A Multifiber Link-Load Correlation (MLLC) model presented in Chapter 4 and [38] is more accurate than the models in [19, 21]. The analytical and simulation results show that a limited number of fibers per link is sufficient to guarantee high network performance in the ring, the mesh-torus, and the NSF T1 backbone networks.

Routing and wavelength assignment algorithms (RWAA) play a key role in WDM networks [16]. The current research on multifiber networks has focused on fixed-path routing (FPR) algorithms, i.e., a request is blocked if no wavelength is free on the pre-selected path between a source-destination (s-d) pair. Alternate-path routing (APR), in which a request blocked on one path is overflowed to an alternate path, can significantly improve the network performance [12] in single-fiber networks. We study the effects of multiple fibers in WDM networks with the APR in this chapter. The question we attempt to answer is how many fibers per link are required to guarantee high performance in a WDM network with the APR. We use and extend the MLLC model in the previous chapter to analyze the performance of WDM networks with the APR. Our model is a generalized model that can be used in both regular and irregular networks. We observe that the number of fibers required to guarantee high performance is slightly higher in the APR than the FPR. However, a limited number of fibers are still sufficient to guarantee that the blocking performance of a multifiber WDM network is similar to the blocking performance of a full-wavelength-convertible network.

This chapter is organized as follows. The MLLC model presented in the previous chapter is extended to analyze the performance of the APR in Section 5.2. An iterative approach is proposed to solve the Erlang-map equation introduced by the APR in multifiber networks. The accuracy of the analytical model is assessed in Section 5.3 by comparing the analytical results to the simulation results. The numerical results show that the performance of the APR is much better than that of the FPR in multifiber networks. The number of required fibers per link is slightly higher in the APR than the

FPR to provide high network performance. However, a small number of fibers per link are still sufficient to guarantee high network performance in both the regular mesh-torus networks and the irregular NSFnet. We make our concluding remarks in Section 5.4.

5.2 Analysis of the Alternate-Path Routing

We have presented the MLLC model for fixed-path routing in the previous chapter. The MLLC model provides a method to analyze the status of each path. Let $Q_\alpha^p(i)$ be the probability that the path connecting s-d pair α has i free wavelength trunks. Let $l(p)$ be the length of path p. Using the results in Chapter 4, $Q_\alpha^p(i)$ is given by

$$Q_\alpha^p(i) = \sum_{y_f=0}^{FW} P_6^{l(p)}(i, y_f) \; . \tag{5.1}$$

where $P_6^{(l)}(\widehat{N}_{f_l}, y_{f_l})$ is the probability that $\widehat{N}_{f_l}$ wavelengths are free on an l-hop path and y_{f_l} LCs are free on hop l. $P_6^{(l)}(\widehat{N}_{f_l}, y_{f_l})$ is given in Eq. 4.8. Thus the stable-state distribution of the number of free wavelength trunks on a path can be computed using Eq. (5.1). The input parameters of the MLLC model is the network traffic specified by the rate of leaving calls from link i (λ_i^l), the rate of entering calls at link j (λ_j^e), and the rate of continuing calls from link i to link j (λ_{ij}^c). Here i, j are the links of a network. The carried network traffic is determined by routing and wavelength assignment algorithms in WDM networks. Different routing algorithms generate different network traffics that determine the network performance. For the fixed-path routing, the link traffics, e.g., the arrival rates of calls entering at link i, λ_i^e, leaving from link j, λ_j^l, and continuing from link i to link j, $\lambda_{i,j}^c$, can be computed using Eqs. (4.10), (4.11), and (4.9), respectively. We analyze the performance of alternate-path routing (APR) in this section. We are interested in finding the effects of multiple fibers in the performance of alternate-path routing, i.e., how many fibers per link are required to ensure high network performance. In the following analysis, we make the following similar assumptions as in Chapter 4:

- We assume Poisson input traffic with arrival rate λ at each node and exponentially distributed call holding time with mean $1/\mu$.

- Each link consists of F fibers, and each fiber consists of W wavelengths.

- An incoming request on one channel can be switched to any output port using OXC as long as the output port has the same wavelength free regardless of which fiber it is on. If the wavelength is not free on all of the F fibers, the request is blocked on this wavelength. No wavelength converter is available at any node.

In the alternate-path routing, a set of paths are precomputed statically for each s-d pair and stored sequentially at the sources nodes according to specified criteria, e.g., the path length. Upon the arrival of a connection request at a source node, the paths are searched sequentially. The first path that has free wavelengths available is selected, and one wavelength is uniformly randomly selected to establish the connection. The request is blocked only if all of the candidate paths have no free wavelengths. Note that the number of paths for each s-d pair is restricted to two for easy discussion in this model. The model can be easily extended to consider more than two paths. However, we assume that the overflowed traffic is still Poisson traffic. This assumption may not be valid if more alternate paths are used. Our simulation results also show that using more than two paths does not significantly improve the network performance.

In the alternate-path routing, the traffic load of a link consists of two parts: (1) the loads carried on the first paths that pass through the link; (2) the loads overflowed from the first paths and carried on the second paths that pass through the link. Thus, the link load cannot be directly obtained from the offered traffic without the knowledge of the blocking probability on each path. The probability of blocking is in turn dependent on the arrival rate to the links. This leads to a system of coupled non-linear equations called the Erlang map [55]. We develop an iterative approach to solve the no-linear equations.

We need the following notations to compute the blocking probability:

- Let R_i^1 be a set of the first paths that use link i, and R_{ij}^1 be a set of the first paths that continue from link i to link j. Let R_i^2 be a set of the second paths that use link i, and R_{ij}^2 be a set of the second paths that continue from link i to link j.

- Let $P_{B_\alpha}^1$ be the blocking probability on the first path of a s-d pair α, and $P_{B_\alpha}^2$ be the blocking probability on the second path of α.
- Denote p_α as a path connecting a s-d pair α.
- Let ϵ be a small positive number that is used as convergence criterion.

The non-linear equations can be solved iteratively using the following procedure:

1. Set $P_B = P_{B_\alpha}^1 = P_{B_\alpha}^2 = 0$;
2. Compute the traffic loads entering at link i (λ_i), leaving from link j (λ_j), and the load continuing from link i to link j (λ_{ij}):

$$\lambda_{ij} = \sum_{p_\alpha \in R_{ij}^1} \lambda_\alpha (1 - P_{B_\alpha}^1) + \sum_{p_\alpha \in R_{ij}^2} \lambda_\alpha P_{B_\alpha}^1 (1 - P_{B_\alpha}^2); \tag{5.2}$$

$$\lambda_i = \sum_{p_\alpha \in R_i^1} \lambda_\alpha (1 - P_{B_\alpha}^1) + \sum_{p_\alpha \in R_i^2} \lambda_\alpha P_{B_\alpha}^1 (1 - P_{B_\alpha}^2) - \lambda_{ij}; \tag{5.3}$$

$$\lambda_j = \sum_{p_\alpha \in R_j^2} \lambda_\alpha (1 - P_{B_\alpha}^1) + \sum_{p_\alpha \in R_j^2} \lambda_\alpha P_{B_\alpha}^1 (1 - P_{B_\alpha}^2) - \lambda_{ij}; \tag{5.4}$$

3. Compute $Q_\alpha^p(i)$ using Eq. 5.1. The new values of the blocking probability on the first and second path of α are

$$\widehat{P_{B_\alpha}^1} = Q_\alpha^{p_1}(0)$$

and

$$\widehat{P_{B_\alpha}^2} = Q_\alpha^{p_2}(0)\ ,$$

respectivelys;

4. Compute the new value of the average blocking probability

$$\widehat{P_B} = \frac{\sum_\alpha \widehat{P_{B_\alpha}^1} \widehat{P_{B_\alpha}^2}}{|R|}$$

5. If ($|P_B - \widehat{P_B}| < \epsilon$), exit; otherwise let $P_{B_\alpha}^1 = \widehat{P_{B_\alpha}^1}$, $P_{B_\alpha}^2 = \widehat{P_{B_\alpha}^2}$, $P_B = \widehat{P_B}$, go to Step 2.

5.3 Numerical Results and Analysis

In this section, we assess the accuracy of our analysis model by comparing it with the simulation results. The MLLC model is applied to a 5×5 mesh-torus network, and an irregular NSF T1 backbone network (NSFnet) with fixed-path routing and Alternate-path routing. We are interested in finding the effect of multifibers on these networks with different routing algorithms. The question we attempted to answer is how many fibers are required to provide similar performance as that in a full-wavelength-convertible network.

In the networks we studied, the link capacity is fixed at 24 light channels, i.e., $FW = 24$ on each link. We vary the number of fibers on each link, F, from $1, 2, 3, 4, 6, 8, 12$ to 24, and the number of wavelengths on each fiber by $W = 24/F$ accordingly. We assume Poisson traffic arrives at each node, and the destination for an arrival request is uniformly distributed among other nodes[1]. We adjust the traffic load such that the blocking probabilities are around 10^{-3}. Each data point in the simulations was obtained using 10^6 call arrivals. In the approximate analysis of the APR, multiple iterations are required and the convergence criterion is set to be 10^{-5} for the blocking probabilities. Wavelength converters are useful to reduce the blocking probability in the mesh-torus networks. We first study a 5×5 mesh-torus network. The call blocking probability against the number of fibers per link is plotted in Figure 5.3. The traffic load is 12 Erlangs per node for the fixed-path routing, and 17 Erlangs per node for the alternate-path routing as shown in Figure 5.3.a and 5.3.b, respectively. The analytical results closely match the simulation results in both the fixed-path routing and the alternate-path routing, which indicates that the model is adequate in analytically predicting the performance of SPR and APR in mesh-torus networks.

We observed from the figures that the network performance of using a full-range wavelength converter (F=24, W=1) at every node is much better than using no wavelength

[1]The MLLC model could also be used for non-uniformly distributed traffic using Eqs. (5.2), (5.3) and (5.4). The uniform distribution assumption is made only for simplicity. Note that link loads in NSFnet are non-uniformly distributed.

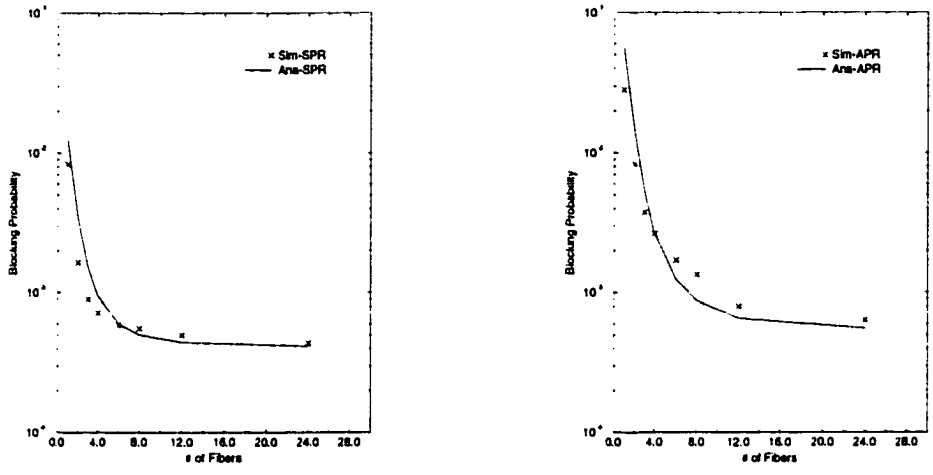

(a) (b)

Figure 5.1 Blocking probability versus the number of fibers ina 5×5 mesh-torus network using (a) fixed-path routing, traffic load is 12 Erlangs per node, and (b) alternate-path routing, traffic load is 17 Erlangs per node. The number of LCs per link are fixed at 24

conversion (F=1, W=24) in the fixed-path routing (more than one order of magnitude). Using full wavelength conversion improves the blocking performance even further, around two order of magnitudes, if the alternate-path routing is used. However, the network blocking probability decreases sharply with the increasing number of fibers per link F, when F is small. The performance improvement becomes less significant after $2-4$ fibers per link are used in the fixed-path routing and $4-6$ fibers per link in the alternate-path routing. Thus, routing algorithms affect the benefits of using multiple fibers per link in WDM networks. The alternate-path routing requires more fibers per link than the fixed-path routing. However, only very limited number of fibers per link are required for both the fixed-path routing and the alternate-path routing.

The mesh-torus network has been intensively studied in the literature [32, 21]. However, few analytical models are applicable to irregular multifiber networks. We apply the analytical model to the NSFnet and show the results in Figure 5.3. The traffic load

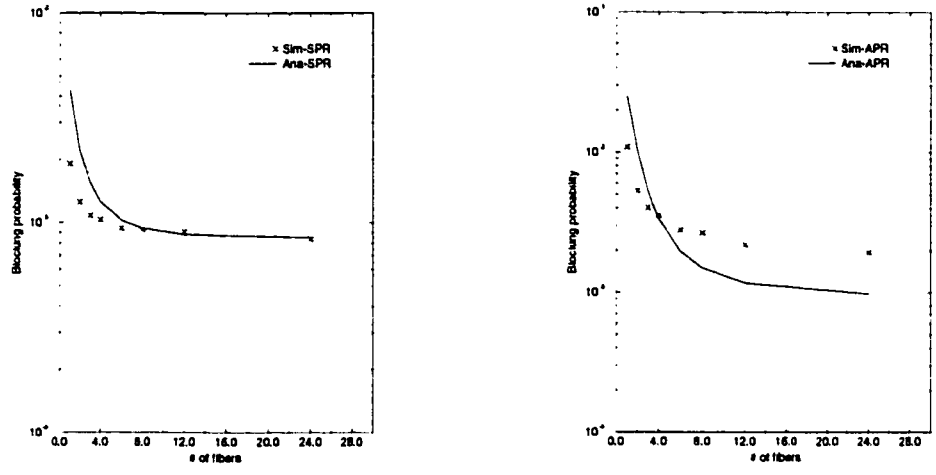

(a) (b)

Figure 5.2 Blocking probability versus the number of fibers in the NSF T1 backbone network using (a) fixed-path routing, traffic load is 12 Erlangs per node, and (b) alternate-path routing, traffic load is 17 Erlangs per node. The number of LCs per link are fixed at 24

per node is 12 Erlangs for the fixed-path routing and 17 Erlangs for the alternate-path routing. It is seen that the analytical results follow the trend of the simulation results for both of the routing algorithms. In the NSFnet, full wavelength conversion (F=24, W=1) at every node does not improve much the performance compared to no wavelength conversion (F=1, W=24). It is also interesting to note that only 4 fibers per link in the fixed-path routing, and 6 fibers per link in the alternate-path routing, are sufficient to provide similar performance to using full wavelength converters in the NSFnet.

5.4 Conclusions

We have studied the effect of multiple fibers in all-optical WDM networks with alternate-path routing in this chapter. We use and extend a multifiber link-load correlation model presented in Chapter 4 to evaluate the blocking performance of such

networks. We have shown that the model is accurate for a variety of network topologies by comparing the analytical results with the simulation results.

We observed that routing algorithms affect the benefits of using multiple fibers on each link in WDM networks. The number of fibers required to provide high performance using alternate-path routing is slightly higher than in the fixed-path routing. However, a limited number of fibers are sufficient to guarantee high performance in both fixed-path routing and alternate-path routing.

6 DYNAMIC ROUTING IN MULTIFIBER WDM NETWORKS

6.1 Introduction

As we have seen in Chapter 2, dynamic routing approaches are more efficient than static routing methods. Analytical and simulation results [12, 16, 18] show that the dynamic routing method can significantly improve the network performance compared to the fixed-path routing and alternate-path routing. However, most of the current research on dynamic routing has focused on single-fiber WDM networks. We study the performance of multifiber WDM networks with the fixed-paths least-congestion (M-FPLC) routing in this chapter.

In the M-FPLC, we first statically compute a set of routes to be used for each source-destination pair in a network and store the route information at each source node. Upon arrival of a connection setup request, the least congested route is selected to set up the request. The request is blocked if no channel is free on any route. Much research has been done in obtaining the call blocking performance of single-fiber WDM networks [17, 31, 39, 47, 65]. The analytical models proposed for multifiber networks with different routing algorithms have been reviewed in Chapter 4 and 5. We use and extend the multifiber link-load correlation (MLLC) model developed in 4 to analyze the performance of multifiber WDM networks with the M-FPLC routing in this chapter. The new analytical model is a generalized model that can be used in both regular and irregular networks.

As we have mentioned in the previous chapter, the cost of a multifiber network is

likely to be higher than a single-fiber network (more amplifiers and multiplexer/demultiplexer). The design goal of a multifiber network is to achieve high network performance with the minimum number of fibers. An important problem in multifiber networks is to decide how many fibers per link are required to guarantee high network performance that is similar to a network with full-range wavelength converters at every node. This fiber requirement may depend on many factors, e.g., the network topology, traffic patterns, the number of wavelengths per fiber, and the routing algorithm employed in the network. We have seen in Chapter 4 and Chapter 5 that a limited number of fibers are sufficient to guarantee that the network performance of a multifiber network is similar to that of a full-wavelength-convertible network. We study the fiber requirement under dynamic traffic in different topologies with dynamic routing in this chapter. We observe that the number of fibers required to provide high performance in a multifiber network with dynamic routing is higher than those multifiber networks with fixed-path routing and alternate-path routing. However, multifiber networks with dynamic routing can still achieve similar blocking performance to full-wavelength-convertible networks with limited number of fibers.

This chapter is organized as follows. The link-load correlation model is extended to analyze the performance of the M-FPLC routing in multifiber WDM networks in Section 6.2. An iterative approach is proposed to solve the Erlang-map equation introduced by the M-FPLC in multifiber networks. The accuracy of the analytical model is assessed in Section 6.3 by comparing the analytical results to the simulation results. The numerical results show that a small number of fibers per link are sufficient to guarantee high network performance in both the regular mesh-torus networks and the irregular NSFnet. We observe from the simulation results that the blocking probability increases slightly with the increasing number of fibers using the above routing algorithm. This counter-intuition observation suggests us to develop a new dynamic routing algorithm in Section 6.4, lightpath (LP)-based M-FPLC, to further improve the blocking performance. We make our concluding remarks in Section 6.5.

6.2 Analytical Model for the M-FPLC Routing in Multifiber WDM Networks

We propose an analytical model to compute the blocking performance of the M-FPLC in this section. In the M-FPLC routing, a set of paths is predetermined for each s-d pair[1]. Upon the arrival of a connection request, the least congested path, i.e., the path that has the maximum number of free wavelength trunks (defined in the Chapter 4), is selected to use. If there is a tie, the first path with free wavelength is selected. A wavelength is randomly selected among the free wavelengths to set up the request. The call is blocked if no free wavelength is found on all of the paths. Note that the least congested path may be computed by a central controller in a network as proposed in [18], or using a distributed algorithm [49, 50]. We focus on the performance analysis of the M-FPLC routing in this chapter.

Following Chapter 5, we define $Q_{P_\alpha}(i)$ be the probability that the path P_α connecting s-d pair α has i free wavelength trunks. Let $l(P_\alpha)$ be the length of path P_α. $Q_{P_\alpha}(i)$ is given by

$$Q_{P_\alpha}(i) = \sum_{y_f=0}^{FW} P_6^{l(P_\alpha)}(i, y_f) \ . \tag{6.1}$$

where $P_6^{(l)}(\widehat{N}_{f_l}, y_{f_l})$ is the probability that $\widehat{N}_{f_l}$ wavelengths are free on an l-hop path and y_{f_l} LCs are free on hop l. $P_6^{(l)}(\widehat{N}_{f_l}, y_{f_l})$ is given in 4.8

$Q_{P_\alpha}(i)$ gives the stable-state distribution of the number of free wavelength trunks on a path. Let P_{B_α} be the probability that a connection request of s-d pair α is blocked. In the M-FPLC routing, a request is blocked if none of the two paths connecting a s-d pair has free wavelength. Thus P_{B_α} is given by

$$P_{B_\alpha} = Q_{P_\alpha^1}(0) Q_{P_\alpha^2}(0) \ . \tag{6.2}$$

Let $|R|$ be the number of s-d pairs in a network, and P_B be the network-wide average

[1]We restrict the number of paths for each s-d pair to two for easy discussion in this chapter. The analytical model can be easily extended to consider more than two paths. However, more than two paths do not significantly improve the blocking performance as observed in our experiments and also shown in [18].

blocking probability. P_B is given by

$$P_B = \sum_{\alpha} P_{B_\alpha} / |R| \ . \tag{6.3}$$

Eq. 6.3 is used to compute the call blocking probability in a multifiber network with the M-FPLC routing. The above analysis assumes that the arrival rates of calls that leave a link, continue from a link on to the next link of a path, and enter at a link, λ_l, λ_c and λ_e respectively, are known. Typically, the traffic in a network is specified in terms of the set of offered loads between s-d pairs. The call arrival rates at links have to be estimated from the arrival rates of calls to node. The complication in estimating the link arrival rates in the M-FPLC routing is that a path for a request is selected using the current network status. Thus the arrival rate on each link is continuously changing. No steady state is reached in the strict sense when the M-FPLC is used. We propose to use a technique based on the Erlang Fixed-Point method for Alternate routing [55] to solve this problem. We need the following further notations:

- Let $R_j^{(1)}$ be a set of the first routes that employ link j, and $R_j^{(2)}$ be a set of the second routes that employ link j.
- Let $R_{i,j}^{(1)}$ be a set of the first routes that have a subset of route from link i to j. Let $R_{i,j}^{(2)}$ be a set of the second routes that have a subset of route from link i to j.
- Let $Pr(P_\alpha^1)$ and $Pr(P_\alpha^2)$ be the probabilities that a call for a s-d pair α is set up on the first and second path, P_α^1 and P_α^2, respectively.

In the M-FPLC, a call request is set up on the first path if the number of free wavelengths on the second path is less than the number of free wavelengths on the first path. Otherwise, it is set up on the second path assuming that the path has at least one free wavelength. Therefore,

$$Pr(P_\alpha^1) = \sum_{i=1}^{F} Q_{P_\alpha^1}(i)(\sum_{n=0}^{i} Q_{P_\alpha^2}(n)), \tag{6.4}$$

$$Pr(P_\alpha^2) = \sum_{i=1}^{F} Q_{P_\alpha^2}(i)(\sum_{n=0}^{i-1} Q_{P_\alpha^1}(n)). \tag{6.5}$$

Recall that λ is the call arrival rate at each node. The arrival rate of calls that enter at link i and continue to link j, $\lambda_c(i,j)$, becomes

$$\lambda_c(i,j) = \sum_{P_j \in R^1_{i,j}} \lambda Pr(P_j) + \sum_{P_j \in R^2_{i,j}} \lambda Pr(P_j). \tag{6.6}$$

The arrival rate of calls that leave from link i, $\lambda_l(i)$, includes calls that use link i as the first or second route, but do not continue to link j,

$$\lambda_l(i) = \sum_{P_i \in R^1_i} \lambda Pr(P_i) + \sum_{P_i \in R^2_i} \lambda Pr(P_i) - \lambda_c(i,j). \tag{6.7}$$

The arrival rate of calls that enter at link j, $\lambda_e(j)$ includes calls that use link j as the first or second route, but do not include calls that continue from link i to link j,

$$\lambda_e(j) = \sum_{P_j \in R^1_j} \lambda Pr(P_j) + \sum_{P_j \in R^2_j} \lambda Pr(P_j) - \lambda_c(i,j). \tag{6.8}$$

Given the arrival rates to each link, the conditional probabilities $S(y_f|x_{pf})$ and $U(z_c|y_f, x_{pf})$, defined in Chapter 2, can be derived using Eqs. (2.1) and (2.2). The probability that $\widehat{N}_{f_2}$ WTs are free on a two-hop path given that $\widehat{X}_{f_1}$ WTs are free on the first hop of the path, y_{f_2} LCs are free on the second hop, and z_{c_2} LCs are busy on both of the link occupied by continuing calss from the first to the second hop, $R_{WTLC}(\widehat{N}_{f_2}|\widehat{X}_{f_1}, y_{f_2}, z_{c_2})$, can be computed using Eq. (4.7). Since $R_{WTLC}(\widehat{N}_{f_2}|\widehat{X}_{f_1}, y_{f_2}, z_{c_2})$ depends only on the number of fibers per link, F, and the number of wavelengths per fiber, W. Let ϵ be a small positive number that is used as convergence criterion. Let J be the number of links in a network. The algorithm given below iteratively computes the approximate average blocking probability.

1. Initialization. For each source-destination pair α let $P_{B_\alpha} = 0$. Choose $\lambda_e(i)$, $\lambda_c(i,j)$, and $\lambda_l(i), i,j = 1,\ldots,J$ arbitrarily for all links.

2. Calculate $Q_{P_\alpha}(i)$ for every path of each s-d pair using Eq. (6.1).

3. Calculate the blocking probability $\bar{P}_{B_\alpha}$ for every s-d pair α using Eq. (6.2). If $\max_\alpha |P_{B_\alpha} - \bar{P}_{B_\alpha}| < \epsilon$ then terminate. Otherwise let $P_{B_\alpha} = \bar{P}_{B_\alpha}$, go to next step .

4. Calculate λ_c, λ_l, and λ_e for each link using Eqs. (6.6), (6.7) and (6.8), then go back to step 2.

Since the arrival rate for each link can be computed individually, this method is suitable for analysis of irregular networks. The method is also applicable to alternate routing approaches with small modifications of Eqs. (6.4) and (6.5).

6.3 Numerical Results and Analysis

In this section, we assess the accuracy of our analysis model by comparing it with the simulation results. The analytical model is applied to a 5×5 mesh-torus network, and an irregular NSF T1 backbone network (NSFnet) with the M-FPLC routing. We are interested in finding the effect of multifibers on the blocking performance of these networks. The question we attempted to answer is how many fibers are required to yield similar performance as that of a full-wavelength-convertible network with dynamic routing.

In the networks we studied, the link capacity is fixed at 24 light channels, i.e., $FW = 24$ on each link. Similar to Chapter 4 and 5, we vary the number of fibers on each link, F, from $1, 2, 3, 4, 6, 8, 12$ to 24, and the number of wavelengths on each fiber by $W = 24/F$ accordingly. We assume Poisson traffic arrives at each node, and the destination for an arrival request is uniformly distributed among other nodes[2]. Each data point in the simulations was obtained using 10^6 call arrivals. In the approximate analysis of the M-FPLC routing, multiple iterations are required and the convergence criteria, ϵ, is set to be 10^{-5}.

The call blocking probability against the number of fibers per link is plotted in Figure 6.1 for a 5×5 mesh-torus network (regular) and in Figure 6.2 for the NSFnet (irregular). The traffic loads are 26 and 17 Erlangs per node for the two networks, respectively. From the figure, we observed that the analytical results follow the trend

[2]The analytical model could also be used for non-uniformly distributed traffic using Eqs. (6.6), (6.7) and (6.8). The uniform distribution assumption is made only for simplicity. Note that link loads in NSFnet are non-uniformly distributed.

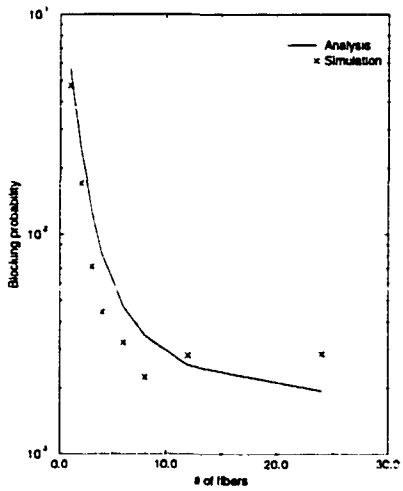

Figure 6.1 Blocking probability versus the number of fibers in a 5×5 mesh-torus network with the M-FPLC routing. Traffic loads are 26 Erlangs per node. The number of LCs per link is fixed at 24

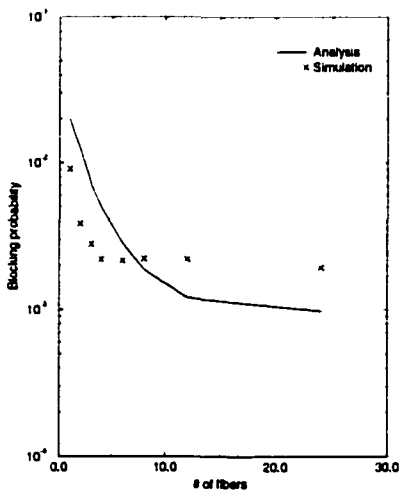

Figure 6.2 Blocking probability versus the number of fibers in the NSFnet using the M-FPLC routing. Traffic loads are 17 Erlangs per node. The number of LCs per link is fixed at 24

of the simulation results. The analytical results are in good agreement with simulation results for small to moderate number of fibers per link ($F < 8$). The analytical model slightly overestimates the blocking probability when F is large. The analytical results closely match the simulation results, which indicates that the model is adequate in analytically predicting the performance of the M-FPLC routing in different networks.

We observed from the figures that the network performance of using a full-range wavelength converter (F=24, W=1) at every node is much better than using no wavelength conversion (F=1, W=24) in the mesh-torus network with M-FPLC routing (more than one order of magnitude). Such performance improvement is not very significant in the irregular NSFnet. However, the network blocking probabilities decrease sharply with the increasing number of fibers per link F in both of the networks, when F is small. The performance improvement becomes less significant after 6 fibers per link are used in the mesh-torus network and 4 fibers per link in the NSFnet. We observe that high network performance using the M-FPLC routing is guaranteed with $F = 4$ and $W = 6$ in the NSFnet.

We also noticed from the simulation results in Figures 6.1 and 6.2 that the best performance is achieved when $F = 8$ in the mesh-torus network and $F = 4$ in the NSFnet. After that, the blocking probability increases slightly with the usage of more fibers. This counter-intuitive observation results from the routing rules. In the M-FPLC routing, the least congested path is the one that has the maximum number of free wavelength trunks in multifiber networks. Since a free wavelength trunk may consists of one or more free lightpaths from a source to a destination (the maximum number is F), a path with more free wavelength trunks is not necessary to have more free lightpaths than the other path. Therefore a path with more free resources may not be selected to set up a connection. The routing rule, the first path is selected if the two paths have the same number of free wavelength trunks, leads the M-FPLC routing to the alternate path routing when $F = 24$, i.e., $W = 1$. It has been shown in Chapter 2 that the alternate path routing performs poorly compared to the FPLC routing in the single-fiber mesh-torus and NSFnet networks. Thus the network performance may be

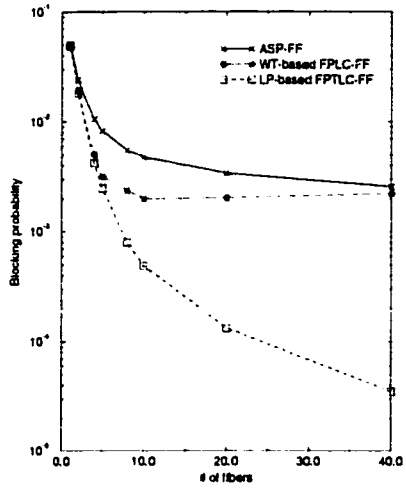

Figure 6.3 Simulation results of a 5×5 mesh-torus network using the M-FPLC routing. Traffic loads are 48 Erlangs per node. The number of LCs per link is fixed at 40

degraded if too many fibers are used in the above M-FPLC routing.

6.4 Lightpath-based M-FPLC Routing

The observation made in the above section suggests a new M-FPLC routing algorithm: instead of counting the number of free wavelength trunks on a path, the least congested path should be determined by the number of free lightpaths on a path. We call this new M-FPLC routing algorithm as an LP-based M-FPLC, and the previous M-FPLC algorithm as WT-based M-FPLC. These two M-FPLC routing algorithms are compared in Figure 6.3 using simulation results. The blocking performance of the alternate path routing [15] is also shown in the figure for comparison.

In the simulation, the link capacity is fixed at 40 light channels, i.e., $FW = 40$ on each link. We vary the number of fibers on each link, F, from $1, 2, 4, 5, 8, 10, 20$ to 40, and the number of wavelengths on each fiber by $W = 40/F$ accordingly. We change the wavelength assignment algorithm from random to first-fit depicted in Chapter 1, i.e.,

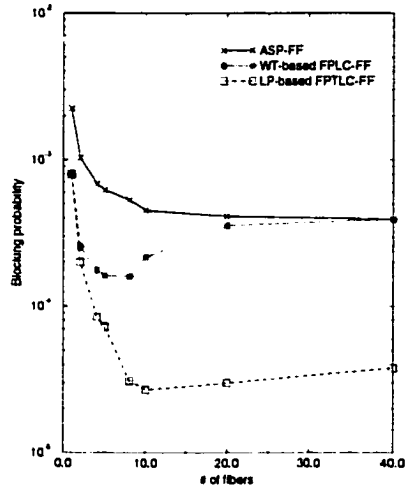

Figure 6.4 Simulation results of the NSFnet network using the M-FPLC routing. Traffic loads are 29 Erlangs per node. The number of LCs per link is fixed at 40

after a path is determined to use, the first free wavelength with the smallest index is selected to set up a connection. The traffic loads are 48 Erlangs per node for the 5×5 mesh-torus network and 29 Erlangs per node for the NSFnet. We observed from Figure 6.3 and 6.4 that the LP-based M-FPLC performs much better than the WT-based M-FPLC and the alternate path routing in both of the networks when multiple fibers are available. The network blocking probability decreases sharply with the increasing number of fibers per link, F. For the mesh-torus network, the blocking performance is improved continuously with the increasing F, but the rate of the performance improvement decreases. For the NSFnet, the best performance is achieved when $F = 10$. After that the blocking probability increases slightly with the increasing F. This observation suggests that employing more fibers help to improve the network performance in the mesh-torus network with LP-based M-FPLC. However, in the irregular NSFnet, the benefit of employing multiple fibers is maximized if we keep the $F = 8$ and $W = 5$. From the wavelength-conversion point of view, the results in Figure 6.3 and 6.4 also suggests that limited wavelength conversion is not only a solution to reduce the cost of

wavelength converters, but also a solution to obtain high network performance.

6.5 Conclusions

We have studied the blocking performance of multifiber WDM networks with the M-FPLC routing. Two M-FPLC routing algorithms, WT-based M-FPLC and LP-based M-FPLC, are proposed and studied. We have developed a new analytical model based on the mutifiber link-load correlation (MLLC) model presented in 4 to evaluate the blocking performance of such networks. We have shown that the analytical model is accurate for a variety of network topologies by comparing the analytical results with the simulation results. We observed that the LP-based M-FPLC routing algorithm can use multiple fibers more efficiently than the WT-based M-FPLC and the alternate path routing algorithms. In both the mesh-torus and NSFnet networks, limited number of fibers is sufficient to guarantee high performance. For the irregular NSFnet, the best performance is achieved with $F = 4$ and $W = 6$. This observation suggests that determining appropriate number of fibers per link is critically important to achieve high network performance.

7 A PARAMETRIC COST MODEL

7.1 Introduction

We have introduced in the previous chapters that using multiple fibers on each link is an alternate solution to overcome the wavelength continuity constraint. Our analysis and simulation results show that a limited number of fibers per link are sufficient to guarantee that the network blocking performance is similar to that of networks with full wavelength conversion at every node. However, the cost of a multifiber network cannot be compared to a wavelength-convertible network without having a good cost model. We develop a parametric system cost model for both multifiber networks and single-fiber wavelength-convertible WDM networks in this chapter. By comparing the cost of different network configurations, we show that a multifiber network is a cost-effective solution with current technology.

7.2 A Cost Model

We study a general network topology represented by $G(V, E, F, W)$, which shows that the network has $|V|$ nodes, $|E|$ links, each link consists of F fibers, and each fiber carries W wavelengths. We consider three cost factors in a WDM network: the cost related to (1) a cable (C_{Cable} cost), (2) to a fiber (C_{Fiber} cost), and (3) to a switch (C_{Switch} cost). We assume that every link has the same configuration, i.e., the number of fibers per link, F, and the number of wavelengths per fiber, W, are same throughout the network.

In a WDM network, the cable cost, C_{Cable}, includes digging cost, leasing cost, right

of way cost, and cable maintenance cost, etc., which are required before any capacity can be used on a link. Different network configurations, i.e., the number of fibers per link (F) and the number of wavelengths per fiber (W), do not affect the cable cost significantly. To simplify the cost comparison, we therefore assume that the cable cost of a multifiber network is the same as that of a single-fiber wavelength-convertible network. This assumption, that either dark fibers are available ($C_{Cable} = 0$) or new fibers have to be laid out in both multifiber and single-fiber networks, is fundamental in our study. In some scenarios, fibers have been exhausted and laying out new fibers is too costly and/or too time-consuming, compared to increasing the number of wavelengths per fiber and employing wavelength conversion. Multifiber WDM networks may not be a viable solution in this case. We consider the general scenarios where optical networks are built from green fields or plenty of dark fibers are available, which is assumed the case in metropolitan-area networks (MAN), or local-area networks (LANs).

The fiber cost, C_{Fiber}, is the combination of costs associated with a fiber. The fiber cost typically consists of the cost of physical fibers, optical amplifiers, dispersion compensation components, multiplexers and demultiplexers to terminate a fiber, and signal regenerators if installed in the network. Since we consider the fiber cost as a combination of the costs associated with the fiber, the number of wavelengths that a fiber carries affects the fiber cost significantly. One reason is that the components handling more wavelengths costs more than the components that handle fewer wavelengths. For example a dispersion compensation component that can handle 80 wavelengths on each fiber may cost several times more than a compensation component that can only compensate the signals on a fiber consisted of 20 wavelengths. Another reason is that the power budget of optical amplifiers such as EDFA decreases with additional wavelengths. As a consequence we either have to increase the laser power or decrease the distance between two optical amplifiers. In each case the cost of optical amplifiers for each fiber increases with the increasing number of wavelengths per fiber. Therefore the number of wavelengths per link, W, has to be considered as a parameter in the fiber cost. We introduce a uniformed parameter, $\bar{C}_{Fiber}(W)$, to describe the fiber cost of a network. $\bar{C}_{Fiber}(W)$ is

defined as the cost of a fiber with one-unit length and carries W wavelengths. Let i be a link of the network, $1 \leq i \leq |E|$. $\bar{C}_{Fiber}(W)$ can be computed as

$$\bar{C}_{Fiber}(W) = \frac{\sum_{i=1}^{|E|} C_{Fiber}(i, W)}{\sum_{i=1}^{|E|} L(i)} , \tag{7.1}$$

where $L(i)$ is the length of link i, and $C_{Fiber}(i, W)$ is the fiber cost of link i. We assume that $C_{Fiber}(i, W)$ is known, or it can be easily calculated by adding up all the cost associated with one fiber on link i together. Thus the fiber cost of a multifiber network with F fibers per link and W wavelengths per fiber is approximately given by

$$C_{Fiber}(F, W) = F \sum_{i=1}^{|E|} \bar{C}_{Fiber}(W) \times L(i) . \tag{7.2}$$

Many components contribute to the cost of a switch, C_{switch}. The actual cost depends on the architecture and technology used in each switch. In our cost model, we take into account the cost of switching elements (C_{SE}) in a switch and the cost of wavelength converters ($C_{converter}(D)$) if equipped. To simplify the cost model of an optical switch, we consider two general switch architectures with and without wavelength converters, as shown in Figures 7.1 and 7.2, respectively. Dedicated converters are used for each output for each wavelength in the switch shown in Figure 7.2. A converter can also be shared by multiple wavelengths. If so, the cost of a wavelength converter would also be shared by multiple wavelengths.

Let j be a node in the network which has $|V|$ nodes, and K_j be the number of incoming/outgoing links at node j. We assume that the optical switch blocks at each node are nonblocking Batcher-Banyan switches made up of 2×2 switching elements. Let M_{WC}^j be the number of switching elements of the switch at node j if node j has wavelength converters. If node j has no wavelength converter in the optical switch, we denote M_{NWC}^j be the number of switching elements of the switch at node j. M_{WC}^j and M_{NWC}^j are given by [21]

$$M_{WC}^j = K_j WF(3 + log_2 K_j WF)(log_2 K_j WF)/4 , \tag{7.3}$$

and

$$M_{NWC}^j = K_j WF(3 + log_2 K_j WF)(log_2 K_j F)/4 , \tag{7.4}$$

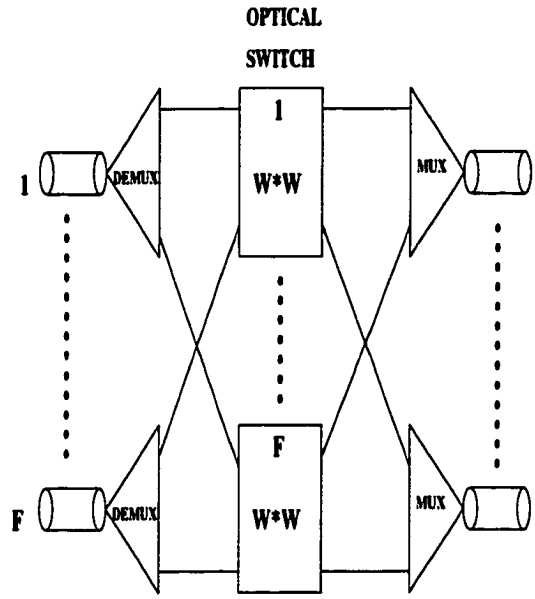

Figure 7.1 A node architecture of a multifiber network without wavelength converter

respectively. As we can see from the above equations, $M^j_{WC} > M^j_{NWC}$ if we fix the product of W and F as constant, i.e., the link capacities are same for both of the two configurations. Thus a wavelength-convertible optical switch may cost more than a switch without wavelength conversion, not only because of the extra cost of converters, but also the cost of increased number of switching elements.

To make a fare comparison, we fix the capacity on each link as constant for both single-fiber and multifiber networks. We denote the constant as D, i.e., $D = WF$. The total switch cost, $C_{Switch-WC}$, for a single-fiber network with wavelength conversion can be computed by

$$C_{Switch-WC} = C_{SE} \times \sum_{j=1}^{|V|} K_j D(3 + log_2 K_j D)(log_2 K_j D)/4 + D \times C_{converter}(D) \ . \quad (7.5)$$

The cost of an optical switch in a multifiber network without wavelength conversion is

$$C_{Switch-NWC} = C_{SE} \times \sum_{j=1}^{|V|} K_j D(3 + log_2 K_j D)(log_2 K_j F)/4 \ . \quad (7.6)$$

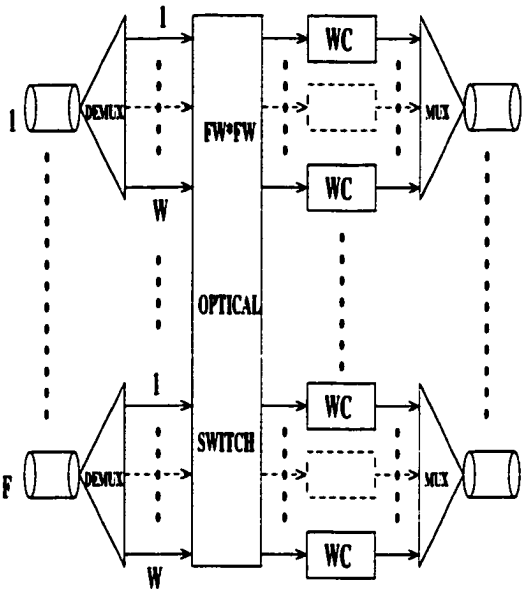

Figure 7.2 A node architecture of a multifiber network with wavelength converter

We know from Eqs. (7.1) and (7.5) that the total cost of a single-fiber network with wavelength conversion, $C_{total-SF}$, is,

$$C_{total-SF} = C_{Cable} + \sum_{i=1}^{|E|} \bar{C}_{Fiber}(D) \times L(i) + C_{SE} \times \sum_{j=1}^{|V|} K_j D(3 + log_2 K_j D)(log_2 K_j D)/4 + D \times C_{converter}(D) \; . \tag{7.7}$$

The total cost of a multifiber network without wavelength conversion, $C_{total-MF}$, is

$$C_{total-MF} = C_{Cable} + F \sum_{i=1}^{|E|} \bar{C}_{Fiber}(W) \times L(i) + C_{SE} \times \sum_{j=1}^{|V|} K_j D(3 + log_2 K_j D)(log_2 K_j F)/4 \; . \tag{7.8}$$

Let C_{diff} be the cost difference between the cost of a single-fiber wavelength-convertible network and the cost of a multifiber network without wavelength conversion. Thus

$$\begin{aligned} C_{diff} &= C_{total-SF} - C_{total-MF} \\ &= \sum_{i=1}^{|E|} (\bar{C}_{Fiber}(D) - F \times \bar{C}_{Fiber}(W)) \times L(i) \end{aligned}$$

$$+C_{SE} \times \sum_{j=1}^{|V|} K_j D(3 + log_2 K_j D)(log_2 K_j W)/4$$
$$+D \times C_{converter}(D) \tag{7.9}$$

We can divide the total cost difference into two parts: (1) link cost difference, and (2) switch cost difference. Let C^l_{diff} be the link cost difference of a single-fiber wavelength-convertible network and a multifiber network without wavelength conversion. Let C^s_{diff} be the switch cost difference of the two networks. Then

$$C^l_{diff} = \sum_{i=1}^{|E|} (\bar{C}_{Fiber}(D) - F \times \bar{C}_{Fiber}(W)) \times L(i) \ , \tag{7.10}$$

and

$$C^s_{diff} = C_{SE} \times \sum_{j=1}^{|V|} K_j D(3 + log_2 K_j D)(log_2 K_j W)/4 + D \times C_{converter}(D) \ . \tag{7.11}$$

Then the cost difference between a single-fiber wavelength-convertible network and a multifiber network, $Cdiff$, becomes

$$C_{diff} = C^l_{diff} + C^s_{diff} \ . \tag{7.12}$$

We can clearly see the tradeoff of using multiple fibers per link or wavelength converters in an optical switch to improve the network performance from Eqs 7.10, 7.11, and 7.12. Since the cost of a single-fiber link is usually less than the cost of a multifiber link with a unit length, i.e., $\bar{C}_{Fiber}(D) < F \times \bar{C}_{Fiber}(W)$, we know from Eq. 7.10 that $C^l_{diff} < 0$. Eq. 7.11 shows that $C^s_{diff} > 0$, that is, the switch of a single-fiber wavelength-convertible network costs more than that in a multifiber WDM network.

To compute the cost difference numerically, we need to unify the cost factors. In Eq. 7.10, we choose $\bar{C}_{Fiber}(W)$ as a base cost unit. Let γ_1 be the cost ratio of a fiber with D wavelengths to a fiber with W wavelengths, that is,

$$\gamma_1 = \frac{\bar{C}_{Fiber}(D)}{\bar{C}_{Fiber}(W)} \ . \tag{7.13}$$

Eq. 7.10 becomes

$$\frac{C^l_{diff}}{\bar{C}_{Fiber}(W)} = \sum_{i=1}^{|E|} (\gamma_1 - F) \times L(i) \ . \tag{7.14}$$

Similarly, in Eq. 7.11 we choose $C_{converter}(D)$ as a base cost unit. Let γ_2 be the cost ratio of a switch element to a wavelength converter, that is,

$$\gamma_2 = \frac{C_{SE}}{C_{converter}(D)} . \tag{7.15}$$

Eq. 7.11 becomes

$$\frac{C^s_{diff}}{C_{converter}(D)} = D(\gamma_2 \sum_{j=1}^{|V|} K_j(3 + log_2 K_j D)(log_2 K_j W)/4 + 1) . \tag{7.16}$$

The total cost difference between a single-fiber wavelength-convertible network and a multifiber network, C_{diff} in Eq. (7.12), becomes

$$\begin{aligned} C_{diff} &= \bar{C}_{Fiber}(W) \sum_{i=1}^{|E|} (\gamma_1 - F) \times L(i) \\ &\quad + C_{converter}(D) D(\gamma_2 \sum_{j=1}^{|V|} K_j(3 + log_2 K_j D)(log_2 K_j W)/4 + 1) . \end{aligned} \tag{7.17}$$

7.3 Numerical Results

The blocking performance of the NSFnet shown in Figure 2.11 has been extensively studied in the previous chapters. We study the cost issue of the NSFnet in this section. We show the tradeoff of using multiple fibers per link to reduce the switch cost but increase the link cost and using wavelength converters to reduce the fiber cost but increase the switch cost.

The NSFnet consists of 14 nodes and 21 links, i.e., $|V| = 14$ and $|E| = 21$. The length of each link, $L(i), i = 1, \ldots, 21$, is shown in Table 7.1. The link-length information obtained from [68] shows the driving distance between two states. We assume here that the driving distance is the route length between two nodes in the NSFnet network.

In the numerical calculation, we assume that the link capacity is fixed at 24, i.e., $D = 24$. In the multifiber configuration of the NSFnst we studied, we fix the number of fibers per link at 4, i.e., $F = 4$, and correspondingly the number of wavelengths per fiber is $W = 6$. We also assume that the cost ratio of a fiber with 24 wavelengths to a fiber with 6 wavelengths, $\gamma_1 = 2$. From Eq. (7.14) we know the link cost difference

Table 7.1 Link lengths in the NSFnet

Link	Length (in miles)	Link	Length (in miles)
NY - MD	375	NY - PA	286
NY - MI	643	NJ - MD	160
NJ - MI	860	NJ - PA	235
MD - TX	1603	PA - GA	883
PA - IL	710	MI - UT	1788
IL - NE	678	NE - CO	428
GA - TX	111	CO - UT	475
CO - TX	813	TX - CA2	1565
CA2 - CA1	345	CA2 - WA	986
WA - IL	2031	UT - CA1	775

between a single-fiber wavelength-convertible NSFnet network and a multifiber NSFnet network becomes

$$\begin{aligned} C^l_{diff} &= \bar{C}_{Fiber}(W)\sum_{i=1}^{24}(-2)L(i) \\ &= \bar{C}_{Fiber}(W) \times (-2) \times 16750 \\ &= -33500\bar{C}_{Fiber}(W)\ . \end{aligned} \tag{7.18}$$

Figure 2.11 shows that among the 24 nodes in the NSFnet, 10 nodes have input/output degrees $K_j = 3$, 2 nodes have $K_j = 4$, and 2 nodes have $K_j = 2$. We assume that the cost ratio of a switch element to a wavelength converter, $\gamma_2 = 0.01$. Thus the switch cost difference in Eq. (7.16) becomes

$$\begin{aligned} C^s_{diff} &= C_{converter}(D) \times 24(0.01(30(3 + log_2 72)(log_2 18) \\ &\quad +4(3 + log_2 48)(log_2 12) \\ &\quad +8(3 + log_2 96)(log_2 24)/4 + 1) \\ &= C_{converter}(D) \times 93.6\ . \end{aligned} \tag{7.19}$$

The overall cost difference between a single-fiber wavelength-convertible NSFnet network and a 4-fiber non-wavelength-convertible NSFnet network with 6 wavelengths on

each fiber becomes

$$\begin{aligned} C_{diff} &= C_{total-SF} - C_{total-MF} \\ &= -33500\bar{C}_{Fiber}(W) + C_{converter}(D) \times 93.6 \end{aligned} \tag{7.20}$$

The cost of a unit-length fiber with W wavelengths on it, $\bar{C}_{Fiber}(W)$, and the cost of a wavelength converter, $C_{converter}(D)$, depend on many factors, e.g., the technologies used in the wavelength conversion and optical amplifiers, and the types of used fibers which may or may not require dispersion compensation. The cost may vary significantly in different cases [66, 67]. The values of overall cost difference C_{diff} with different $\bar{C}_{Fiber}(W)$ and $C_{converter}(D)$ are listed in Table 7.2.

Table 7.2 The values of overall cost difference with different parameters

$\bar{C}_{Fiber}(6)$	$C_{converter}(24)$	C_{diff}
2	800	7880
4	1000	-40400
1	500	13300

Let γ_3 be the ratio of the cost of a W-wavelength fiber with unit length to the cost of a wavelength converter, i.e.,

$$\gamma_3 = \frac{\bar{C}_{Fiber}(W)}{C_{converter}(D)} .$$

We know from Eq. (7.20) that the overall cost difference between the two network configurations is zero if $\gamma_3 = 358$. Thus the multifiber network (F=4,W=6) has the same cost as the single-fiber wavelength-convertible network if the cost of a wavelength converter is 357 times more than that of a unit-length fiber with 6 wavelengths on it. New technologies of installing fibers in metropolitan-area networks and local-area networks have been developed to reduce the fiber cost [66]. In these networks, optical amplifiers may not be required because of the short distance between any two nodes. Therefore the fiber cost may not play a significant role in the overall network cost in

metropolitan-area networks and local-area networks. However, the technologies of all-optical networking have not been mature yet. The cost of wavelength converters is likely to remain high in the near future. Thus multifiber networks is a cost-effective solution in metropolitan-area networks or local-area networks with current technology.

7.4 Conclusions

We develop a parametric system cost model for all-optical WDM networks in this chapter. The model can be applied to both single-fiber and multifiber networks. It is also applicable to both wavelength-convertible and non-wavelength-convertible networks. The tradeoff of using multiple fibers to reduce the switch cost but increase the fiber cost and using wavelength converters to reduce the fiber cost but increase the switch cost has been clearly observed from the cost model and the numerical results. By comparing the cost of different network configurations, we show that a multifiber network is a cost-effective solution with current technology.

8 CONCLUSIONS AND FUTURE WORK

WDM technology has revolutionized wide-area networks (WAN) by enabling huge increase in the capacity of a single fiber. Wavelength-routed all-optical networks cost-effectively improve the scalability, flexibility, and reliability of not only backbone networks, but also metropolitan-area networks (MAN) and local-access networks (LAN). In all-optical WDM networks, routing and wavelength assignment (RWA) algorithms play a key role in conquering the wavelength continuity constraint. The primary focus of this dissertation is to develop dynamic routing algorithms and study the impacts of dynamic routing on the performance of WDM networks.

In WDM networks, multiple paths may exist for each source-destination (s-d) pair. Dynamic routing algorithms select a route to establish a connection according to the current network status. We developed new dynamic routing algorithms, fixed-path least-congestion (FPLC) routing and routing using neighborhood information, in Chapter 2. In the FPLC, the number of paths for each s-d pair is preselected and fixed. The least-congested path is chosen to set up a connection. We developed analytical models for Poisson traffic to evaluate the blocking probability of WDM networks with FPLC routing. Our analytical model takes the important effects of link-load correlation into account. Numerical results show that the fixed-paths least-congestion routing with the first-fit wavelength assignment method significantly improves network performance compared to the alternate-paths routing and shortest-path routing algorithms. The reason of the improvement is that more wavelengths are left free on a network when the FPLC with the first-fit wavelength assignment method is used. However, the FPLC routing algorithm still has higher setup delay and higher control overhead. The neighborhood-

information-based routing algorithm is employed as a trade-off between network performance in terms of blocking probability versus setup delay and control overhead when using dynamic routing algorithms. It is shown that the routing using neighborhood information method achieves good performance when compared to static routing approaches. 1-neighborhood information is sufficient to ensure network performance in a 4×4 mesh-torus network and in the NSF T1 backbone network.

The blocking performance of WDM networks can be significantly improved by using dynamic routing algorithms. The algorithms we developed in Chapter 2 can be used in networks with or without wavelength conversion. However, the performance gap still exists between the networks without wavelength conversion and the networks with wavelength converters at every node. Since the cost of an all-optical wavelength converter is likely to remain high in the near future, sparse-wavelength-convertible networks, in which only a few nodes having wavelength conversion capability, becomes a cost-effective solution. An interesting problem in such networks is how to place a small number of converters so that the network performance is optimized. We considered the optimal converter placement problem for a given number of converters on a path topology in Chapter 3. We first proposed and proved that optimal placement considering end-to-end calls are obtained when the segments on a path have equal success probability. Then the theory was used to achieve optimal converter placement using both the link-load independence model and the link-load correlation model. Three implementation algorithms with linear complexity were introduced.

Different technologies of converting one wavelength to another wavelength have been demonstrated in laboratories. However, none of them is currently available in the market yet. The cost of an all-optical wavelength converter is likely to remain high in the near future. Multifiber WDM networks are an alternative solutions to conquer the wavelength continuity constraint. In multifiber WDM networks, each link consists of multiple fibers, and each fiber carries information on multiple wavelengths. A wavelength that cannot continue on the next hop can be switched to another fiber using an optical cross-connect (OXC) if the same wavelength is free on one of the other fibers. We study

the effect of multiple fibers in all-optical WDM networks in Chapter 4. To evaluate the blocking performance of such networks, we developed an analytical model with the consideration of the link-load correlation. The results show that the analytical model is accurate for a variety of network topologies. A multifiber network has similar blocking performance as that of a full-wavelength-convertible network, if we select the wavelength-fiber-pairs adequately. A limited number of fibers are sufficient to guarantee high network performance.

We continue the investigation of multifiber WDM networks with alternate-path routing and fixed-path least-congestion routing in Chapter 5 and Chapter 6, respectively. The effects of multiple fibers on the performances of networks with different routing and wavelength assignment algorithms are studied. The question we attempted to answer in these chapters is how many fibers are required to achieve high performance. The multifiber link-load correlation model is extended to analyze the performance of multifiber networks with different routing algorithms. The results show that routing algorithms affect the benefits of using multiple fibers on each link in WDM networks. The number of fibers required to achieve high performance using alternate-path routing is slightly higher than in the fixed-path routing. Even more fibers are required in a multifiber network with fixed-path least-congestion routing to provide similar blocking performance to that of a network with full wavelength converters at every node. However, a limited number of fibers are still sufficient to guarantee high performance in both alternate-path and fixed-path least-congestion routing.

The research reported in this dissertation can be extended in several different ways. The model we presented in Chapter 2 assumed that the traffic arrives at each node follows Poisson distribution. However, the Poisson distribution may not model current network traffic, especially data traffic, accurately. Non-Poisson traffic has been studied in [57] with the assumption of fixed-path routing. More studies are required to understand the behavior of networks with Non-Poisson input traffic and using dynamic routing algorithms. We also assumed in Chapter 2 that the traffic arrives at each link is still Poisson in the dynamic routing algorithms. This assumption is not valid in the strict

sense because the path selected to establish a connection is not randomly determined, but according to the network status. The accuracy and complexity of the model may be further improved if Non-Poisson traffic is used to model the link traffic.

The efficient algorithms we developed in Chapter 3 can only be used in path or ring networks. A possible direction is to extend the algorithms to new heuristic solutions to place wavelength converters in other topologies.

Using multiple fibers on each link to conquer the wavelength continuity constraint is a new concept in the literature. A precise and comprehensive network cost model would be useful to determine if multifiber networks are preferable to the networks with wavelength conversion. We have evaluated the network performance using random and first-fit wavelength assignment and different routing algorithms. More sophisticated wavelength assignment algorithms should also be investigated in multifiber WDM network in the future.

APPENDIX

The following is a proof of lemma 1 in Chapter 3:

Proof: Let $\sum_{i=1}^{K+1} z_i = C$, where C is a constant. Let $g(z_i) = 1 - (1 - e^{z_i})^F$. We show below that $z_i^{opt} = C/(K+1), i = 1, 2, \ldots, K+1$ is an optimal vector to maximize $G(Z)$. To prove this, we need to show that

$$(K+1)\ln g(z_i^{opt}) \geq \sum_{i=1}^{K+1} \ln g(z_i)$$

where z_i^{opt} is an element of the optimal vector and z_i's are the elements of a feasible vector. Since z_i is in a convex set, we need to show that $\ln g(z)$ is a concave function of the continuous variable $z \in [-\infty, 0]$. Let $H(z) = \ln g(z)$. The second derivative of $H(z)$ is

$$H''(z) = \frac{g''(z)g(z) - [g'(z)]^2}{g^2(z)}.$$

Evaluating $g(z)$, $g'(z)$, and $g''(z)$ and substituting in the above equation, we obtain

$$H''(z) = \frac{Fe^z(1-e^z)^{F-2}(1 - Fe^z - (1-e^z)^F)}{g^2(z)}.$$

Note that for every $-\infty \leq z \leq 0$ and $F \geq 1$, $(Fe^z + (1-e^z)^F)$ is a non-decreasing function of z and is lower bounded by 1. Since the remaining factors are all positive, $H''(z) \leq 0$. ■

BIBLIOGRAPHY

[1] M. Shariff, "Packet over SONET Fuels New IP Transport Paradigm", *Lightwave Mag.*, p. 33, April 1998.

[2] Douglas C. Dowden, Richard D. Gitlin, and Robert L. Martin, "Next-Generation Networks", *BELL LABS Technology Journal*, Vol. 3, No. 4, pp. 3-14, Oct-Dec. 1999.

[3] Larry Rabiner, "Research Vision, Challenges, Endstate", AT&T Research Forum, http://www.research.att.com/forum/archive/19990526.html, 1999.

[4] Rod C. Alferness, Paul A. Bonerfant, Curtis J. Newton, Kevin A. Sparks, and Eve L. Varma, "A Practical Vision for Optical Transport Networking", *BELL LABS Technology Journal*, pp. 3-19, Jan. 1999.

[5] N. K. Cheung, G. Nosu, and G. Winzer, "Special issue on dense WDM networks", *IEEE J. Sel. Areas Comm.*, Vol. 8, no. 6, Aug. 1990.

[6] B. Mukherjee, *Optical Communication Networks*, Mc-Graw-Hill, NY, NY, 1997.

[7] R. Ramaswami and K.N. Sivarajan, *Optical networks: a practical perspective*, Morgan-Kaufman, San Francisco, CA, 1998.

[8] B. Mukherjee, D. Banerjee, S. Ramamurthy, A. Mukherjee, "Some principles for Designing a Wide-Are WDM Optical Network", *IEEE Journal on Selected Areas in Communications*, Vol. 4, No. 5, pp. 684-696, Oct. 1996.

[9] R. Ramaswami, K. N. Sivarajan, "Design of Logical Topologies for Wavelength-Routed Optical Networks", *IEEE Journal on Selected Areas in Communications*, Vol. 14, No. 5, pp. 840-851, Oct. 1996.

[10] Gerald R. Ash, Dynamic Routing in Telecommunications Networks, *McGraw-Hill*, NY, NY, 1997.

[11] D. Bertsekas and R. Gallager, *Data Networks*, Prentice Hall, Englewood Cliffs, NJ, 1992.

[12] H. Harai, M.Murata and H.Miyahara, "Performance of Alternate Routing Methods in All-Optical Switching Networks", *Proc. IEEE INFOCOM '97*, Vol. 2, pp. 517-525, April 1997.

[13] S. Ramamurthy and B. Mukherjee, "Fixed-Alternate Routing and Wavelength Conversion in Wavelength-Routed Optical Networks," *Proc. IEEE Globecom '98*, Vol. 4, pp. 2295-2303, Sydney, Australia, Nov. 1998.

[14] Ling Li and Arun K. Somani, "Fiber Requirement in Multifiber WDM Networks with Alternate-Path Routing", *Proc. ICCCN '99*, Boston, MA, 1999.

[15] Ling Li and Arun K. Somani, "Dynamic Wavelength Routing Using Congestion and Neighborhood Information", *IEEE/ACM Trans. On Networking*, pp. 779-786, Oct. 1999.

[16] A. Mokhtar and M. Azizoğlu, "Adaptive Wavelength Routing in All-Optical Networks", *IEEE/ACM Transactions on Networking*, pp. 197-206, Vol. 6, No. 2, April 1998.

[17] M. Kovačević and A. Acampora, "Benefits of Wavelength Translation in All-Optical Clear-Channel Networks", *IEEE Journal on Selected Areas in Communications*, Vol. 14, pp. 868-880, June 1996.

[18] E. Karasan and E. Ayanoglu, "Effects of Wavelength Routing and Selection Algorithms on Wavelength Conversion Gain in WDM Optical Networks", *IEEE/ACM Transactions on Networking*, pp. 186-196, Vol. 6, No 2, April 1998.

[19] S. Subramaniam and R. Barry, "Dynamic Wavelength Assignment in Fixed Routing WDM Networks", *Proc. IEEE ICC '97*, pp. 406-410, Montreal, Canada, Nov. 1997.

[20] X. Zhang and C. Qiao, "Wavelength Assignment for Dynamic Traffic in Multi-fiber WDM Networks", *Proc. ICCCN '98*, pp. 479-485, 1998.

[21] G. Jeong and E. Aynoglu, "Comparison of Wavelength-Interchanging and Wavelength-Selective Cross-Connects in Multiwavelength All-Optical Networks", *Proc. IEEE INFOCOM '96*, pp. 156–163, 1996.

[22] J. M. Wiesenfeld, "Wavelength conversion techniques," *Proc. OFC '96*, pp. 71–72, paper TuP 1, 1996.

[23] R. W. Tkach, A.R. Chraplyvy, F. Forghieri,A. H. Gnauck, R. M. Derosier, "Four-photon mixing and high-speed WDM systems," *IEEE/OSA J. Lightwave Technology*, Vol. 13, pp. 841–849, May 1995.

[24] R. Schnabel, U. Hilbk,T. Hermes, P. Meissner, C. Helmolt, K. Magari, F. Raub ,W. Pieper,F. J. Westphal, R. Ludwig, L. Kuller, H. G. Weber, "Polarization insensitive frequency conversion of a 10channel OFDM signal using fourwave mixing in a semiconductor laser amplifier," *IEEE Photon. Technology Letter*, Vol. 6, pp. 56–58, Jan. 1994.

[25] S. J. B. Yoo, "Wavelength conversion technologies for WDM network applications," *IEEE/OSA J. Lightwave Technology*, Vol. 14, pp. 955–966, June 1996.

[26] T. Durhuus, B. Mikkelsen, C. Joergensen, S. L. Danielsen, K. E. Stubkjaer, "All-optical wavelength conversion by semiconductor optical amplifiers," *IEEE/OSA J. Lightwave Technology*, Vol. 14, pp. 942–954, June 1996.

[27] M. Eiselt, W. Pieper, and H. G. Weber, "Decision gate for alloptical retiming using a semiconductor laser amplifier in a loop mirror configuration," *IEE Elect. Letters*, Vol. 29, pp. 107–109, Jan. 1993.

[28] H. Yasaka, H. Sanjoh, H. Ishii, Y. Yoshikuni, K. Oe, "Finely tunable 10Gb/s signal wavelength conversion from 1530 to 1560nm region using a super structure grating

distributed Bragg reflector laser," *IEEE Photonic Technology Letters*, Vol. 8, pp. 764–766, June 1996.

[29] B. S. Glance, J. M. Wiesenfeld, U. Koren, and R. W. Wilson, "New advances in optical components needed for fdm optical networks", *Journal of Lightwave Technology*, 11(5/6):882–890, May/June 1993.

[30] S. Subramaniam. "All-Optical Networks with Sparse Wavelength Conversion". *Ph.D. Dissertation*. University of Washington, 1997.

[31] S. Subramaniam, M. Azizoğlu, and A. K. Somani, "All-Optical Networks with Sparse Wavelength Conversion", *IEEE/ACM Transactions on Networking*, Vol.4, pp.544-557, Aug. 1996.

[32] J. Yates, J. Lacey, D. Everitt, and M. Summerfield, "Limited-range wavelength translation in all-optical networks", *Proc. IEEE INFOCOM '96*, pp. 954-961, March 1996.

[33] S. Subramaniam, M. Azizoglu, and A. K. Somani, "On the optimal placement of wavelength converters in wavelength-routed networks", *Proc. IEEE INFOCOM '98*, pp. 902-909, April 1998.

[34] S. Thiagarajan, A. K. Somani, "An efficient algorithm for optimal wavelength converter placement on wavelength-routed networks with arbitrary topologies", *Proc. IEEE INFOCOM '99*, Vol. 2, pp. 916-923, April 1999.

[35] Ling Li and Arun K. Somani, "Efficient Algorithms for Wavelength Converter Placement in All-Optical Networks", *Proc. Conference on Information Sciences and Systems*, Maryland, March 1999.

[36] K. R., Venugopal,M. Shivakumar, P. S. Kumar, "A heuristic for placement of limited range wavelength converters in all-optical networks", *Proc. IEEE INFOCOM '99*, Vol. 2, pp. 908-915, April 1999.

[37] D. Banerjee and B. Mukherjee, "Practical approaches for routing and wavelength assignment in all-optical wavelength-routed networks," *IEEE Journal on Selected Areas in Communications*, Vol. 14, pp. 903-908, June 1996.

[38] Ling Li and Arun K. Somani, "A New Analytical Model for Multifiber WDM Networks", *Proc. Globecom '99*, pp. 1007 - 1011, Rio de Janeiro, Brazil, December 1999.

[39] A. Birman, "Computing Approximate Blocking Probabilities for a Class of All-Optical Networks", *IEEE Journal on Selected Areas in Communications*, Vol. 14, pp. 852-857, June 1996.

[40] A. Birman and A. Kershenbaum, "Routing and Wavelength Assignment Methods in Single-Hop All-Optical Networks with Blocking", *IEEE INFOCOM '95*, 1995.

[41] S.-P. Chung, A.Kashper, and K.W. Ross, "Computing Approximate Blocking Probabilities for Large Loss Networks with State-Dependent Routing", *IEEE/ACM Transactions on Networking*, Vol. 1, pp.105-115, February, 1993.

[42] K. Chan, and T. P. Yum, "Analysis of Least Congested Path Routing in WDM Lightwave Networks", *Proc. IEEE INFOCOM '94*, Vol. 2, pp. 962-969, 1994.

[43] E. D. Lowe and D. K. Hunter, "Performance of Dynamic Path Optical Networks", *IEE Proceedings-Optoelectronics*, Vol. 144, No. 4, pp. 235-9, Aug. 1997.

[44] Ling Li and Arun K. Somani, "Blocking Performance Analysis of Fixed-Paths Least-Congestion Routing in Multifiber WDM Networks", *Proc. SPIE Photonics East '99*, Boston, MA, 1999.

[45] Z. Zhang and A. S. Acampora, "A heuristic wavelength assignment algorithm for multihop WDM networks with wavelength routing and wavelength re-use," *IEEE/ACM Trans. Networking*, Vol. 3, no. 5, pp. 281–288, June 1995.

[46] O. Gerstel and S. Kutten, "Dynamic wavelength allocation in all-optical ring networks," *Proc. IEEE ICC '97*, Vol.1, pp. 432-436, June 1997.

[47] R. A. Barry and P. A. Humblet, "Models of blocking probability in all-optical networks with and without wavelength changers", *IEEE Journal on Selected Areas in Communications*, Vol. 14, pp. 858–867, June 1996.

[48] R. A. Barry and D. Marquis, "An improved model of blocking probability in all-optical networks", *LEOS 1995 Summer Topical Meeting*, pp. 43-44, Aug. 1995.

[49] R. Ramaswami and A. Segall, "Distributed Network Control for Wavelength Routed Optical Networks," *Proc. IEEE INFOCOM '96*, Vol. 1, pp. 138-147, 1996.

[50] Y. Mei and C. Qiao, "Efficient Distributed Control Protocol for WDM All-Optical Networks", *Proc. ICCCN*, pp. 150 -153, Sept, 1997.

[51] S. Ramamurthy and B. Mukherjee, "Survivable WDM Mesh Networks, Part I - Protection," *Proc. IEEE INFOCOM '99*, Vol. 2, pp. 744-751, New York, March 1999.

[52] S. Ramamurthy and B. Mukherjee, "Survivable WDM Mesh Networks, Part II - Restoration," *Proc. IEEE International Conference on Communications (ICC '99)*, Vol. 3, pp. 2023-2030, Vancouver, Canada, June 1999.

[53] G. Mohan and A. K. Somani, "Routing Dependable Connections With Specified Failure Restoration Guarantees in WDM Networks ", to appear in *Proc. INFOCOM '2000*, March 2000.

[54] Ling Li, "Optimal Resource Placement in Multifiber Mesh-Survivable WDM Networks", *Proc. On-going Student Research, FTCS '99*, Madison, Wisconsin, June 1999.

[55] A. Girard, *Routing and Dimensioning in Circuit-Switched Networks*, Addison-Wesley, Reading, MA, 1990.

[56] A. K. Somani and M. Azizoglu, "All Optical LAN Interconnection with a Wavelength Selective Router," *Proc. IEEE INFOCOM '97*, pp. 1278-1285, April 1997.

[57] S. Subramaniam, M. Azizoğlu, and A. K. Somani, "A Performance Model for Wavelength Conversion with Non-Poisson Traffic", *Proc. IEEE INFOCOM '97*, pp. 499-506, 1997.

[58] K. C. Lee and O. K. Li, "A wavelength-convertible optical network", *IEEE Journal on Lightwave Technology*, Vol. 11, pp. 962-970, May/June, 1993.

[59] H. Obara, H. Masuda, K. Suzuki, and K. Aida, "Multifiber wavelength-division multiplexed ring network architecture for Tera-bit/s throughput", *Proc. IEEE ICC '98*, Vol. 2, pp. 921-925, June 1998.

[60] S. Baroni, P. Bayvel, R. Gibbens and S. K. Korotky, "Analysis and Design of Resilient Multifiber Wavelength-Routed Optical Transport Networks", *Journal of Lightwave Technology*, Vol. 17, No. 5, pp. 743-758, May 1999.

[61] O. Gerstel, R. Ramaswami, and G.H. Sasaki, "Fault tolerant multiwavelength optical rings with limited wavelength conversion", *IEEE Journal on Selected Areas in Communications*, Vol. 16, No. 7, pp. 1166-1178, Sept. 1998.

[62] H. Harai, M. Murata, and H. Miyahara, "Performance analysis of wavelength assignment policies in all-optical networks with limited-range wavelength conversion", *IEEE Journal on Selected Areas in Communications*, Vol. 16, pp. 1051-1060, Sept. 1998.

[63] V. Sharma and E. A. Varvarigos, "Limited wavelength translation in all-optical WDM mesh networks", *Proc. IEEE INFOCOM '98*, Vol. 2, pp. 893-901, March 1998.

[64] T. Tripathi and K. N. Sivarajan, "Computing approximate blocking probabilities in wavelength routed all-optical networks with limited-range wavelength conversion", *Proc. IEEE INFOCOM '99*, Vol. 1, pp. 329 -336, March 1999.

[65] Y. Zhu, G. N. Rouskas, H. G. Perros, "Blocking in Wavelength Routing Networks, Part I: The Single Path Case", *Proc. IEEE INFOCOM '99*, pp. 321-328, March, 1999.

[66] http://www.siemens.com/telcom/articles/e0297/297boec.htm.

[67] http://www.light-wave.com.

[68] http://www.mapquest.com.